CHARACTERISATION OF CYTOPLASMIC URIDYL TRANSFERASES IN YEAST AND HUMAN CELLS

Marie-Joëlle Schmidt

University of Oxford
Sir William Dunn School of Pathology
Lincoln College

Thesis submitted for the degree of Doctor of Philosophy
at the University of Oxford
Trinity Term 2011

ABSTRACT

Marie-Joëlle Schmidt
Lincoln College

A thesis submitted for the degree of Doctor of Philosophy
Trinity Term 2011

Characterisation of Cytoplasmic Uridyl Transferases in Yeast and Human Cells

Regulation of gene expression by terminal addition of uridyl residues to RNA substrates has recently emerged as a widespread phenomenon in eukaryotes. Studies in organisms ranging from fission yeast to human cells have shown that uridylation of RNA 3' ends stimulates rapid RNA degradation. However, many questions regarding the specificity of the uridyl transferases, the broad range of their substrates and the consequences of their loss are still unanswered. In light of this, the uridyl transferases Cid1 in *Schizosaccharomyces pombe* and ZCCHC11 in human cells and their roles in the regulation of gene expression were further characterised in this study.
To begin with, the biochemistry of the Cid1 protein complex responsible for uridylation in *Schizosaccharomyces pombe* was analysed in more detail by mass spectrometry and *in vitro* assays. These experiments provided insights into the modulation of Cid1 activity by accessory factors. Next, the role of the human uridyl transferase ZCCHC11 in the regulation of replication-dependent histone mRNAs was examined. Results showed that ZCCHC11 is required for efficient destabilisation of histone mRNAs following inhibition or completion of DNA replication. In agreement with this finding, cDNA sequencing experiments showed that ZCCHC11-mediated uridylation is particularly prevalent at the end of S phase. Finally, this thesis also explored the phenotype resulting from ZCCHC11 knock-down with respect to the human cell cycle. Depletion of ZCCHC11 led to the occurrence of DNA damage and activation of the DNA integrity checkpoint, which in turn resulted in cell cycle delay. Taken together, the data presented in this thesis extend current knowledge of the uridyl transferases and their actions in fission yeast and human cells and provide a link between RNA regulation and cell cycle control.

ACKNOWLEDGEMENTS

This work would not have been completed without the support of numerous people and I would like to take this opportunity to acknowledge them here. First and foremost, I would like to thank my mentor and supervisor for giving me the opportunity to work on this exciting project in his lab and for all the support, encouragement and fun during the last four years.

Many thanks go to all lab members, past and present, particularly Olivia R., Li Phing L. and Abigail S. who have introduced me to *S. pombe* and Andrea M., Kumi G., Daniel S. and Sophie F. for their supportive presence and help during my mammalian years. Special thanks to Sophie F. for always being there to listen and comment whether it be scientifically or personally and for making my French improve so much! Best of luck to Erdem A, who has inherited the ZCCHC11 project! Thanks also to Jenny T. for a short but great time and experience in the lab!

I am hugely thankful to Nick Proudfoot for his support and advice as a graduate advisor but also for being such a great musical colleague! I was fortunate to collaborate with David Tollervey and Sander Granneman from the University of Edinburgh on a genome-wide project. Thanks to everyone from the Tollervey lab for a great experience!

This thesis would have been unachievable without the technical help, scientific advice and most of all, infinite love from Steve. A couple of sentences would not do justice, but thanks for your sweet support and for persevering hard in acquainting myself with the British humour!

Finally, I owe biggest thanks to my family for the moral support and absolute faith in me during all my highs and lows. I would not be writing this without you standing behind me!

Table of Contents

List of Figures

List of Tables

Glossary of Abbreviations

AMP	Adenosine monophosphate
ATP	Adenosine triphosphate
BSA	Bovine serum albumin
Cid	Caffeine induced death suppressor
DAPI	4',6-diamidino-2-phenylindole
DMSO	Dimethyl sulphoxide
DSB	Double strand break
E. coli	*Escherichia coli*
HU	hydroxyurea
Lsm	Sm-like
miRNA	microRNA
MMS	Methyl methanesulfonate
mRNA	Messenger RNA
MS	Mass spectrometry
ncPAP	Non-canonical PAP
NTP	Nucleotide triphosphate
OD	Optical density
PABP	Poly(A) binding protein
PAP	Poly(A) polymerase
PEG	Polyethylene glycol
PI	Propidium iodide
PIKK	phosphoinositide 3-kinase related kinases
PUP	Poly(U) polymerase
qPCR	Quantitative polymerase chain reaction
RACE	Rapid amplification of cDNA ends
RBD	RNA binding domain
RNA	Ribonucleic acid
RNAi	RNA interference
RRM	RNA recognition motif
rRNA	Ribosomal RNA
RT-PCR	Reverse Transcription followed by PCR
S. cerevisiae	*Saccharomyces cerevisiae*
S. pombe	*Schizosaccharomyces pombe*
shRNA	Short hairpin RNA
siRNA	Small interfering RNA
SLBP	Stem-loop binding protein
snRNA	Small nuclear RNA
TAP	Tobacco acid pyrophosphatase
tRNA	Transfer RNA
TUTase	Terminal U transferase
UMP	Uridine monophosphate
UTP	Uridine triphosphate
UTR	Untranslated region
WT	Wild type

Role of Author

The research presented in this Thesis has not been submitted for any other degree. The experimental work presented was performed wholly by me.

Financial Statement

I would like to acknowledge the trustees of the E.P. Abraham Trust for a graduate scholarship and the Lincoln College research fund for financial support during this DPhil.

CHAPTER I. INTRODUCTION

This thesis focuses on mechanisms that oversee the life span of mRNA, particularly at the stage when it has fulfilled its function in translation. I investigate a specific enzyme in fission yeast (Cid1) and its orthologue in human cells (ZCCHC11) that is involved in targeting RNAs for destruction in order to avoid detrimental accumulation of RNA molecules in the cell. In brief, Chapter III reports on studies using the *Schizosaccharomyces pombe* (*S. pombe*) model system regarding the biochemistry of the protein complex of Cid1 with the aim of finding factors that regulate Cid1 activity. Chapter IV describes a ZCCHC11–dependent role in the destruction of mRNAs and specifically histone mRNAs. I find that ZCCHC11 is required for rapid and efficient degradation of histone mRNAs at specific times during the human cell cycle. Finally, Chapter V details the cell cycle phenotype of human cells in which ZCCHC11 has been depleted. I describe a cell cycle defect associated with loss of ZCCHC11 and potentially attributable to its role in histone mRNA turnover.

This introductory chapter reviews current knowledge of RNA 3' ends and their function in cytoplasmic RNA decay, as well as the family of non-canonical poly(A) polymerases, to which Cid1 and ZCCHC11 belong. In addition, histone mRNA processing and, finally, regulation of cell cycle phases relevant to this study will also be introduced. As both yeast and mammalian systems were used in this study, information relevant to both is incorporated, whilst conservation and variations between these systems are emphasised.

I.1. mRNA 3' ends

The life cycle of an RNA starts with its transcription by RNA polymerase and ends with its degradation by various endo- and exonucleases. The quantity of RNA produced in the cell is tremendous, implying a high metabolic cost for their synthesis. Moreover, several processing steps are needed in order to produce mature and functioning RNA molecules, which mostly operate as RNA-protein complexes. These steps include capping, splicing, polyadenylation, and RNA editing (Wahle and Ruegsegger 1999; Shatkin and Manley 2000; Hastings and Krainer 2001). Many of these reactions occur co-transcriptionally, revealing a spatially and temporally close association between transcription and RNA processing (Proudfoot et al. 2002). Mature RNA molecules are exported from the nucleus to the cytoplasm, whereas the remaining fragments (introns, 3´ trailers, extensions and internal spacers) are thought to be rapidly degraded in the nucleus (Kim et al. 2004; West et al. 2004). There is mounting evidence that all maturation processes are continuously monitored by surveillance mechanisms (Houseley et al. 2006).

In the following section, 3´ end processing of mRNAs will be reviewed in further detail. Their formation involves an endonucleolytic cleavage at specific sites and subsequent extension with a long poly(A) tract. Polyadenylation of mRNAs (with the exception of histone transcripts of higher eukaryotes) is carried out by poly(A) polymerases (PAP), the best known member of the β family of related nucleotidyltransferases (Holm and Sander 1995; Aravind and Koonin 1999).

3' end cleavage and PAP-mediated polyadenylation of mRNAs have multiple functions in eukaryotes: promotion of transcription termination, mRNA stability, facilitation of mRNA export and, finally, initiation of translation (Huang and Carmichael 1996; Sachs et al. 1997; Carpousis et al. 1999). The presence of an intact poly(A) tail on mRNAs in eukaryotes is a hallmark of a mature transcript. In contrast, poly(A) tails on mRNAs in bacteria promote

their removal by creating a 'landing pad' for the RNA degradation machinery (Kushner 2002). As such, the impact of poly(A) tails on RNA stability appears at almost complete variance between bacteria and eukaryotes. Importantly, poly(A) tails in bacteria are too short to be bound by protective poly(A) binding proteins (Feng et al. 2001), whereas long poly(A) tails present on all mature mRNAs in eukaryotes are rapidly bound by the poly(A) binding protein PABP in higher eukaryotes (Pab1p in yeast). As such, PABP protects the transcript from deadenylation in the cytoplasm (Caponigro and Parker 1995).

For a long time the function of poly(A) tails in eukaryotes was believed to be restricted to the stabilisation of mRNAs. However, a new function for poly(A) tails in promoting the degradation of aberrant non-coding RNAs and cryptic unstable transcripts was revealed by several studies in *S. cerevisiae* (Kadaba et al. 2004; LaCava et al. 2005; Vanacova et al. 2005; Wyers et al. 2005). This activity is performed by the so-called TRAMP complex, which consists of the poly(A) polymerase Trf4 or Trf5, the RNA helicase Mtr4 and either of the two zinc finger proteins Air1 and Air2. Poly(A)-mediated degradation was later also found in human cells (West et al. 2006; Shcherbik et al. 2010) and will be discussed in more detail in section I.3.3.

In addition to polyadenylation, it was found that cytoplasmic uridylation of mRNA 3' ends could also serve to stimulate RNA degradation (Song and Kiledjian 2007; Mullen and Marzluff 2008; Rissland and Norbury 2009). Non-templated uridyl residues have been found on non-coding RNAs including decay intermediates of micro-RNA (miRNA) directed cleavage products (Shen and Goodman 2004), small RNAs (Li et al. 2005; van Wolfswinkel et al. 2009) and micro-RNAs (Heo et al. 2008; Hagan et al. 2009; Heo et al. 2009; Jones et al. 2009; Lehrbach et al. 2009). The mechanism of uridylation-mediated decay of cytoplasmic mRNAs will be explained in further details in the following section. Uridylation-mediated turnover of miRNAs is emphasised in section I.3.3.5.

I.2. mRNA decay in the cytoplasm

I.2.1. Deadenylation-mediated decay

Most of the current knowledge of cytoplasmic mRNA decay comes from studies in budding yeast, where the initial step is the removal of the poly(A) tail (Decker and Parker 1993). This step ultimately leads to removal of the 5' cap and exonucleolytic degradation by either a 5' exonuclease or the cytoplasmic RNA exosome (Coller and Parker 2004). Shortening of the poly(A) tail by deadenylases is predominantly thought to prevent binding of the poly(A) tail by PAPB, and instead results in recruitment of the Lsm1-7 complex (Tharun and Parker 2001). The Lsm1-7 complex is a protein ring structure composed of seven Sm-like proteins, which was shown to stimulate decapping *in vivo* (Tharun et al. 2000) and which preferentially binds short teminal A- and U-tracts (Chowdhury et al. 2007). The Lsm1-7 complex then recruits the heterodimer Dcp1-Dcp2, consisting of the decapping activator Dcp1 and the decapping enzyme Dcp2, which removes the cap of the substrates. As a consequence of decapping, the accessible 5' end of the RNA can be degraded by the cytoplasmic 5'-3' exonuclease Xrn1. Alternatively, deadenylation can also lead to degradation of the transcript from the 3' end. This is achieved by the cytoplasmic exosome, a multi-subunit protein complex with 3'-5' exo- and endonuclease activity (Lykke-Andersen et al. 2009).

Rates of RNA decay are specific for each mRNA species, though mechanisms defining the half-life of RNAs are still poorly understood. Probably the best-characterised *cis* elements influencing RNA stability are the AU-rich elements located in downstream un-translated regions of mRNAs (3'UTR), which can trigger deadenylation and decapping in budding yeast (Vasudevan and Peltz 2001) and mammals (Gao et al. 2001).

I.2.2. Uridylation-mediated decay

First indications that uridine residues on RNA 3' ends could be involved in promoting decapping and 5'-3' exonucleolytic degradation came from a study in plants investigating decay intermediates of miRNA-directed cleavage products (Shen and Goodman 2004). When complementary to their mRNA target, plant miRNAs directed endonucleolytic cleavage of mRNAs, resulting in two RNA fragments (Jones-Rhoades et al. 2006). These authors found stretches of non-templated uridines (1-4 nucleotides in average) on the 3' ends of 5' cleavage products of mRNA targets. Interestingly, the majority of uridylated transcripts had undergone substantial exonucleolytic degradation from the 5' end, suggesting that uridine residues could stimulate decapping and subsequent RNA decay. *In vitro* studies later showed that an oligouridine tract of 5 uridine residues on an RNA 3' end stimulates decapping, 5'-3' RNA decay and inhibites 3'-5' decay (Song and Kiledjian 2007). These authors also found that decapping is promoted by the interaction of the Lsm1-7 complex with the oligouridine tract. They proposed a model whereby the Lsm1-7 complex binds a non-templated uridine tract and recruits the decapping complex to the 5' end of the substrate, followed by decapping and exonucleolytic degradation.

Subsequent investigations in fission yeast from our laboratory and others in human cells have confirmed the role of uridylation in promoting mRNA decay via the Lsm1-7 complex *in vivo* (Mullen and Marzluff 2008; Rissland and Norbury 2009; Norbury 2010). Initially, uridine residues were found on polyadenylated actin messages in *S. pombe* and were attributed to the activity of the cytoplasmic nucleotidyl transferase Cid1 (Rissland et al. 2007). For more details about the identification of Cid1, see section I.3.2.1. Subsequent sequencing of circularised polyadenylated messages in *S. pombe* established a link between Cid1-mediated uridylation and 5'-3' mRNA decay (Rissland and Norbury 2009). Importantly, uridylated messages accumulate to a significant degree in strains defective in the decapping

activator Dcp1 or Lsm1, suggesting that uridylation precedes decapping. The length of these oligouridine tracts is on average 1-3 nucleotides, which is in accordance with the length of oligouridine tracts found in *Arabidopsis* previously (Shen and Goodman 2004). It is worthwhile mentioning that equivalent sequencing analyses performed on actin transcripts in *S. cerevisiae* did not reveal indications of mRNA uridylation in budding yeast (Rissland and Norbury 2009), and neither have investigations by others (personal communication Laura Milligan and David Tollervey). These observations imply a greater complexity of decay pathways in fission yeast, and by extension higher eukaryotes, than in budding yeast.

Non-templated uridine residues were also found on human replication-dependent histone mRNAs (Mullen and Marzluff 2008). These are the only metazoan mRNAs that are not polyadenylated (for more details on histone mRNA expression, see Chapter I.4). This study initially found that Lsm1 physically interactes with the characteristic 3' end histone stem-loop binding protein SLBP (see below for more details). In addition, the decapping enzyme Dcp2, the 5'-3' exonuclease Xrn1 and the 3'-5' exosome are required to stimulate efficient degradation of replication-dependent histone mRNAs. Following sequence investigations of circularised histone mRNAs (cRACE) as well as histone mRNA 3' ends (3'RACE), the authors observed oligouridine tracts on the mature 3' ends of these messages. Because histone degradation intermediates with substantial nucleotide removal from both RNA ends were also found, it was concluded that 5'-3' and 3'-5' degradation simultaneously contributes to histone mRNA decay, stimulated by prior addition of oligouridine tracts. Interestingly this study, which found uridine tracts of up to 10 nucleotides in length, is the only report to date of such long U-tails. Two enzymes responsible for uridylation of histone mRNAs were identified, although the identity of the uridyl transferase remained controversial and constitutes a focal point of this thesis.

Several subsequent reports described the involvement of uridylation in destabilisation of cytoplasmic non-coding RNAs in mammals and worms, and will be reviewed in more detail below.

The enzymes responsible for the addition of non-templated ribonucleotides to RNA 3' ends are, like the canonical poly(A) polymerase PAP, also members of the Pol β superfamily, but belong to a distinct subclass of nucleotidyl transferases, the so-called non-canonical (nc) PAPs (Schmidt and Norbury 2010). Members of the ncPAP family in fission yeast and humans will be introduced in the following section.

I.3. Non-canonical poly(A) polymerases

I.3.1. Common features

Despite having very different functions in the cell, all nc-PAPs share some common characteristics. In-depth coverage of structural and catalytic features of canonical PAPs can be found elsewhere (Martin et al. 2008). In brief, PAPs catalyse template-independent incorporation of ribonucleoside monophosphate to the 3' hydroxyl end of RNAs via a two-metal ion catalytic mechanism. The catalytic domain contains the signature helix-turn motif of the Pol β superfamily, which is conserved from yeast to human cells (Figure I.1). A hallmark of this motif is the highly conserved triad of aspartates that is essential for catalytic activity. These residues are important for the coordination of the metal ions and the incoming nucleotide within the active site. The catalytic domain is accompanied by a PAP-associated domain, which is also highly conserved among ncPAPs (Figure I.1).

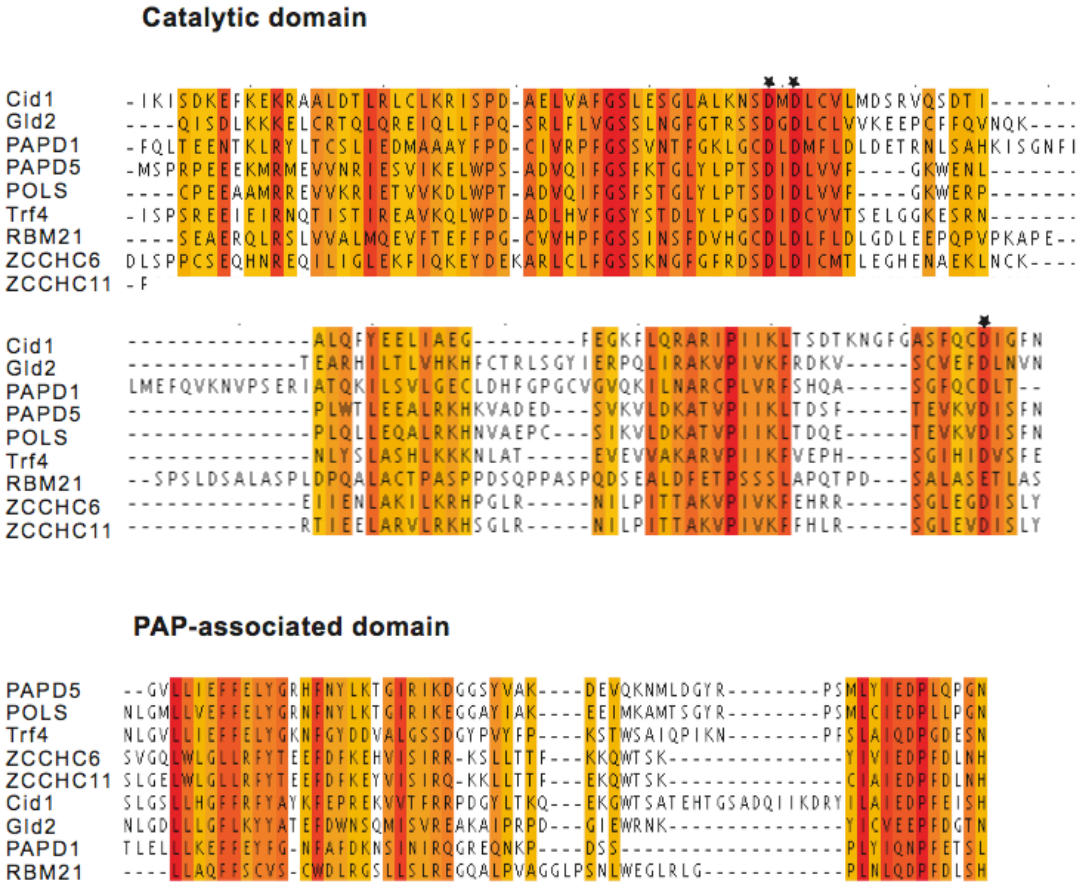

Figure I.1 NcPAPs are conserved amongst eukaryotes.

Alignment of the catalytic and PAP-associated domains of the human nc-PAPs together with *S. pombe* Cid1 and *S. cerevisiae* Trf4. Colours ranging from yellow over orange to red indicate percentage similarity from 30% to 100% identity. The asterisks denote the catalytic triad consisting of 3 aspartates.

In general, ncPAPs show pronounced selectivity for specific nucleotides *in vivo*, raising the question of how such selectivity is achieved. Structural and kinetic analyses of canonical PAPs and the related trypanosomal RNA-editing terminal U-transferases (TUTases) have suggested the involvement of multiple factors including non-polar and water-mediated interactions between specific amino acid residues and the nucleotides (Deng et al. 2005; Balbo and Bohm 2007). While most if not all ncPAPs select specific nucleotides *in vivo*, they can show greater flexibility in accepting alternative nucleotides *in vitro* (Rissland et al. 2007; Bai et al. 2011). Understanding nucleotide specificity at the molecular level will require precise structural information that is lacking for most of the ncPAPs.

In contrast to the canonical PAP, ncPAPs do not contain canonical RNA-recognition motifs (RRMs), with the exception of RBM21, the U6 TUTase (Figure I.2). Instead, ncPAPs typically act in a complex with RNA-binding protein(s) in order to recognize target RNAs or, in one unusual case, as a dimer (Bai et al. 2011). Moreover, *in vitro* activities of isolated proteins very often differ from their activity *in vivo*. For example, the canonical PAP displays distributive activity in the absence of specific interacting factors, while it exhibits processive activity as part of the characteristic mRNA 3' end processing complex (Kaufmann et al. 2004). In contrast, *S. pombe* Cid1, which is discussed in more detail below, has robust poly(U) polymerase (PUP) activity *in vitro*. In light of this, it is therefore surprising that *in vivo* Cid1 appears to add only one to three terminal UMPs (Rissland et al. 2007).

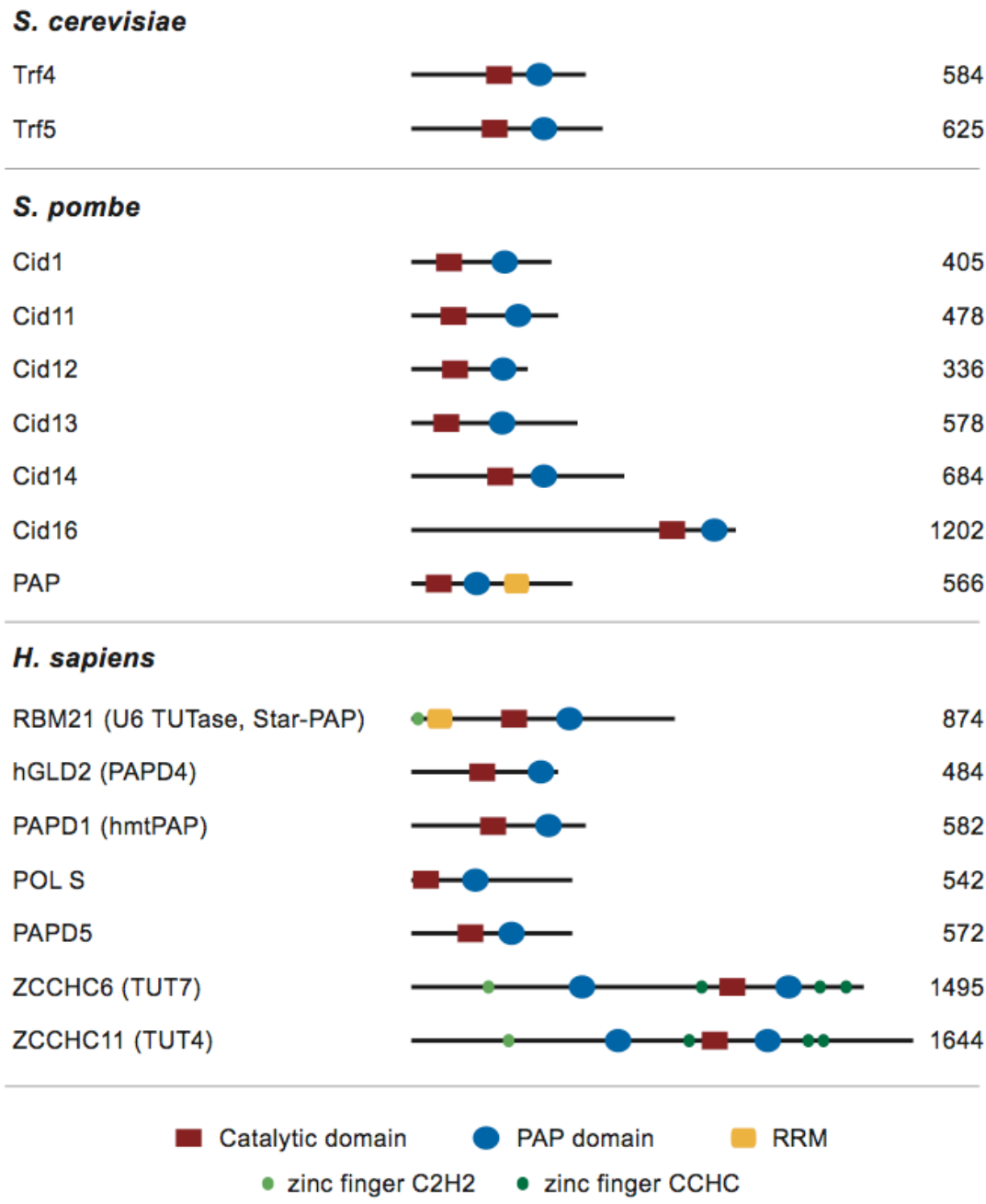

Figure I.2 Domain organisation of ncPAPs in yeast and human cells

The features highlighted are: catalytic domain (red), PAP-associated domain (blue), RNA recognition motif (yellow), zinc finger C2H2 (light green) and CCHC (dark green). The size of each protein is indicated in amino acids. Names in brackets indicate alternative names used in the literature.

I.3.2. Nc-PAPs in fission yeast

I.3.2.1. Cid1

The description of Cid1 in fission yeast provided one of the first insights into the biological functions of ncPAPs. Cid1 (for caffeine induced death suppressor) was discovered through a screen designed to identify genes involved in the DNA replication stress response using a combination of the drugs caffeine and hydroxyurea (HU) (Wang et al. 1999). By inhibiting the checkpoint kinase Rad3 in *S. pombe* (ATR in humans, see Chapter I.5 for more details), caffeine can override the S-M checkpoint that normally prevents entry into mitosis when DNA replication is perturbed. HU causes depletion of dNTP pools by inhibition of ribonucleotide reductase, which results in S phase arrest. Therefore, exposure of cells to the combination of caffeine and HU promotes premature entry into mitosis and cell death, a phenotype that can be suppressed by overexpression of Cid1. In addition, overexpression of Cid1 confers partial resistance to the HU sensitivity of checkpoint mutants whilst *cid1* deletion causes sensitivity to the combination of HU and caffeine (Wang et al. 2000). As such, Cid1 was suggested to be required for S-M checkpoint integrity in response to DNA replication stress.

Its amino acid sequence shows that Cid1 is a member of the Pol β superfamily of nucleotidyl transferases and more specifically the Cid family of non-canonical poly(A) polymerases in *S. pombe* (Figure I.2*)*. Fluorescence microscopy showed that Cid1 is exclusively cytoplasmic in exponentially growing cells as well as in cells undergoing DNA replication stress (Read et al. 2002). Biochemical investigations of the *in vitro* activity of Cid1 suggested that Cid1 is a poly(A) polymerase, albeit with roles distinct from that of the nuclear canonical PAP. Surprisingly, it was later revealed that its major activity is uridylation of mRNA substrates, both *in vivo* and *in vitro* (Rissland et al. 2007). It was shown that Cid1 possesses strong and processive poly(U) polymerase (PUP) activity as a recombinant protein and as a native protein

complex isolated from yeast cells. Importantly, the PUP activity of recombinant Cid1 is able to out-compete effectively its PAP activity. Furthermore, the authors reported the presence of one or two uridyl residues on the 3' ends of polyadenylated actin mRNAs *in vivo*, which were attributable to Cid1. This observation raised the question as to why only few uridine residues can be found *in vivo*, when *in vitro* Cid1 is able to polymerase hundreds of nucleotides within minutes; a question that constitutes a key aspect of this thesis. The presence of uridine residues on mRNA 3' ends was subsequently demonstrated to stimulate decapping and exonucleolytic decay as described in section I.2.2 and thereby to play a previously uncharacterised role in mRNA turnover in the cytoplasm (Rissland and Norbury 2009).

I.3.2.2. Other non-canonical PAPs in S. pombe

In addition to Cid1, the *S. pombe* genome encodes five other members of the family of ncPAPs, named Cid11-Cid16 (Stevenson and Norbury 2006). As the yeast-related part of this thesis focuses on Cid1, the other Cid-members will only be mentioned briefly in the following section.

Cid13

Like Cid1, Cid13 was discovered in screens designed to identify genes involved in the DNA replication stress response (Read et al. 2002; Saitoh et al. 2002). Cid13 is also cytoplasmic and appears to regulate dNTP pools by polyadenylation of an mRNA encoding a subunit of ribonucleotide reductase.

Cid14

S. pombe Cid14 is the homologue of *S. cerevisiae* Trf4 and Trf5 and was also found in a TRAMP-like complex containing the zinc-knuckle protein Air1 and the RNA helicase Mtr4 (Bühler et al. 2007; Keller et al. 2010). In *S. cerevisiae*, there is a degree of functional redundancy between Trf4 and Trf5, such that cells lacking either one are viable while loss of both is lethal. This essential function can be provided in *trans* by *S. pombe* Cid14, the only demonstration

of cross-species functional homology in the ncPAP family so far reported (Win et al. 2006a), but curiously Cid14 is not essential for viability in fission yeast. Cid14 is involved in nuclear polyadenylation and degradation of rRNAs, suggesting that the pathway of polyadenylation-assisted degradation of nuclear RNAs is conserved in eukaryotes. Indeed, the same pathway has recently also been found in human cells and is described in section I.3.3.4 (Shcherbik et al. 2010). Studies in *S. cerevisiae* and *S. pombe* have indicated an additional role of the TRAMP complex in chromatin remodelling, which is reviewed in detail elsewhere (Houseley and Tollervey 2008).

Cid12

Cid12, which is predominantly localised to the nucleus, was shown to function in RNAi-mediated heterochromatin assembly on centromeric DNA repeats as part of the RNA-directed RNA polymerase (RdRP) complex (Motamedi et al. 2004). The catalytic activity of Cid12 was suggested to be important for its function, as mutation of residues critical for this activity results in loss of centromeric silencing (Win et al. 2006b). However, the exact role of Cid12 remains to be elucidated as well as its nucleotide preference. Finally, Cid12 not only interacts with components of the RNAi machinery but also with numerous splicing factors and in this context may provide a link between spliceosomal complexes and the RNAi pathway (Bayne et al. 2008).

Cid11 and Cid16

Two further ncPAPs exist in *S. pombe*: Cid11 and Cid16. Cid11 is expressed during meiosis (Mata et al. 2002) and is thought to be localised to both the nucleus and cytoplasm, whereas Cid16 shows enrichment in cytoplasmic speckles (Matsuyama et al. 2006). The roles of these two proteins are yet to be characterised, however it is likely that they exhibit ribonucleotidyl transferase activity based on their clear sequence similarity to other ncPAPs.

I.3.3. NcPAPs in human beings

The human genome encodes seven potential ncPAPs (Figure I.2): RBM21 (U6 TUTase, also called Star-PAP), PAPD1 (hmtPAP), PAPD4 (hGLD2), POLS, PAPD5, ZCCHC6 and ZCCHC11. Based on sequence alignments, POLS and PAPD5 are orthologous to *S. cerevisiae* Trf4/Trf5, whereas ZCCHC6 and ZCCHC11 are in some respects most similar to Cid1. No clear orthologue of RBM21, PAPD1 or PAPD4 can be identified among the ncPAPs in *S. pombe*. Some of these human enzymes, such as RBM21, PAPD1 and PAPD4 have been studied in considerable detail whereas the functions of others, such as POLS and ZCCHC6, are yet to be characterised. Here, an overview of the current knowledge of the different human ncPAPs and their biological roles is provided.

I.3.3.1. RBM21 (U6 TUTase / Star-PAP)

RBM21 (U6 TUTase) was identified as an essential enzyme responsible for the 3' terminal addition of up to four UMP residues on spliceosomal U6 snRNA in the nucleolus (Trippe et al. 1998; Trippe et al. 2006). Interestingly, when RBM21 is presented with total RNA either in recombinant form or in native protein complexes purified from mammalian cells, the enzyme exclusively accepts U6 snRNA as a substrate.

Recently, RBM21 has also been identified independently as a PAP involved in signalling pathways that are regulated by nuclear phosphoinositides (Mellman et al. 2008; Mellman and Anderson 2009; Laishram and Anderson 2010). The enzyme was termed Star-PAP (nuclear speckle targeted PIPKIα-regulated poly(A) polymerase), based on its localisation to nuclear speckles and its functional interaction with type I phosphatidylinositol 4-phosphate 5-kinases (PIPKIα). Through its association both with 3' end processing factors and with signalling stimuli, RBM21 was suggested to be involved in the regulated 3' end cleavage of specific target mRNAs. It will be interesting to

follow up on the dual functionality of this protein in the future. Given its apparent role in stabilisation of U6 snRNA, it would be surprising if knock-down of RBM21 did not affect overall splicing efficiency; such an effect may underlie the lethality seen on its knock-down in some studies, and will necessarily complicate the investigation of other, non-essential roles of this ncPAP.

I.3.3.2. PAPD4 (hGLD2)

Non-canonical polyadenylation by GLD2 has been implicated in a wide range of cellular processes including germline development, control of cell division and synaptic plasticity (Richter 2007). GLD2 was first described in *C. elegans* as a cytoplasmic ncPAP (Wang et al. 2002) important for translational activation of cytoplasmic mRNAs. Together with the RNA binding protein GLD3, GLD2 functions by positively regulating the expression of dormant mRNAs through elongation of the poly(A) tail. Although GLD2 alone has weak PAP activity, recruitment of GLD3 is sufficient to stimulate polyadenylation *in vitro*. As such, GLD2 provides another example of a ncPAP acting in concert with an RNA-binding protein to target specific transcripts. The ability of an RNA binding protein to stimulate murine and human GLD2 PAP activity was later confirmed using a tethered approach in *Xenopus* oocytes (Kwak et al. 2004). Surprisingly, GLD2 in Xenopus (xGLD2) is localised to both the nucleus and cytoplasm (Rouhana et al. 2005). The same is true for murine and human GLD2, which localise predominantly to the nucleus (Nakanishi et al. 2006), but the biological significance of this nuclear ncPAP is not yet understood. In contrast, *Drosophila* GLD2 is restricted to the cytoplasm (Benoit et al. 2008; Kwak et al. 2008).

One feature of xGLD2, not so far described for any other ncPAP, is its ability to activate its own mRNA by polyadenylation during *Xenopus* oocyte maturation (Rouhana and Wickens 2007). Conservation of the relevant regulatory sequences and proteins suggests that a similar positive feedback circuit is likely to occur in mammals. In addition to the functions of GLD2

described above, the protein has recently also been implicated in the regulation of murine miRNAs (Katoh et al. 2009), discussed in section I.3.3.5.

I.3.3.3. PAPD1 (hmtPAP)

The function of polyadenylation in human mitochondria is not yet fully understood; observations of truncated and polyadenylated mitochondrial transcripts suggest that part of this function may be related to the degradation-stimulating role of polyadenylation in bacteria or in plant chloroplasts and mitochondria (Slomovic et al. 2005; Schuster and Stern 2009). On the other hand, the addition of AMP residues to the 3' end of mitochondrial mRNAs in humans serves to complete the UAA stop codon in some mitochondrial mRNAs, presumably reflecting the extreme evolutionary pressure to reduce mitochondrial genome size (Ojala et al. 1981). The enzyme that polyadenylates mitochondrial RNAs is called PAPD1 or hmtPAP. As judged by immunofluoresence microscopy, this protein is exclusively mitochondrial (Tomecki et al. 2004; Nagaike et al. 2005). The consequences of polyadenylation regarding mitochondrial mRNA stability remain controversial. One study showed steady state levels of mRNAs and their translational products to be markedly decreased following PAPD1 siRNA knock-down (Nagaike et al. 2005), while no hmtPAP-dependent effects on mRNA stability were observed by others (Tomecki et al. 2004).

Very recently, the structure of PAPD1 has been determined by crystallography (Bai et al. 2011), the first and only structure of a human ncPAP to be unveiled to date. The catalytic and PAP-associated domain of PAPD1 proved to be very similar to that of canonical PAP. However, the structure revealed a previously unrecognised domain in the N-terminal region that resembled RNA-binding domains (RBD) and was consequently termed the RL (RBD-like) domain. It was also found that dimerisation of PAPD1, mediated by the RL domain, is essential for catalytic activity. Furthermore, *in vitro* polymerisation assays showed that PAPD1 is able to use all four nucleotides, but displays a preference for ATP and UTP. Kinetic analyses of

recombinant PAPD1 showed that it possesses 9-fold greater PAP than PUP activity.

In addition to the role of PAPD1 in polyadenylation of mitochondrial mRNAs, it has intriguingly also been implicated in the degradation of replication-dependent histone mRNAs (Mullen and Marzluff 2008). As outlined in Chapter I.2.2, the replication-dependent histone mRNAs are rapidly degraded following uridylation of the 3' end of histone mRNAs. Together with PAPD5 (see section I.3.3.4), PAPD1 was suggested to be responsible for the modification of histone mRNAs. Further work will be needed to clarify the apparent dual role of PAPD1 in uridylation of histone mRNAs in the cytoplasm and the polyadenylation of mRNAs in mitochondria.

I.3.3.4. Human Trf4 / Trf5 orthologs

As components of TRAMP complexes, budding yeast Trf4 and Trf5 together with the RNA helicase Mtr4 and the zinc finger proteins Air1 and Air2 are involved in targeting a wide range of nuclear RNA substrates for degradation by the nuclear exosome. Two human Trf4 orthologues, PAPD5 and POLS, can be identified on the basis of sequence comparison, but the biological functions of these enzymes are largely unknown. Recent structural analysis of a heterodimer of *S. cerevisiae* Trf4 and Air2 revealed a highly conserved interaction surface between the central domain of Trf4 and the zinc knuckles of Air2 (Hamill et al. 2010). This conservation amongst eukaryotes suggests that human cells might contain a similar TRAMP complex. It seems likely that a PAP-mediated surveillance mechanism similar to that described in yeast also takes place in the mammalian nucleus as some pre-mRNA cleavage products were found to have non-templated A-rich tails. These cleavage products did not appear to be added by the canonical nuclear PAP but were degraded by the exosome (West et al. 2006). Furthermore, incomplete pre-rRNA transcripts were recently found to undergo PAPD5-dependent polyadenylation and exosome-dependent degradation in murine cells (Shcherbik et al. 2010). Additional evidence for a Trf4-like protein in human

cells was very recently provided by a study investigating the biochemistry of PAPD5 (Rammelt et al. 2011). The authors showed that PAPD5 localises to the nucleus and catalyses the addition of adenyl residues to various RNA substrates. In contrast to Trf4 however, PAPD5 is able to bind its substrates and is active without a cofactor. Deep sequencing of PAPD5-associated transcripts suggested that rRNAs are the primary targets of PAPD5. Interestingly, it was shown that spliced-out introns represent a significant proportion of TRAMP substrates in *S. cerevisiae* (San Paolo et al. 2009). It can be speculated that a similar mechanism of intron turnover in the human nucleus may account for a major function of human Trf4 orthologues, as most polymerase II transcription in human cells generates intronic RNA. It will be interesting to investigate adenylated exosome substrates in human cells in the future.

As mentioned above, PAPD5 has been suggested to be involved in the turnover of replication-dependent histone mRNAs by uridylation of their 3' ends (Mullen and Marzluff 2008). In the same study, immunofluorescence microscopy of epitope-tagged PAPD5 indicated a cytoplasmic, rather than nuclear, distribution. These results suggest a role for PAPD5 that is quite distinct from the function of nuclear Trf4 in yeast. The implication of PAPD5 in histone mRNA degradation argues for possible functional redundancy between the different ncPAPs and is challenged in this work (Chapter IV.6). Additional clarification will also be needed to dissect the role of Gld4; another name that has been given to PAPD5. In brief, Gld4 has been found in the cytoplasm in *C. elegans* (Schmid et al. 2009) and was suggested to be involved in the cytoplasmic polyadenylation and regulation of p53 mRNA in a manner that depends on Gld2 (see section I.3.3.2) and the cytoplasmic polyadenylation element binding protein (Burns et al. 2011).

In summary, PAPD5 is probably the ncPAP, to which the most different functions have been attributed but further experiments are awaited that will clarify its distinct roles.

I.3.3.5. ZCCHC6 and ZCCHC11 and small RNA uridylation

Based on sequence alignments and biochemical analyses, two human orthologues of the fission yeast RNA uridyl transferase Cid1 have been identified (Kwak and Wickens 2007; Rissland et al. 2007). These relatively large proteins (171 kDa and 185 kDa, respectively, in comparison with 46 kDa for Cid1) each contain two PAP-associated domains and one catalytically active nucleotidyl transferase domain (Figure I.2). They also possess multiple zinc finger motifs that are likely to be involved in protein–protein and/or RNA–protein interactions. Analysis of ZCCHC6 expressed in *Xenopus* oocytes or purified by tandem affinity from human cells showed robust PUP activity and marginal activity with ATP, CTP or GTP (Kwak and Wickens 2007; Rissland et al. 2007). Human ZCCHC11 is present in the cytoplasm (Heo et al. 2009) and ZCCHC6 localises to stress granules in human cells following their induction by arsenite (Andrea Mikulasova and Chris Norbury, unpublished results), suggesting a role in stress-induced metabolism of RNAs.

Recent studies have identified a role for ZCCHC11 in the regulation of microRNAs (miRNAs) (Hagan et al. 2009; Heo et al. 2009; Jones et al. 2009; Lehrbach et al. 2009). Regulation of miRNA biogenesis and turnover has only recently been explored, beginning with the finding that the RNA-binding protein Lin28 represses the biogenesis of *let-7* miRNA post-transcriptionally (Heo et al. 2008; Newman et al. 2008; Rybak et al. 2008). Lin28 has key functions in development and disease, as for example in specification of the stem cell phenotype and induction of pluripotency in somatic cells (Yu et al. 2007) or as a proto-oncogene (Viswanathan et al. 2009). Lin28 interacts with the cytoplasmic precursor form of *let-7* (pre-*let-7*) and mediates the terminal addition of uridine residues to its 3' end, a modification that inhibits Dicer processing and stimulates decay (Heo et al. 2008). Three groups have then independently identified ZCCHC11 as the pre-*let-7* TUTase in *C. elegans*, mouse and human cells (Hagan et al. 2009; Heo et al. 2009; Lehrbach et al.

2009). ZCCHC11 has also been named TUT4 in humans and PUP-2 in *C. elegans*, but for simplicity it is referred to ZCCHC11 here. In all three organisms, ZCCHC11 forms a complex with Lin28 and pre-*let-7* in the cytoplasm. Uridylation of pre-*let-7 in vitro* requires the catalytic activity of ZCCHC11 and depends on Lin28. *In vitro*, recruitment of ZCCHC11 to pre-*let-7* is mediated by the association of Lin28 with a conserved sequence motif in the terminal loop of pre-*let-7* in mammals (Heo et al. 2009). Single-molecule approaches later confirmed that Lin28 acts as a uridylation processivity factor by magnifying the interaction between ZCCHC11 and pre-*let-7* up to 200-fold (Yeom et al. 2011). In *C. elegans*, however, the terminal loop sequence of pre-*let-7* is not conserved and was shown to be dispensable for Lin28 regulation *in vivo* (Lehrbach et al. 2009). Pre-*let-7* levels decrease in mouse embryonic stem (ES) cells and in *C. elegans* when Lin28 and/or ZCCHC11 are depleted. In contrast, mature *let-7* transcripts accumulate, indicating that uridylation of the precursor selectively inhibits *let-7* maturation (Hagan et al. 2009; Heo et al. 2009; Lehrbach et al. 2009). Microarray experiments showed that the *let-7* family is selectively targeted by the combined action of ZCCHC11 and Lin28 in mouse embryonic stem (ES) cells (Hagan et al. 2009; Heo et al. 2009). As expected, inhibition of ZCCHC11 also leads to repression of *let-7* target gene products, as demonstrated by luciferase reporter assays (Hagan et al. 2009). Finally, ZCCHC11 was suggested to contribute to the maintenance of pluripotency in mouse ES cells (Heo et al. 2009) and to regulate larval development in *C. elegans* (Lehrbach et al. 2009).

In an earlier study, ZCCHC11 was implicated in the regulation of cytokine expression (Minoda et al. 2006). The underlying mechanism has since been shown to involve ZCCHC11-mediated regulation of the cytokine-targeting miRNA family *miR-26* (Jones et al. 2009). ZCCHC11-dependent uridylation of mature *miR-26* was shown to abrogate the silencing effect of *miR-26* on cytokine expression. Consequently, depletion of ZCCHC11 results in decrease of specific cytokine levels and, interestingly, in shortening of the

poly(A) tail length of the corresponding cytokine mRNAs. Deep sequencing of small RNAs revealed the presence of 1-3 non-templated uridine residues at the 3' end of *miR-26*, which are lost upon siRNA-mediated knock-down of ZCCHC11. Consistent with a role of ZCCHC11 in inflammation and immunity, ZCCHC11 protein is ubiquitously expressed but with a predominance in organs of the immune system (Jones et al. 2009). Selective uridylation of pre-miRNA and mature miRNAs by ZCCHC11 raises the question of how this substrate specificity is achieved. It is unlikely that ZCCHC11 itself selects its target, as it is capable of uridylating a broad range of substrates (Jones et al. 2009). In the case of pre-miRNAs, Lin28 recruits ZCCHC11 to pre-*let-7* (Hagan et al. 2009; Heo et al. 2009; Lehrbach et al. 2009). It remains to be seen whether Lin28 also targets ZCCHC11 to mature miRNAs, or whether an as yet uncharacterised protein performs this function.

Mass spectrometric analysis of *miR-122* in mammals revealed the presence of non-templated terminal adenosine and uridine residues at the 3' ends (Katoh et al. 2009). In contrast to uridylation, adenylation of *miR-122* appears to stabilise the miRNA. This modification is catalysed by PAPD4 (hGLD2) and occurs after processing of the pre-miRNA by Dicer. The authors proposed a model in which miRNAs are subject to a delicate balance between selective stabilisation and degradation. The type of nucleotide added determines steady state levels of the miRNA, and hence further RNAi-related processes. The presence of non-templated adenine and uridine residues has since then been confirmed by multiple reports in fish, flies and mammalian cells and have mainly been attributed to Gld2 and ZCCHC11. However, one very recent study using RNA interference combined with extensive deep sequencing implicated every single ncPAP in the modification of small RNAs, the significance of which will be interesting to investigate in the future (Wyman et al. 2011).

Other small RNAs have also been shown to be uridylated by Cid1-like ncPAPs. A recent study in *C. elegans* has linked uridylation of siRNAs with a

Cid1 orthologue, CDE-1, in worms (van Wolfswinkel et al. 2009). CDE-1 shares similarities with *S. pombe* Cid1, Cid11 and, perhaps most clearly, Cid12. Firstly, CDE-1 has RNA uridylation activity *in vitro*. Secondly, loss of function results in meiotic and mitotic defects and thirdly, CDE-1 is required for RNAi-related processes. More importantly, CDE-1 was shown to uridylate and, as a consequence, repress siRNAs generated by the RdRP complex. CDE-1 was proposed to play a role in restricting siRNAs to distinct RNAi pathways, as depletion of CDE-1 leads to disruption of diverse silencing events. These findings may provide a useful framework for further investigations of Cid12 function in *S. pombe*.

I.4. Regulation of mammalian histone mRNAs

In higher eukaryotes, histone mRNAs differ significantly from canonical mRNAs with their characteristic 3' end structure and their tight coordination with DNA synthesis (Marzluff et al. 2008). Histone mRNA expression is highly prominent during S phase when DNA replication takes place and rapidly declines as cells complete S phase and enter G2. Replication-dependent histone mRNAs consequently require a unique set of processing and regulatory factors in order to coordinate histone expression with DNA replication and to meet the needs of chromatin duplication during S phase. In the following section the regulation of replication-dependent histone mRNAs and the regulatory factors relevant to this study will be introduced in more detail.

I.4.1. Organisation of replication-dependent histone genes

The core histones are encoded by a set of replication-dependent genes that have remained clustered together during evolution. These clusters contain multiple copies of genes encoding all four core histones (H2A, H2B, H3 and H4) and also H1. The histones H2A, H2B, H3 and H4 are assembled within nucleosomes while H1 is found between nucleosomes as a linker (Kornberg 1977). The histone variant H2A.X, which is involved in recognition of DNA damage within chromatin (Thiriet and Hayes 2005) is encoded outside the canonical histone gene cluster as are other rare isoforms of histone proteins (Marzluff 2005).

Canonical histone mRNAs have a 7-methyl-guanosine cap at their 5' end. However, they do not contain introns and are the only known metazoan mRNAs that are not polyadenylated. Instead, they share a characteristic and highly conserved stem-loop structure at their 3' end. The stem-loop

sequence is regarded as the main player in histone mRNA processing as well as in the regulation of histone mRNA levels during the cell cycle.

I.4.2. 3' ends of replication-dependent histone mRNAs

The stem-loop sequence of every metazoan histone mRNA consists of six base pairs for the stem and four bases constituting the loop (Figure I.3A). Five nucleotides on both ends adjacent to the stem are also highly conserved and together with the stem-loop form the characteristic structure of 26 nucleotides, which is recognised by the stem-loop binding protein (SLBP) (Wang et al. 1996; Martin et al. 1997). The stem-loop sequence is located no further than 60 nucleotides downstream from the stop codon in all metazoan histone mRNAs (Marzluff et al. 2008). Processing of histone mRNAs requires the stem-loop sequence and a purine-rich sequence element called the histone downstream element. Formation of mature histone 3' ends is initiated by binding of the stem-loop by SLBP (Dominski and Marzluff 2007). Next, the histone downstream element base-pairs with the U7 snRNA, a component of the U7 snRNP with an Sm-binding site that is distinct from the spliceosomal snRNAs (Strub and Birnstiel 1986; Mowry and Steitz 1987). SLBP and the U7 snRNP recruit 3' end cleavage factors common to the canonical cleavage and polyadenylation machinery (Kolev and Steitz 2005). Release of the transcript from its template occurs through cleavage by the conserved endonuclease CPSF-73 (Dominski et al. 2005) at the position ACCCA (Figure I.3A, arrow) following the 3' arm of the stem-loop (Scharl and Steitz 1994).

I.4.3. Translation of replication-dependent histone mRNAs

Once matured, histone mRNAs are efficiently exported to the cytoplasm where they are translated. Though SLBP is not needed for cytoplasmic export of histone mRNAs (Erkmann et al. 2005), SLBP also binds histone mRNAs in the cytoplasm (Whitfield et al. 2004). Similar to the poly(A) tail of canonical mRNAs, the stem-loop sequence of histone mRNAs is required for cap-dependent translation (Gallie et al. 1996). It is thought that SLBP, like

PABP, helps to circularise histone messages through interaction with cap-bound factors and thereby stimulates efficient translation on polyribosomes (Sanchez and Marzluff 2002; Gorgoni et al. 2005).

I.4.4. Degradation of replication-dependent histone mRNAs

Following translation of histone proteins, levels of histone mRNAs rapidly decrease upon completion of DNA replication. In contrast to *S. cerevisiae,* where histone mRNA levels are mainly controlled through the rate of transcription (Osley 1991), mammalian histone mRNA levels are regulated post-transcriptionally. The decrease in histone mRNA levels in mammals occurs as a result of rapid shortening of their half-life by RNA degradation when DNA replication is completed or inhibited (Marzluff and Duronio 2002).

As in histone mRNA processing and translation, the *cis* element mediating the regulation of histone mRNA half-life is the stem-loop sequence and by extension, SLBP (Pandey and Marzluff 1987). Degradation of histone mRNAs also requires active translation; inhibition of translation was found to stabilise histone transcripts (Stimac et al. 1984; Kaygun and Marzluff 2005b). In addition, the position of the stop codon in close proximity to the stem-loop is essential for histone mRNA degradation (Graves et al. 1987; Kaygun and Marzluff 2005b). These findings suggested that histone mRNA degradation occurs on actively translating polyribosomes. In agreement with this hypothesis, it was also shown that Upf1, a protein involved in translation termination and nonsense-mediated decay (Chang et al. 2007) is also needed for histone mRNA degradation. Upf1 was shown to interact directly with SLBP following inhibition of DNA replication and is believed to recruit further RNA turnover components (Kaygun and Marzluff 2005a). First insights into the cytoplasmic degradation mechanism of histone mRNAs were provided by a study of Mullen and Marzluff (2008), which revealed that many factors common to the degradation of polyadenylated messages were also required for histone mRNA degradation despite the absence of a poly(A) tail (Mullen and Marzluff 2008). These factors include: Lsm1, the decapping component

Dcp2, the cytoplasmic 5'-3' exonuclease Xrn1, the exosome component Rrp41 and intriguingly, the 3'-5' exonuclease PM/Scl-100 (also called hRrp6) that is strongly enriched in nucleoli, although small amounts of hRrp6 can be found in the cytoplasm (Tomecki et al. 2010). Analysis of decay intermediates showed that degradation of histone mRNAs most likely occurred from both 3' and 5' ends, which is in agreement with the requirement of both exonucleolytic components (Mullen and Marzluff 2008). This analysis also revealed the presence of oligouridine tails at the 3' end following inhibition or completion of DNA replication. It is thought that this modification represents the first step in initiating rapid histone mRNA decay by recruiting Lsm1 and by extension the Lsm1-7 complex to the newly added uridine tail. The Lsm1-7 complex then stimulates decapping and degradation as described in Chapter I.2. Notably, the uridylation- and Lsm1-mediated mechanism of cytoplasmic mRNA degradation has recently also been described for polyadenylated messages in fission yeast in our laboratory (Rissland and Norbury 2009).

I.4.5. Cell cycle regulation of replication-dependent histone mRNAs

Replication-dependent histone mRNAs are among the most regulated RNAs during the cell cycle (Figure I.3B), as their synthesis is highly induced in S phase when DNA replication takes place. During S phase, histone mRNA levels increase 15- to 30-fold in mammalian cells and rapidly decline when DNA replication is completed (Osley 1991). It is thought that post-transcriptional regulation of mammalian histone mRNAs accounts for most of the control of their RNA levels (Marzluff 2005). Major determinants of the post-transcriptional regulation of histone mRNAs are the stem-loop and its binding partner, SLBP (Lüscher et al. 1985; Harris et al. 1991). SLBP, whose levels are stoichiometrically equivalent to histone mRNA levels as each mature histone mRNA has one SLBP bound to its stem-loop during its life cycle, is itself cell cycle-regulated (Zheng et al. 2003). SLBP protein is synthesised when cells enter S phase and rapidly degraded at the end of S phase upon phosphorylation of the protein, thereby paralleling the

expression of histone mRNA levels. As a result, the SLBP protein represents a major determinant in the control of histone mRNAs. In contrast to histone mRNA levels however, SLBP is not coupled to active DNA replication, as SLBP protein levels remain elevated during S phase even when DNA replication is inhibited (Whitfield et al. 2004). Similarly, stabilisation of SLBP at the end of S phase does not prevent histone mRNA degradation (Zheng et al. 2003), implicating a higher complexity in regulating histone mRNA half-life during S phase.

Besides SLBP, other factors are known to be important for the regulation of histone mRNA levels, particularly at the transcriptional level. These include the U7 snRNP, which is involved in histone mRNA processing as mentioned above, and which is thought to be essential for the progression of cells from G1 to S phase (Wagner and Marzluff 2006). Synthesis of histone mRNAs at the beginning of S phase also requires activation of cyclin E-CDK2 (cyclin-dependent kinase 2) and phosphorylation of the nuclear protein NPAT, thereby stimulating histone gene transcription (Ma et al. 2000; Zhao et al. 2000). Phosphorylation of SLBP at the S/G2 transition is dependent on cyclin A-CDK1 (Koseoglu et al. 2008). This event triggers SLBP degradation along with histone mRNA decline and completes the life cycle of histone mRNAs.

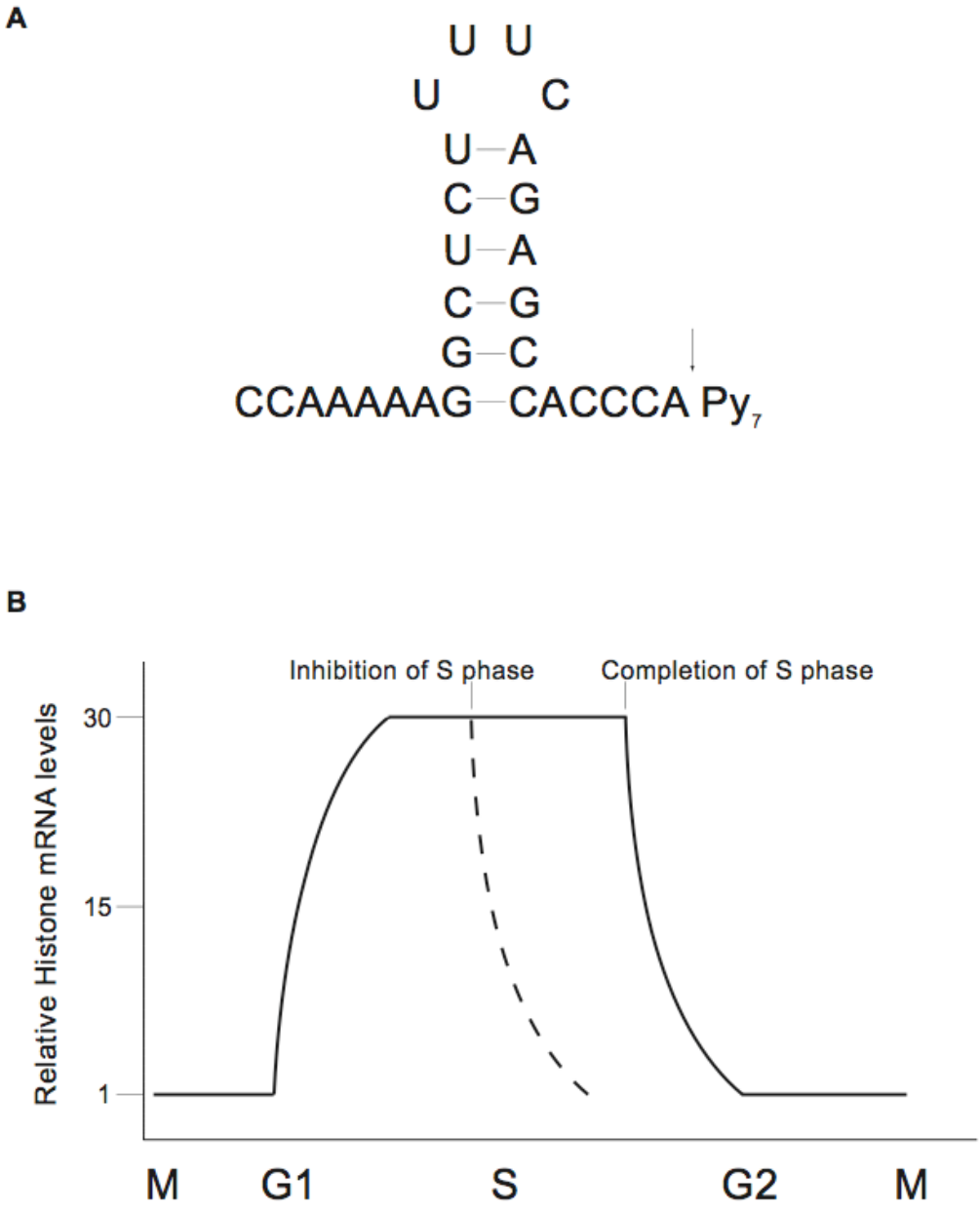

Figure I.3 Characteristics of mammalian replication-dependent histone mRNAs

(A) The sequence of the conserved stem-loop at the 3' end of histone mRNAs is depicted. The arrow indicates the position of cleavage and the mature 3' end. (B) Relative changes in histone mRNA levels during the cell cycle are shown. Levels increase rapidly when cells enter S phase and decline upon completion or inhibition (dotted line) of S phase.

I.5. The DNA integrity checkpoint

All DNA must be replicated faithfully in S phase and segregated properly during mitosis to ensure genome integrity. As cells encounter multiple events that can damage genomes during these processes, checkpoint mechanisms have evolved to prevent potentially harmful consequences of genome instability. These mechanisms have the ability to halt the progression of the cell cycle and to activate DNA repair mechanisms. Once the DNA damage is repaired, cells can resume progression through the cell cycle. If the damage is irreparable, multi-cellular organisms have the ability to permanently arrest the cell cycle or stimulate apoptosis in the affected cell. In contrast, unicellular organisms such as yeast depend on cell survival and re-activate cell cycle progression despite the risks of defective DNA content.

This section deals with the cellular response to genomic damage and how the cell cycle is affected as a consequence. The mammalian system will be emphasised in the following; information about the fission yeast system will be included when relevant.

I.5.1. Causes of DNA damage

Genome instability can be caused at various stages of the cell cycle by multiple events that activate a wide range of repair mechanisms (Zhou and Elledge 2000; Hoeijmakers 2001; Nyberg et al. 2002). Very common forms of DNA damage that result from spontaneous hydrolysis and oxidation or from environmental factors such as ultraviolet radiation include depurination, deamination, alkylation and formation of pyrimidine dimers. These defects affect only one DNA strand and can usually be repaired by base excision or nucleotide excision repair, mechanisms which remove and replace the damaged nucleotide.

More severe DNA damage affects both DNA strands, such as double strand breaks (DSBs) that have the potential to fragment chromosomes. DSBs are caused by ionising radiation or exposure to chemicals such as bleomycin. The default repair mechanism for DSBs in mammalian cells is non-homologous end joining, which simply ligates both broken ends together. Alternatively and more accurately, the damage can be repaired by homologous recombination between the broken chromatid and a homologous sequence in a sister chromatid or, much more rarely, a homologous chromosome.

Other events triggering checkpoint activation include aberrant replication forks during DNA replication in S phase (Branzei and Foiani 2005). These occur, for example, when dNTP pools are depleted by the ribonucleotide reductase inhibitor HU, or when forks encounter physical obstacles during DNA replication. Slowed or stalled replication forks elicit checkpoint responses such as a block to mitotic entry or the inhibition of further initiation of DNA synthesis. Mechanisms are in place to stabilise replication forks while DNA repair takes place so that stalled forks can resume DNA replication following the repair.

The pathways causing genome instability may appear very distinct. However, the responses and cell cycle-related actions to DNA damage and replication stress share many common components. The major elements involved in checkpoint activation are summarised in Figure I.4 and will be introduced in more detail in the following section.

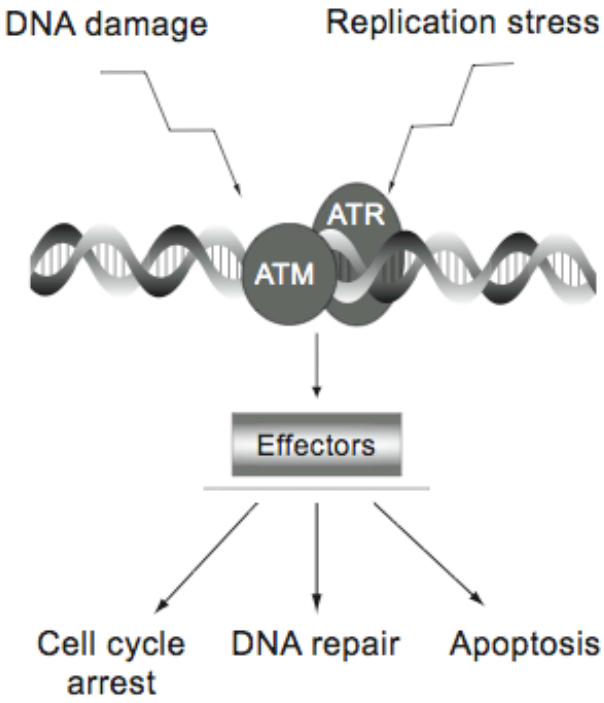

Figure I.4 Signal transduction during the DNA integrity response

Upon DNA damage or replication stress, the PIKKs ATM / ATR activate down-stream effectors, which in turn trigger cell cycle arrest, DNA repair and in metazoans, apoptosis. See text for more detail.

I.5.2. The DNA integrity response

I.5.2.1. Initiation of the response

Central players acting in response to DNA damage are a pair of conserved protein kinases called ATM (ataxia telangiectasia mutated) and ATR (ATM and Rad3 related) in mammalian cells and Tel1 and Rad3 in *S. pombe*. They belong to the family of phosphoinositide 3-kinase-related kinases (PIKK) whose various substrates mediate the response to DNA checkpoint activation. In vertebrates, a model is emerging that both proteins in parallel are important for the DNA damage response and checkpoint activation, with ATM mainly responding to DNA damage such as DSBs and ATR to replication stress (Zhou and Elledge 2000). In contrast, Rad3 in *S. pombe* is required for the activation of the replication checkpoint as well as the DNA damage response. Upon detection of DNA damage by sensors such as the MRN complex (Mre11–Rad50–Nbs1) and ATRIP (ATR-interacting protein), ATM and ATR are recruited to sites of DNA damage and are activated by auto-phosphorylation. ATM and ATR possess serine/threonine kinase activity and once activated, trigger a cascade of signals that ultimately lead to cell cycle arrest, DNA repair and potentially cell death (Bartek and Lukas 2007).

Investigations of ATM / ATR substrates responding to DNA damage have been performed on a proteome-wide scale in yeast and human cells using immunoprecipitation with phospho-specific antibodies for ATM/ATR consensus sites combined with MS (Matsuoka et al. 2007; Smolka et al. 2007). Numerous candidates identified in this way are proteins involved in RNA processing, amongst them the uridyl transferase ZCCHC11 studied here in great detail. Although most of these results were not validated by other experimental means, they suggested a wider network responding to the activation of the DNA integrity checkpoint than originally anticipated.

I.5.2.2. Effecting the response

Major effectors in the checkpoint response are two kinases, Chk1 and Chk2 (Chk1 and Cds1 in fission yeast) that transmit signals initiated by ATM and ATR. Chk1 and Chk2 are serine/threonine kinases that share overlapping substrates despite being structurally unrelated (Zhou and Elledge 2000). By phosphorylating numerous downstream targets, together with other effectors they activate DNA repair and recombination mechanisms and inhibit cell cycle progression. Chk1 is thought to be present in S phase and G2, whereas Chk2 is a stable protein detectable throughout the cell cycle (Lukas et al. 2001). Originally, a strict concept divided the two kinases into two pathways (Bartek and Lukas 2003): ATM phosphorylates Chk2 in response to DSBs, thereby triggering DNA repair whilst ATR activates Chk1 in response to replication stress and as a result promotes cell cycle arrest. This concept has been refined as numerous studies observed overlapping functions of ATM, ATR, Chk1 and Chk2 in effecting responses to various types of genotoxic stress. For example, Chk1 was also found to be phosphorylated by ATM upon ionising radiation (Gatei et al. 2003).

Chk1 and Chk2 are recruited to DNA damage sites by adaptor or mediator proteins, which in turn interact with modified chromatin upon DNA damage. A well-studied example is the variant form of H2A, H2A.X that is phosphorylated by ATM in response to DSBs in foci surrounding the DNA damage. This modification (γ-H2A.X) provides new binding sites for additional DNA damage mediators and DSBs-specific DNA repair components (Stucki et al. 2005). Furthermore, H2A.X was also found to be phosphorylated by ATR upon replication stress triggered for example by HU (Ward and Chen 2001). Although not essential, γ-H2A.X substantially contributes to the durable propagation of the DNA checkpoint response (Celeste et al. 2003).

I.5.3. DNA checkpoints in the cell cycle

The major role of DNA checkpoints is to halt cell cycle progression while DNA repair occurs, in order to prevent replication of aberrant DNA and to avoid the propagation of genomic damage (Weinert and Hartwell 1988). Consequently, loss of checkpoint control leads to DNA rearrangements and chromosome loss (Hartwell and Kastan 1994). Equally important is the relief of the cell cycle blockade once DNA damage is repaired, so that cells can resume proliferation. In the following section, the different checkpoints during the cycle will be explained.

I.5.3.1. G1 checkpoint

Higher eukaryotes possess a robust G1 checkpoint that ensures fidelity of the DNA template prior to DNA replication (Nyberg et al. 2002; Sancar et al. 2004). This checkpoint results in a pronounced delay of S phase entry when activated. Initiation of the arrest involves ATM-dependent phosphorylation of the kinase Chk2 leading to inactivation of the phosphatase Cdc25A and inhibition of CDK activity, the essential component driving S phase entry. Maintenance of the arrest requires phosphorylation of the tumour suppressor p53, ultimately also resulting in inhibition of CDK activity. Long-term p53 activation may lead to apoptosis in many cell types. The precise mechanism of recovery from G1 arrest as well as the various responses to p53 are still poorly understood (Yee and Vousden 2005).

I.5.3.2. S phase checkpoint

The S phase checkpoint can be divided into three categories (Bartek and Lukas 2007). Firstly, the DNA replication checkpoint becomes activated when replication forks are stalled either by nucleotide depletion, polymerase inhibition or encounter of DNA damage. Secondly, the intra-S phase checkpoint senses DSBs independently of active replication. Both of these

checkpoints result in inhibition of further DNA synthesis by blocking origin firing. Thirdly, the S-M checkpoint ensures complete and faithful duplication of chromosomes prior to mitosis. When activated, it also prevents entry into mitosis. Although the three pathways appear distinct, they are closely coordinated and share common components previously introduced in section I.5.2.

Blockage of origin firing depends on inactivation of Cdc25A and CDK activity, similarly to the response in G1. It is thought that these signals are mediated by ATM-Chk2 in the case of DSBs and ATR-Chk1 when replication forks are stalled, although crosstalk between both pathways does occur as mentioned above. Besides Chk2, several additional ATM substrates are important for the intra-S phase checkpoint including a component of cohesin, which is involved in sister chromatid cohesion, and hence homologous recombinational repair (Kim et al. 2002; Yazdi et al. 2002). Furthermore, ATM-mediated phosphorylation of H2A.X during S phase can spread over megabase lengths surrounding the DNA lesion (Rogakou et al. 1999), thereby providing the basis for assembly of DNA repair components. In order to preserve genome integrity throughout generations, the S-M checkpoint blocks entry into mitosis upon DNA damage. There is also increasing evidence that mitosis is blocked by the S-M checkpoint in unperturbed cells while DNA replication is ongoing (Sorensen et al. 2004). The molecular mechanism is similar to the G2/M checkpoint and is therefore discussed below.

I.5.3.3. G2/M checkpoint

Much of the current knowledge regarding the G2/M checkpoint stems from studies in yeast, particularly fission yeast. However, this checkpoint is conserved in eukaryotes and both lower and higher eukaryotes share a common mechanism that depends on the phosphorylation state of CDK1 to block mitotic entry (Nyberg et al. 2002). Upon DNA damage in S phase or in G2, the cell cycle is arrested until the damage is repaired to ensure genome

integrity during cell division. Similar to the other checkpoints discussed above, the central players in the G2/M checkpoint activation are ATM and ATR and their downstream effectors Chk1 and Chk2. The primary function of the G2/M checkpoint is the inhibition of the mitosis-promoting protein kinase cyclin B-CDK1. In brief, CDK1 activity is inhibited by phosphorylation by the mitosis-inhibiting kinase Wee1 during S phase (Murakami and Nurse 2000). As cyclin B levels rise towards the onset of mitosis, cyclin B-CDK1 complexes are activated by Cdc25-mediated de-phosphorylation, thereby triggering entry into mitosis. This entry can be blocked by Chk1/Chk2-mediated phosphorylation of Cdc25 and as a consequence inactivation of the protein (Bartek and Lukas 2007). Importantly, phosphorylated Cdc25 is bound by a 14-3-3 protein (Rad24 in *S. pombe*), and sequestered in the cytoplasm, thus preventing activation of CDK1 in the nucleus. In addition, Chk1/Chk2-mediated up-regulation of Wee1 also contributes to blocking mitotic entry. Recovery from the G2/M checkpoint and resumption of the cell cycle is still poorly understood. Nevertheless, several mechanisms have been suggested to play a role in checkpoint recovery including de-phosphorylation of Chk1 and ubiquitin-mediated proteolysis of Chk1 co-factors (Calonge and O'Connell 2008).

I.6. Aims of the thesis

This thesis is concerned with a novel RNA turnover mechanism that involves uridylation of cytoplasmic RNAs. In particular, it investigates how RNAs that have fulfilled their function are targeted for degradation and how cells deal with failure of this mechanism. Central to this thesis are the uridyl transferases, Cid1 in fission yeast and ZCCHC11 in mammalian cells, that modify RNAs prior to their degradation. Investigations were carried out in both *S. pombe* and human cell systems in order to gain knowledge about the generality and evolutionary conservation of cytoplasmic RNA degradation mechanisms. With this in mind, this thesis aims at identifying:

- Accessory factors in fission yeast involved in cytoplasmic RNA decay
- The enzyme responsible for histone mRNA uridylation in human cells
- The nature of the phenotype associated with defects in uridylation-dependent RNA decay

In brief, Chapter III studies the biochemistry of the protein complex containing the uridyl transferase Cid1 using the *S. pombe* model system. Chapter IV investigates human ZCCHC11 and identifies a role for this enzyme in the destruction of replication-dependent histone mRNAs. Finally, Chapter V explores the consequences of depleting ZCCHC11 in human cells with respect to the cell cycle. Taken together, the results presented in this thesis extend our understanding of uridylation-mediated RNA degradation in both systems and, importantly, reveal the necessity of efficient mRNA decay for cellular function.

CHAPTER II. MATERIALS AND METHODS

II.1. General methods

II.1.1. DNA methods

II.1.1.1. Determination of DNA concentration

The concentration of DNA preparations was determined by measuring the absorbance at 260nm using an Eppendorf Biophotometer. An A_{260} of 1.0 was taken to be the equivalent of 50μg/ml dsDNA. Pure DNA had an OD_{260}/OD_{280} ratio of 1.8.

II.1.1.2. PCR using a DNA template

PCR reactions comprised when not otherwise stated: 100ng DNA template, 0.5mM dNTPs (Bioline), 0.5 units Simple Red Taq polymerase (Fisher Scientific), 1x Taq buffer, 0.5μM of each oligonucleotide (synthesised by Sigma Aldrich) and made up to 50μl with dH_2O. Reactions were thermally cycled in a Veriti® Thermal Cycler (Applied Biosystems) as follows: 95°C for 2 min, followed by 25 cycles of {94°C for 30 sec, annealing temperature for 30 sec, 72°C for 30 sec per kb} and a final 7 min hold at 72°C, before chilling to 4°C. The annealing temperature (T_m) varied depending on the GC/AT ratio of the oligonucleotides and was calculated using the equation: $T_m=4(G+C)+2(A+T)°C$.

II.1.1.3. Agarose Gel Electrophoresis

Samples were supplemented with 0.2 volumes of 6x DNA loading dye prior to loading on 1-2% agarose gels prepared with 1 x TBE buffer and containing 0.5μg/ml ethidium bromide (Sigma). Electrophoresis was carried out at 2-10V/cm^2 in 1 x TBE running buffer. 2.5μl of a size marker (Hyperladder™ I or IV, Bioline) was run alongside. DNA was visualised using a UV transilluminator (UVP).

1 x TBE
10mM Tris, 10mM H_3BO_3, 2mM EDTA pH8.0

6 x DNA loading buffer
30% sucrose, 100mM EDTA pH8.0, 0.01 % bromophenol blue

II.1.1.4. Restriction Enzyme Digestion

Digests comprised in a 20μl reaction: 0.2 - 1μg DNA, 1x restriction buffer, 5 units of restriction enzyme and 100μg/ml of bovine serum albumin (BSA) if necessary. Reactions were incubated at the optimum temperature (usually 37°C) for 1-2 hours and digestion was verified by agarose gel electrophoresis.

II.1.1.5. Ethanol precipitation

To concentrate nucleic acids, 2.5 volumes of 100% ethanol and 0.1 volumes of 2M sodium acetate pH 5.2 were added, mixed and incubated at -20°C for 1 hour. Samples were centrifuged (16000 x *g*, 10 min, room temperature), washed carefully in 150μl 70% ethanol, air-dried and re-suspended in dH_2O.

II.1.1.6. Phenol extraction

To remove protein and lipid contaminants, an equal volume of phenol:chloroform:isoamylalcohol (25:24:1) was added to nucleic acid solutions and mixed by vortexing for 20 sec. Samples were centrifuged

(16000 x *g*, 5 min, room temperature) and the aqueous layer removed to a fresh tube.

II.1.1.7. DNA sequencing

Dideoxy-DNA sequencing was carried out using the BigDye™ Terminator Cycle Sequencing Kit (Department of Zoology, Oxford). 1μl BigDye reagent was mixed with 50-200ng DNA template, 3.2pmol oligonucleotide primer, 1.5μl 5x buffer and made up to 10μl with dH_2O. Reactions were thermally cycled in a Veriti® Thermal Cycler (Applied Biosystems) as follows: 96°C for 4 min, followed by 25 cycles of {96°C for 30 sec, 50°C for 10 sec, 60°C for 4 min}. Samples were ethanol precipitated and DNA pellets stored at 4°C prior to analysis using a 3730*xl* DNA Analyzer (Applied Biosystems) carried out by the Geneservice (Source BioScience). The resulting DNA was analysed using ApE Universal software.

II.1.1.8. Gel extraction

DNA was purified from agarose gel slices using the filter from a 1ml filter tip (Anachem). The gel slice was transferred onto the filter, placed in an Eppendorf tube and spun (16000 x *g*, 10sec). The filter was discarded and the resulting DNA in the liquid was subsequently ethanol precipitated and re-suspended in 10-20μl dH_2O.

II.1.1.9. TA Ligation

If needed, 3' deoxy-adenosine overhangs were added to gel-purified PCR products by incubating the DNA with 0.1mM dATP, 0.1 units Taq polymerase and 1x Taq buffer for 10 min at 72°C. The DNA was subsequently ligated in a 10μl reaction containing 10 units of T4 DNA ligase (Roche), 1x ligase buffer and 12ng linearised pCR 2.1® vector with 3' deoxy-thymidine overhangs (Invitrogen). Reactions were incubated at 18°C overnight and transformed into bacteria, as described (II.1.2.3).

II.1.2. Bacterial methods

XL1-Blue chemically competent *E. coli* (*recA1 endA1 gyrA96 thi-1 hsdR17 supE44 relA1 lac [F´ proAB lacI^{q}ZΔM15 Tn^{10} (TetR)]*) was used to amplify plasmid DNA. BL21(DE3)pLysS (*F$^-$ ompT gal dcm lon hsdS$_B$(r$_B^-$ m$_B^-$) λ(DE3) pLysS(cm^R)*) chemically competent *E. coli* was used for recombinant protein expression. Both strains were grown in LB (Luria Bertani) medium. The medium of BL21 cells was supplemented with 34μg/ml chloramphenicol for maintenance of the pLysS plasmid.

II.1.2.1. Competent cell preparation of XL1-Blue

200μl of an overnight LB culture was diluted into 50ml of fresh SOB and incubated at 37°C for 2-2.5 hours. At OD_{600} of 0.3-0.5, the culture was cooled on ice for 30 min and harvested by centrifugation (3000 x g, 10min, 4°C). The cell pellet was re-suspended in 5ml cold TSB and incubated on ice for 10 min. Aliquots of 100μl were dispensed, snap-frozen in liquid nitrogen and stored at -80°C.

SOB
2% Bactotryptone, 0.5% Yeast extract, 10 mM NaCl. 2.5 mM KCl, 10 mM $MgCl_2$, autoclaved

TSB
10% PEG (6000), 5% DMSO, 20 mM $MgCl_2$, in LB

II.1.2.2. Competent cell preparation of BL21(DE3)pLysS

An overnight culture was diluted 1:100 in LB + chloramphenicol. 45ml of the cells were harvested at OD_{600} of 0.4-0.6 by centrifugation (3000 x *g*, 15 min, 4°C). The pelleted cells were re-suspended in 20ml of cold 50mM $CaCl_2$ and incubated on ice for 30 min. Cells were centrifuged as above and re-suspended in 5ml ice-cold $CaCl_2$. Following incubation on ice of at least 30 min, cells were ready for transformation.

II.1.2.3. Transformation of E. coli

The DNA ligation was mixed with 20µl of 5 x KCM and dH_2O to a final volume of 100µl and cooled down on ice. When plasmids were transformed without prior ligation, the addition of 5x KCM was omitted. The DNA was incubated with 100µl of competent cells on ice for 20-30 min prior to heat-shock (42°C, 45sec) and quick chill on ice. 700µL of LB was added and cells were incubated at 37°C shaking for one hour. Cells were centrifuged (3000 x *g*, 1 min, room temperature), re-suspended in 200µl LB, plated on LB-agar containing selective antibiotic and incubated overnight at 37°C.

5 x KCM
0.5 M KCl, 0.15 M $CaCl_2$, 0.25 M $MgCl_2$, filter-sterilised

II.1.2.4. Purification of plasmid DNA

Large-scale preparations of pure plasmid DNA were carried out using a Plasmid Maxi kit (Qiagen) according to the manufacturer's instructions. Small-scale plasmid preparations were carried out similarly to the Plasmid Mini kit (Qiagen). However, instead of using silica-gel columns, the DNA was recovered by ethanol precipitation.

II.1.3. Cloning

II.1.3.1. Site-directed mutagenesis

Point mutations were obtained by site-directed mutagenesis following the instruction manual of QuickChange® XL Site-Directed Mutagenesis Kit (Stratagene). In brief, a PCR reaction was performed using 125 ng of complementary oligos spanning the mutation site (30-40 base pairs in length), 10ng of template vector DNA and 5 units of PfuTurbo® DNA polymerase (Stratagene), whereby half of the polymerase was added in the beginning and the second half after 9 PCR cycles. Thermal cycling conditions were as follows: 95°C for 1min, 18 cycles of {95°C for 50 sec,

60°C for 50 sec, 68°C for 1 min / kb of plasmid length} and a 7 min hold at 68°C. Following the PCR reaction, the non-mutated parental DNA was digested by adding 10 units of the restriction enzyme *Dpn*I (New England Biolabs) to the reaction and incubating at 37°C for 1 hour. Samples were transformed into *E.coli* as described (II.1.2.3). A control reaction lacking the DNA polymerase was performed in parallel.

II.1.3.2. GeneClip™ U1 Hairpin Cloning Systems

To create plasmid constructs for gene silencing in mammalian cells, the GeneClip™ U1 Hairpin Cloning System (Promega) was used. Complementary oligonucleotides containing the desired siRNA hairpin target sequence were designed using the online Promega siRNA designer (www.promega.com/siRNADesigner/). Complementary hairpin primers were annealed and ligated into the linearised pGeneClip™ Vector following the manufacturer's instructions. The vectors containing the insert were transformed into *E.coli* as described (II.1.2.3). Clones were screened by *Pst*I enzymatic digestion (II.1.1.4), with the desired ligation products resulting in two specific DNA fragments of 3.2 and 1.4kb in length.

II.1.4. Protein methods

II.1.4.1. Denaturing protein gel electrophoresis (SDS-PAGE)

Protein samples were mixed with appropriate amounts of 4x sample buffer and heated (98°C, 5 min) prior to loading onto mini 6-12% SDS-PAGE gels (with 6% stacking gel) along with 5 μl of protein marker (ColorPlus Prestained Protein Ladder, New England Biolabs). Gels were run at 80V through the stacking gel and at 150V through the separating gel using 1x SDS running buffer.

4x Sample buffer
200mM Tris-Cl pH6.8, 40% glycerol, 8% SDS, 4% β-mercapto ethanol, 0.02% bromophenol blue

Separating gel
375mM Tris-CL pH 8.8, 0.1% SDS, 6-15% acrylamide:bisacrylamide (37.5:1, Fisher Scientific), 0.03% APS, 0.2% TEMED

Stacking gel
125mM Tris-CL pH 6.8, 0.1% SDS, 6% acrylamide:bisacrylamide (37.5:1, Fisher Scientific), 0.03% APS, 0.2% TEMED

SDS running buffer
25mM Tris pH8.3, 0.1% SDS, 190mM glycine

II.1.4.2. Total protein staining

SDS-PAGE gels were stained with Coomassie staining solution and destained using destaining solution. For increased sensitivity, gels were washed in dH_2O three times 5 min and incubated for 1 hour in Sypro Ruby (BioRad), a fluorescent dye visualised at 532nm using a FLA5000 scanner (Fuji).

Coomassie staining solution
50% ethanol, 10% acetic acid, 0.1% coomassie brilliant blue

Destaining solution
10% ethanol, 10% acetic acid

II.1.4.3. Western blotting

Following SDS-PAGE, gel, Hybond™ nitrocellulose membrane (Amersham) and 3MM Whatman paper were briefly soaked in transfer buffer. Proteins were transferred to the membrane using a semi-dry blotter (BioRad) according to the manufacturer's instructions (constant voltage of 10V for 40 min). Membranes were blocked in 1x TBS-T containing 5% dry milk for 1-2 hours and incubated with primary antibody, diluted in the blocking solution according to Table II.1 below at 4°C. Then the membrane was washed 3-4 times with 1x TBS-T followed by incubation with the secondary HRP-conjugated antibody diluted in blocking solution at room temperature. The membrane was again washed 3-4 times before performing the ECL reaction. Equal volumes of ECL solutions A and B (Santa Cruz) were added to the

membrane for 1 min, excess liquid was drained and chemoluminescence was detected by exposure to X-ray films RX-NIF (Fujifilm). Antibodies used in this study are given in Table II.1below.

1x TSB-T
50mM Tris pH7.4, 150mMNaCl, 0.05% Tween

Western transfer buffer
48mM Tris pH8.3, 39mM glycine, 1.3mM SDS, 10% methanol

Name	Type	Dilution	Incubation	Source
α-ZCCHC11 (CN91)	Rabbit polyclonal	1:1000	Overnight	Lab stock
α-ZCCHC6 (CN90)	Rabbit polyclonal	1:1000	Overnight	Lab stock
α-Chk1	Mouse monoclonal	1:2000	Overnight	Sigma
α-phChk1	Rabbit monoclonal	1:500	Overnight	Bethyl
α-Cid1 (CN43)	Rabbit polyclonal	1:500	Overnight	Lab stock
α-Tubulin (TAT-1)	Mouse monoclonal	1:5000	30-60 min	Keith Gull
α-HA-HRP	Mouse monoclonal	1:2000	30-60 min	Roche
α-mouse-HRP	Goat polyclonal	1:2000	30-60 min	Sigma
α-rabbit-HRP	Goat polyclonal	1:2000	30-60 min	Sigma
α-TOP2a	Rabbit polyclonal	1:2000	2 hours	Ian Hickson

Table II.1 Antibodies used for western blot in this study

II.1.4.4. Induction of recombinant antigens in E. coli

An overnight culture of BL21(DE3)pLysS cells transformed with pGEX6P was diluted 1:100 into 200ml LB + ampicillin (without chloramphenicol) and incubated at 37°C. When the culture reached an A_{600} of 0.5, protein expression was induced by the addition of Isopropyl β-D-1-thiogalactopyranoside to the medium to a final concentration of 100μM. Bacteria were grown for additional 3 hours at 37°C and harvested by centrifugation (4000 x *g*, 15min, 4°C).

II.1.4.5. GST purification of recombinant antigens

Harvested cells were washed once in cold PBS prior to re-suspension in 2ml BugBuster (Novagen) supplemented with 2μl Benzonase (Novagen) per 50ml

bacterial culture. Cells were lysed for 15 min rotating at 4°C. The lysate was clarified by centrifugation (16000 x *g*, 25 min, 4°C) and the supernatant incubated with 40µl packed glutathione-sepharose (pre-equilibrated in PBS, Amersham) for 1 hour, rocking at 4°C. Beads were washed four times for 10 min in 1ml cold HBS prior to elution of the recombinant protein. Beads were incubated in 100µl elution buffer for 10 min six times. The elution fractions were snap-frozen in liquid nitrogen and analysed on a 10% SDS-PAGE.

PBS
0.14mM NaCl, 3.4µM KCl, 10µM Na_2HPO_4, 1.8µM KH_2HPO

HBS
40mM HEPES pH 7.0, 200 mM NaCl

Elution buffer
20mM Tris pH8.0, 150mM NaCl, 10% glycerol, 25mM glutathione

II.1.4.6. Affinity purification of antibodies by western blot

Combined elutions from the GST purification containing the recombinant antigen were diluted in sample buffer to a final volume of 1ml and run on a large 10% SDS-PAGE gel (Protean II) for 4-5 hours. A vertical strip of the gel was stained with Coomassie to localise the antigen. The gel area containing the recombinant antigen was excised and transferred to an Immobilon-P PVDF membrane (Fisher Scientific) as described (Chapter I.1.4.3.), but the membrane was soaked in 100% methanol prior to soaking in transfer buffer. Following transfer at constant 0.04 mA for 2 hours, the membrane was blocked for 2 hours in 5% milk PBS-T. 2ml of crude serum were diluted 1:1 in milk PBS-T and incubated with the membrane overnight, rotating at 4°C. The membrane was subsequently washed 3 times in TBS-T for 10 min. The antibody was eluted by addition of 1ml of 0.1M glycine pH 5.2 to the membrane for 5 min at 4°C. The solution was subsequently neutralised with 120ml of 1M Tris-HCl pH 8.0. The concentration of the antibody was determined by comparison to different concentrations of BSA on 10% SDS-PAGE. The antibody was stored at 4°C.

II.2. Fission yeast

II.2.1. Growth and maintenance of *S. pombe*

All *S. pombe* strains were grown at 30°C in liquid cultures in YE5S medium or supplemented Edinburgh Minimal Medium (EMM2) and maintained on YE5S agar or minimal agar with the appropriate supplement. Strains were stored at -80°C in YE5S medium containing 25% glycerol. Strains used in this study are shown in Table II.2 below and medium recipes are given in Appendix D.

Strain	Genotype	Source
wildtype	*h⁻ leu1-32*	Lab stock
cid1-TAP	*h⁻ cid1-TAP::kanMX6 leu1-32*	S.W. Wang
cid1-myc	*h⁻ cid1-myc::kanMX6 leu1-32 ura4-D18 ade6*	This study
cid1-HA	*h⁻ cid1-HA::kanMX6 leu1-32 ura4-D18*	S.W. Wang
mlo3-myc	*h⁻ mlo3-myc::kanMX6 leu1-32 ura4-D18 ade6*	This study
mlo3-myc cid1-HA	*h⁻ cid1-HA::kanMX6 mlo3-myc::kanMX6 leu1-32 ura4-D18 ade6*	This study
hyd1-HA	*h⁻ hyd1-HA::kanMX6 leu1-32 ura4-D18 ade6*	A. Stevenson
hyd1-HA cid1-myc	*h⁻ hyd1-HA::kanMX6 cid1-myc::kanMX leu1-32 ura4-D18 ade6*	This study
scp160-HA	*h⁻ scp160-HA::kanMX6 leu1-32 ura4-D18 ade6*	A. Stevenson
scp160-HA cid1-GFP	*h⁻ scp160-HA::kanMX6 cid1-GFP::kanMX6 leu1-32 ura4-D18 ade6*	A. Stevenson
pab1-HA	*h⁺ pab1-H::kanMX leu1-32, ura4D-18, ade6*	A. Stevenson
cid1-myc pabp1-HA	*h⁻ cid1-myc::kanMX6 pab1-H::kanMX leu1-32 ura4-D18 ade6*	This study
cid1Δ	*h⁻ cid1-myc::ura4⁺ leu1-32 ura4-D18*	Wang et al. 2000

Table II.2 *S. pombe* strains used in this study

II.2.2. Strain crosses and random spore analysis

Strains of opposite mating types were crossed by mixing cells on ME4S agar inducing starvation-dependent conjugation after 2 days at 25°C. The mixed cells were treated with 2% glusulase (30°C, 1 hour) to digest cell walls and

release ascospores. Progeny of the required genotype were obtained by plating onto selective agar plates.

II.2.3. Gene tagging in *S. pombe* using homologous recombination

II.2.3.1. PCR amplification of fragments for transformation

The tagged strains Cid1-myc and Mlo3-myc were obtained following the one-step targeted recombination method as described by (Bähler et al. 1998) with small modifications. Fragments were amplified in one PCR reaction using long oligos (Appendix C), the plasmid pFA6A-13Myc-kanMX6 as a template and Expand High Fidelity polymerase (Roche). The PCR product was gel-purified as described (II.1.1.8) and served as a template for additional 10 PCR reactions. PCR reactions were pooled, the DNA extracted with an equal volume of phenol / chloroform / isoamyl alcohol (25:24:1, Sigma) and precipitated with ethanol. The washed and re-suspended DNA was directly used in subsequent yeast transformation steps.

II.2.3.2. Transformation by the lithium acetate procedure

1 x 10^9 cells grown to mid-exponential phase were harvested by centrifugation (4000 x *g*, 3 min, room temperature), washed twice with dH_2O, once with 1ml LiAc /TE and re-suspended in 500μl LiAc/TE. For each transformation, 100μl cells were incubated with 100ng transforming DNA plasmid or concentrated PCR products and 20μg of herring sperm carrier DNA for 10 min at room temperature. 260μl LiAc/TE containing 50% of PEG_{4000} was added to each reaction, mixed gently and incubated at 30°C for 1 hour. 43μl DMSO was added prior to heat-shock (5min, 42°C). Cells were harvested by centrifugation (2000 x g, 2 min, room temperature), washed once in dH_2O and re-suspended in 500μl dH_2O. 50-500μl cells were plated onto selective agar and incubated at 30°C for 3-5 days. Successful transformants were identified by colony PCR and western blot following TCA extraction.

LiAc/TE
10mM LiAc, 10mM Tris pH 7.5, 1mM EDTA

II.2.3.3. Colony PCR from yeast cells

A single colony from *S. pombe* was re-suspended in 20μl dH_2O, vortexed and boiled at 95°C for 5 min. 1-5μl of this suspension served as a template in a standard 50μl PCR reaction using Taq polymerase and 35 cycles as described (II.1.1.2).

II.2.4. Overexpression using the *nmt1* promoter

Proteins were overexpressed in *S. pombe leu1-32* strain using the pREPNTAP vector, which drives expression from the thiamine-repressible *nmt1* promoter. Plasmids were transformed into *S. pombe* as described (II.2.3.2) and selected using the *LEU2* marker by plating onto minimal agar without leucine. Expression was repressed by adding 30μM thiamine to the medium. For subsequent *in vitro* activity assays (see below), protein expression was fully induced by removing thiamine from overnight liquid pre-cultures by washing the cells four times in water. Full induction was achieved after a further 18 hours growth in liquid culture without thiamine. For protein identification experiments by MS, *nmt1*-driven expression was reduced by the addition of 0.1μM thiamine to the medium.

II.2.5. Denatured protein extraction (TCA extraction)

5 x 10^7 cells grown to mid-exponential phase were harvested by centrifugation (4000 x *g*, 3 min, 4°C), washed once with water, once in 1ml stop buffer, once in 1ml ice-cold 20% Trichloroacetic acid **(**TCA) and re-suspended in 200μl of 20% TCA. A pellet volume of acid-washed glass beads (Sigma) was added and samples were processed three times in a Bioline bead-beater (full speed, 30 sec), incubating 2 min on ice between runs. 400μl of 5% TCA was added and the suspension transferred to a fresh

tube prior to centrifugation (16000 x *g*, 10 min, 4°C). The pellet containing the proteins was re-suspended in 100µl TCA sample buffer. Protein samples were stored at -20°C.

Stop buffer
1x PBS, 50mM NaF, 10mM NaN_3

TCA sample buffer
200mM Tris-HCL pH 8.0, 1% SDS, 1% β-mercaptoethanol, 5% glycerol, 0.05% bromophenol blue

II.2.6. Native protein extraction

Cells from mid-exponential phase cultures were harvested by centrifugation (4000 x g, 3 min, 4°C). Pelleted cells were re-suspended in an equal volume of lysis buffer and frozen as drops in liquid nitrogen using a syringe and a needle. Lysis was achieved by grinding cells in liquid nitrogen using a mortar and a pestle or a Retsch RM100 motorised grinder and monitored by light microscopy. The cell lysate was clarified by centrifugation (16000 x g, 10 min, 4°C), transferred to a fresh tube and processed as indicated below.

Lysis buffer
6mM $NaHPO_4$, 4mM NaH_2PO, 0.1% NP-40, 2mM EDTA, 2mM EGTA, 50mM NaF, 0.1mM Na_3VO_4
add to 1 ml buffer before use: 1mM DTT, 2mM PMSF, 1mM Benzamidine, 20 µl of 1 proteinase inhibitors tablet (Complete™; Roche) dissolved in 1ml water

II.2.7. Yeast TAP purification

II.2.7.1. Small scale TAP purification for in vitro assays

2 x 10^9 cells of a Cid1-TAP-tagged strain or a strain transformed with a TAP-containing vector were harvested as described (II.2.6). Cell pellets were re-suspended in 1 ml of cold lysis buffer. One pellet volume of acid-washed glass beads was added and samples were processed three times in a Bioline bead-beater (full speed, 30 sec), incubating 2 min on ice between runs. Cell extracts were clarified by centrifugation (10000 x *g*, 5 min, 4°C) and

incubated for one hour with 100 µl IgG FastFlow™ Sepharose slurry (Amersham), which had been rinsed three times in lysis buffer beforehand. IgG Sepharose with immobilised Cid1 was washed twice in lysis buffer and three times in HBS and was subsequently used in *in vitro* assays (II.2.10.2).

Lysis buffer
6mM $NaHPO_4$, 4mM NaH_2PO, 1% NP-40, 2mM EDTA, 2mM EGTA, 50mM NaF, 0.1mM Na_3VO_4
add to 1 ml buffer before use: 1mM DTT, 2mM PMSF, 1mM Benzamidine, 20 µl of 1 proteinase inhibitors tablet (Complete™; Roche) dissolved in 1ml water

HBS
40 mM HEPES pH 7.0, 200 mM NaCl

II.2.7.2. Large scale TAP purification for protein identification

1 x 10^{11} cells of strains, transformed with pREPNTAP and pREPNTAP-Cid1, were grown to A_{600} of 1.0 and harvested by centrifugation (4000 x *g*, 15 min, 4°C). Native protein lysates were prepared as described (II.2.6) and stored at -80°C. After grinding in a motorised grinder (1 hour per 1L culture), extracts were clarified by centrifugation (16000 x *g*, 20 min, 4°C). 1ml IgG FastFlow™ Sepharose was washed three times in lysis buffer and incubated with the clarified extract, rotating at 4°C for 2 hours. The beads were washed once with lysis buffer, twice with TEV cleavage buffer 1 (15 min, 4°C), transferred to a Polyprep column (Biorad) and washed once by gravity flow with TEV cleavage buffer 2. The column was sealed at the bottom and bound proteins were eluted from the beads by incubation with 1 ml of TEV cleavage buffer 2 containing 1/20 volume of TEV protease (Invitrogen) at 16°C for 90 min with occasional flicking of the column. The TEV eluate plus four additional rinses with 1 ml TEV buffer 2 were collected by gravity flow and snap frozen in liquid nitrogen. The concentration of the tagged protein was monitored by Western blot using a specific antibody. The first three elutions were pooled and concentrated by acetone precipitation. Four times the sample volume of 100% ice-cold acetone was added to the samples and incubated at -20°C for 1-2 hours. Precipitated proteins were pelleted by centrifugation (16000 x *g*, 20 min, 4°C) and washed with 90% cold acetone (16000 x *g*, 5 min, 4°C).

The protein pellet was briefly air-dried at room temperature and re-suspended in 30μl 2x sample buffer (Invitrogen), supplemented with 1mM DTT (Invitrogen). For visualisation of the proteins, a 1μl aliquot was run on precast mini NuPAGE® Novex® Bis-Tris Gels (Invitrogen) according to the manufacturer's instructions and stained with Sypro Ruby as described (II.1.4.2).

Lysis buffer
6mM $NaHPO_4$, 4mM NaH_2PO, 0.1% NP-40, 2mM EDTA, 2mM EGTA, 50mM NaF, 0.1mM Na_3VO_4
add to 1 ml buffer before use: 1mM DTT, 2mM PMSF, 1mM Benzamidine, 20 μl of 1 proteinase inhibitors tablet (Complete™; Roche) dissolved in 1ml water

TEV cleavage buffer 1
10mM Tris-Cl pH 8.0, 300mM NaCl, 0.5mM EDTA pH 8.0, 0.1% NP-40, 1mM DTT

TEV cleavage buffer 2
10mM Tris-Cl pH 8.0, 150mM NaCl, 0.5mM EDTA pH 8.0, 0.1% NP-40, 1mM DTT

II.2.8. Protein identification by electro-spray ionisation mass spectrometry

Remaining protein samples from the large scale TAP purification were separated on precast Bis-Tris gels and visualised using Sypro Ruby stain. The entire gel lanes containing the proteins were divided into 10 strips, each cut into 10mm^2 squares using a clean scalpel and transferred into 10 tubes, which were stored at 4°C. Subsequent steps were performed by Dr. Benjamin Thomas at the Dunn School of Pathology. The gel squares were washed twice for 30 min in fresh ambic solution (50mM ammonium bicarbonate dissolved in 10% acetonitrile), soaked in 100% acetonitrile for 10 min and air-dried. 10mM DTT was added to the gel squares for 30 min followed by two washes with 25mM ammonium bicarbonate and one wash in 100% acetonitrile. 55mM iodoacetamine was added for 60 min in the dark followed by two washes in ambic solution and one wash in 100% acetonitrile. After drying the gel squares, they were incubated with a trypsin solution containing 20ng/μl trypsin (Promega) in 25mM ammonium bicarbonate overnight at 37°C. The digestion was stopped by addition of 1%

formic acid and the supernatant transferred to fresh tubes. Additional peptides were extracted from the gel pieces by incubation with 50% formic acid + 25% acetonitrile for 30 min. Supernatants of corresponding gel slices were pooled and dried completely using a Speed-Vac (Thermo Finigan). Samples were injected into a Thermo Orbitrap coupled to a Dionex U3000 nano HPLC. Peptide identities were searched using MASCOT (www.matrixscience.com) against the SwissProt database (www.expasy.org/sprot).

II.2.9. Co-immunoprecipitation of tagged proteins from yeast

Native protein lysate was prepared from 2 x10^9 cells of a tagged strain, as described (II.2.6). Protein-G sepharose (Sigma) was pre-equilibrated in lysis buffer by washing the beads three times. 1ml of protein lysate was pre-cleared by incubation with 20μl of equilibrated protein-G sepharose, rotating for 1 hour at 4°C. The beads were removed by centrifugation (short pulse) and a 50 μl aliquot of the supernatant was saved prior to dividing the lysate in two. Each lysate was incubated with 2μl of either α-HA or α-myc antibody for 1-2 hours, rotating at 4°C. 10μl of protein-G sepharose was added and incubated for further 30 min. The beads were washed four times with lysis buffer containing 0.1%-1% NP-40 and re-suspended in 2x sample buffer. Immunoprecipitation and input samples (diluted in 4x sample buffer) were analysed by SDS-PAGE and western blot (II.1.4)

Lysis buffer
6mM $NaHPO_4$, 4mM NaH_2PO, 0.1% NP-40, 2mM EDTA, 2mM EGTA, 50mM NaF, 0.1mM Na_3VO_4
add to 1 ml buffer before use: 1mM DTT, 2mM PMSF, 1mM benzamidine, 20 μl of 1 proteinase inhibitors tablet (Complete™; Roche) dissolved in 1ml water

II.2.10. In vitro assays

II.2.10.1. 5' end labelling of RNA

In a total volume of 20μl the following was assembled and incubated for 30 min at room temperature: 200 pmoles of $(U)_{15}$ or $(A)_{15}$ RNA oligo (Thermo Scientific), 1x T4 PNK buffer, 10 units T4 PNK (New England Biolabs), 16 pmoles γ-^{32}P-ATP and RNase-free water. Reactions were stopped by the addition of 20μl stop buffer. Radio-labelled RNA was purified by centrifugation (1500 x *g*, 4 min, room temperature) using Quick Mini.Spin column (Roche). The eluate was ethanol precipitated and re-suspended in 20μl RNase-free water.

Stop buffer
20mM Tris-Cl pH7.5, 0.1M NaCl, 10 mM EDTA

II.2.10.2. Template-independent polymerisation assays

To test the activity of overexpressed Cid1, 2-5μl IgG Sepharose with immobilised protein complexes were used in a 10μl reaction. 1x PAP buffer, 0.5mM of the appropriate nucleotide, 1mM $MgCl_2$ and 1μl of 5' end labelled RNA was added and incubated at 30°C for 40 min. For activity tests of endogenous Cid1, 30μl of IgG beads were used in a reaction volume of 40μl and incubated for 1 hour. Twice the reaction volume of stop buffer was added after incubation. Samples were ethanol precipitated and analysed by denaturing PAGE.

5x PAP buffer
100mM Tris-Cl pH 7.5, 250mM KCl, 3.5mM $MnCl_2$, 1mM EDTA, 500ng/ml acetylated BSA, 50% glycerol

II.2.10.3. Denaturing PAGE

Precipitated *in vitro* assay reactions were re-suspended in FA loading buffer and separated on 15% polyacrylamide gels, run at 35W for 2 hours. Gels were transferred to 3MM Whatman paper, dried and exposed to a phosphor-screen (Molecular Dynamics) for 1 hour to overnight. Screens were scanned using a FLA5000 phosphoimager (Fuji) and analysed using the AIDA™ analysis software.

FA loading buffer
95% deionised formamide, 20 mM EDTA, 0.05% bromophenol blue, 0.05% w/v xylene cyanol

Denaturing gel
8M Urea, 1x TBE, 15% acrylamide:bisacrylamide (19:1, BioRad), 0.05% APS, 0.05% TEMED

II.3. Mammalian cells

II.3.1. General Methods

II.3.1.1. Mammalian cell lines

Mammalian work as described in Chapters IV and V was performed on the following cell lines. The HeLa human cervical cancer cell line (kind gift from Steven West and Nick Proudfoot) was used in synchronisation experiments and for fluorescent microscopy. The 293 (T) human embryonic kidney cell lines (kind gifts from Dawn O'Reilly and Shona Murphy) were used for all other experiments in this study.

II.3.1.2. Mammalian tissue culture

All cell lines were cultured in 37°C incubators with 5% CO_2 and grown in DMEM, supplemented with 10% Foetal Calf Serum (FCS) and 0.1mg/ml (1X) Penicillin / Streptomycin antibiotics (Gibco and PAA Laboratories). Cells were split and passaged by trypsinisation using PET solution (PBS, 1mM EDTA,

0.125% Trypsin) to detach adherent cells. Cells were prepared for storage by re-suspending trypsinised cells in 1ml of 90% DMEM / 10% DMSO solution in cryo-vials and freezing in polystyrene racks at -80°C. Frozen cells were revived by rapid thawing at 37°C, washing and re-suspension in DMEM growth media.

II.3.1.3. Cell transfection

Transfection of cells for experiments discussed in Chapter IV was performed using OptiMEM media (Gibco) and Lipfectamine$^{TM-2000}$ (Invitrogen) according to the manufacturer's instructions. 6-well plates containing 20-30% confluent 293T cells were transfected with 5µg pGeneClip (see section II.1.3.2) overnight before changing to antibiotic-containing medium. If needed, 293T cells were transfected with 1µg pcDNA3.1 prior to harvesting the cells for relevant experiments 72 hours post pGeneClip transfection. HeLa cells were transfected identically but 3µg of pGeneclip was used. For experiments discussed in Chapter V, Attractene (Qiagen) was utilised for pGeneClip transfection of 293 cells and HeLa cells (1µg per 10cm^2 dish) according to the manufacturer's instructions. If necessary, pGeneClip transfected HeLa and 293 cells were selected by incubation into medium containing 1.5 and 3µg/ml puromycin (Sigma), respectively.

II.3.2. Protein methods

II.3.2.1. Total protein lysates

~10^6 HEK293T were washed twice in cold PBS, taken off the plate and re-suspended in 200µl RIPA lysis buffer, supplemented with proteinase inhibitors and phosphatase inhibitors if needed. Cells were allowed to lyse for 10mins on ice and centrifuged (16000 x *g*, 10min, 4°C). The supernatant containing protein lysates was transferred to a fresh tube and the total protein concentration was measured using a nanodrop spectrophotometer

(kindly provided by Susan Lea). Subsequent steps were performed as described in (II.1.4). Antibodies for western blot were used according to Table II.1.

RIPA buffer
50mM Tris pH 7.5, 150mM NaCl, 1% Triton X100, 0.1% SDS, 0.5% DOC, 10% glycerol
add to 1 ml buffer before use: 1mM DTT, 2mM PMSF, 1mM Benzamidine, 20 μl of 1 proteinase inhibitors tablet (Complete™; Roche) dissolved in 1ml water

II.3.2.2. Nuclear and cytoplasmic extracts

All steps were carried out in a coldroom at 4°C. Pelleted HEK293T cells were re-suspended in 500μl of lysis buffer and incubated on ice for 5 min. The suspension was carefully under-layered with 500μl of lysis buffer containing 24% (w/v) sucrose and centrifuged (16000 x *g*, 10 min, 4°C). The top 200μl were used as cytoplasmic extracts. Nuclear extracts were obtained by re-suspending the pellet in 200μl RIPA buffer (described above). Fractionated samples were analysed by western blot. Antibodies directed against α-Tubulin and α-Topoisomerase II-α (TOP2a) served as control for cytoplasmic and nuclear partition, respectively.

Lysis buffer
50mM Tris-HCl pH 7.5, 140 mM NaCl, 1.5 mM $MgCl_2$, 0.5% NP-40
add to 1 ml buffer before use: 1mM DTT, 2mM PMSF, 1mM benzamidine, 20 μl of 1 proteinase inhibitors tablet (Complete™; Roche) dissolved in 1ml water

II.3.2.3. ZCCHC11 immunoprecipitation

Cytoplasmic extracts were obtained by re-suspending harvested HEK293T cells in 1ml lysis buffer on ice for 5 min. Cell debris and nuclei were pelleted at 3000 x *g* for 40 secs. Lysates were clarified by centrifugation (16000 x *g*, 15 min, 4°C) and pre-cleared with protein A agarose. An input sample was saved and the remaining lysate was divided in two. One sample was incubated with 5μl α-ZCCHC11 for 1 hour at 4°C prior to adding protein A agarose for 30 min to both samples. Complexes were washed 4 times with

washing buffer and eluted from the beads by boiling them in sample buffer 5 min before loading on a 6% SDS-PAGE gel.

Lysis buffer
10 mM Tris-HCl pH 7.5, 2.5 mM $MgCl_2$, 100 mM NaCl, 35 μg/ml digitonin
add to 1 ml buffer before use: 1mM DTT, 2mM PMSF, 1mM benzamidine, 20 μl of 1 proteinase inhibitors tablet (Complete™; Roche) dissolved in 1ml water

Wash buffer
10 mM Tris-HCl pH 7.5, 2.5mM $MgCl_2$, 100 mM NaCl, 0.05% Triton X-100

II.3.3. RNA methods

II.3.3.1. RNA extraction

Total RNA was isolated using Tri-Reagent (Applied Biosystems) followed by chloroform extraction and isopropanol precipitation of RNA. The purity and concentration of the re-suspended RNA was measured using a nanodrop spectrophotometer.

II.3.3.2. Reverse transcription

5 μg of total RNA was treated with DNase (Promega) for 2 hours at 37°C (with an extra 1μl of DNase added after the initial hour) followed by heat inactivation of the DNase at 70°C for 15 min. The RNA was then reverse-transcribed for 40 min at 55°C using 10 pmol random hexamers (Invitrogen) or gene-specific primers as stated and the reverse-transcriptase Superscript III (Invitrogen) according the manufacturer's guidelines. For each sample, an additional reaction was performed in the absence of reverse transcriptase to control for contaminating DNA.

II.3.3.3. Quantitative PCR

cDNA samples were diluted 1:1 with water and 1μl of the dilution was mixed with 1x SYBR Green mix (SensiMix Bioline) and gene-specific primers in a 10μl qPCR reaction. All qPCR reactions were carried out in triplicates in a

Corbett Rotorgene 6000 machine using 72-reaction plates and quantitated using the Rotorgene 3000 software. All resulting values were normalised to GAPDH mRNA and shown as a ratio to the corresponding control sample. Additional controls were performed on the ACTB transcript to confirm stable GAPDH levels in all conditions. Cycling conditions included denaturation at 95°C for 10 min, followed by up to 45 cycles of {95°C 10 secs, 60°C 10 secs, 72°C 10 secs} and a hold at 72°C for 10 min. A SYBR Green melt curve (1°C rise; range 72°C – 95°C) was concurrently performed for every sample in order to confirm the integrity and similar identity of the resultant PCR products. Furthermore, the integrity of PCR products for each primer pair was also confirmed by agarose gel electrophoresis. All primer sequences are listed in Appendix C.

II.3.3.4. Circularised rapid amplification of cDNA ends (cRACE)

cRACE was performed essentially as described previously (Mullen and Marzluff 2008; Rissland and Norbury 2009). In order to capture capped transcripts, 10 µg of total RNA were incubated with Tobacco Acid Pyrophosphatase (Cambio) for one hour at 37°C. The RNA was ethanol precipitated and subjected to intra-molecular RNA ligation overnight at room temperature using 1 unit of RNA ligase (New England Biolabs) in a 400µl reaction. Half of the precipitated and washed ligated RNA was subsequently reverse-transcribed as described (II.3.3.2) using a gene-specific primer. One-twentieth of the cDNA was amplified in 30 PCR cycles using divergent gene-specific primers across the ligation site. Resulting PCR products were purified through an agarose gel, precipitated and ligated into a TA vector as described in section II.1.1. XL1-Blue bacteria were transformed with the ligation and plated on LB plates containing 20 µg/ml 5-bromo-4-chloro-3-indolyl-β-D-galactopyranoside for blue/white screening. Positive clones were confirmed by colony PCR using gene-specific primers and subsequently sequenced using M13 primers. Individual clones containing gene-specific sequences from both 5' and 3' ends of the mRNA were divided into 2

groups: mRNAs with and without un-templated uridine residues at the site of ligation. Statistical analyses were performed using a χ^2 test comparing control and knock-down samples.

II.3.3.5. RNA immunoprecipitation

~10^6 HEK293T cells in a 10cm dish were cross-linked using 1% formaldehyde for 10 min while shaking at 37°C. The reaction was quenched by the addition of glycine at a final concentration of 0.25M for 5 min at 37°C. Subsequent steps were performed at 4ºC. Cells were washed twice with cold PBS and re-suspended in 1ml RIPA buffer containing proteinase inhibitors, sonicated using a diagenode Bioruptor ('high' 30 secs on/off pulse for 8min) and centrifuged (16000 x *g*, 10 min, 4°C) to remove debris. The supernatant was supplemented with 10mM vanadyl ribonucleoside complex (NEB) and pre-cleared with protein-A agarose beads (20µl packed beads per 1ml lysate, equilibrated in PBS) to reduce non-specific background. 50µl were saved as input, the remaining lysate was diluted 1:2 and divided into 'no antibody' control and immunoprecipitation with 10µl anti-ZCCHC11 or anti-ZCCHC6 antibody. After 2 hours, 10µl protein-A beads were added to the reactions for further 30-60 min. The beads were centrifuged (2000 x *g*, 1 min) and washed with buffers A, B, C for 5 min each and rinsed with buffer D twice before RNA was eluted in 300 µl elution buffer. Cross-links were reversed by incubating samples at 65°C for 45 min with occasional vortexing. RNA was subsequently extracted using Tri-Reagent, DNase-treated and reverse-transcribed as described (II.3.3.2). Semi-quantitative PCR was carried out 28-35 cycles. Products were resolved and visualised on a 2% agarose gel. For absolute quantitation of co-precipitated RNA, qPCR was carried out in triplicate on all samples (input, no antibody control and immunoprecipitate). Values of immunoprecipitates were normalised to GAPDH and are expressed in relation to control samples without antibody.

RIPA buffer
50mM Tris pH 7.5, 150mM NaCl, 1% NP-40, 0.05% SDS, 0.5% DOC
add to1 ml buffer before use: 1mM DTT, 2mM PMSF, 1mM Benzamidine, 20 µl of 1 proteinase inhibitor tablet (Complete™; Roche) dissolved in 1ml water

Wash solution A
20mM Tris pH 8.0, 150mM NaCl, 0.1% SDS, 1% Triton X10, 2mM EDTA

Wash solution B
20mM Tris pH 8.0, 500mM NaCl, 0.1% SDS, 1% Triton X10, 2mM EDTA

Wash solution C
10mM Tris pH 8.0, 250mM LiCl, 1% DOC, 1% NP-40, 1mM EDTA

Wash solution D
10mM Tris pH 8.0, 1mM EDTA

Resuspension solution
50mM Tris pH 7.0, 300mM NaCl, 5mM EDTA, 1% SDS, 1mM DTT

II.3.4. Cell cycle analysis

II.3.4.1. Cell synchronisation

Following pGeneClip transfection, HeLa cells were synchronised at the G1 / S phase border using a double thymidine block as described (Whitfield et al. 2000). In brief, 36 hours post transfection, cells were blocked for the first time by adding 2mM thymidine (Sigma) to the medium for 18 hours. Following a release of 8 hours by removal of thymidine through washing cells with PBS two times, cells were blocked again for 16 hours and subsequently released into S phase. Timepoints were taken as indicated in the experiments. Successful cell synchronisation was monitored by flow cytometry (II.3.4.2).

II.3.4.2. Flow cytometry

~$5x10^6$ HEK293 or HeLa cells were washed twice in cold PBS and re-suspended in 2ml cold 70% ethanol by adding the ethanol slowly while vortexing the suspension. Cells were fixed at 4°C for at least 30 min or stored at 4°C until further processing. Following fixation, cells were washed twice in PBS, re-suspended in 1ml PBS containing 40 µg/ml propidium iodide and 100 µg/ml RNAse A and incubated at room temperature for 15min in the

dark. The DNA content of the cells was monitored with a FACScan or FACScalibur (Becton Dickinson) and analysed using the Cell Quest software.

II.3.4.3. 5-Bromo-2-deoxyuridine (BrdU) incorporation

~10^7 HEK293 cells were pulse labelled for 30 min or 24 hours with BrdU, added to the growth medium to a final concentration of 10μM. Cells were harvested and fixed as detailed above (II.3.4.2). After fixation, cells were washed twice in PBS and incubated with 2ml 2M HCl for 30 min at room temperature to allow histone extraction. Cells were washed twice in PBS and once in blocking solution. A 1:500 dilution of anti-BrdU antibody (Sigma) in blocking solution was subsequently added to the cells and incubated for 1 hour at room temperature on a rotating wheel. Unbound antibody was removed by washing twice in blocking solution prior to a 30 min incubation with anti-mouse antibody conjugated to FITC (Sigma) diluted 1:200 in blocking solution at room temperature in the dark. Following one wash in PBS, cells were re-suspended in PBS containing 40 μg/ml propidium iodide and 100 μg/ml RNAse A and analysed as described (II.3.4.2).

Blocking solution
PBS containing 0.1% BSA and 0. 2% Tween

II.3.4.4. Immunofluorescence microscopy

~10^5 HeLa cells were seeded on 11mm coverslips and incubated overnight in 6 well plates. RNAi was performed as detailed above using 0.2μg pGeneClip and 0.6μl Attractene transfection reagent diluted in 2ml DMEM per well. If needed, cells were treated with appropriate drugs as indicated. On the harvest day, cells were fixed in 4% paraformaldehyde for 10 min followed by three rinses in PBS. Cells were permeabilised in PBS containing 0.5% Triton X-100 for 5 min followed by three rinses in PBS. For BrdU staining, histones were extracted in 2M HCl for 20 min. If needed, unspecific binding of antibodies was reduced by blocking coverslips in blocking buffer for 1 hour at room temperature. The primary antibody was diluted in blocking buffer

according to Table II.3 below and added to the cells for 1-16 hours depending on the antibody. Cells were washed 3 times in PBS+0.1% Triton X-100 for 10 min and incubated with the diluted secondary antibody for 30-60 min. Following three washes in PBS-Triton, coverslips were mounted on 6μl mounting solution containing DAPI (Vectashield) and examined using an Axioplan 2e CCD-fluorescence microscope (Zeiss) and Metamorph™ software (Molecular Devices).

Blocking buffer
PBS containing 0.1% Triton X-100, 1% BSA (Sigma) and 0.1% cold fish skin gelatin (Sigma)

Name	Type	Dilution	Incubation time	Source
α-phH3	Rabbit polyclonal	1:500	30 min	Molecular Probes
α-γH2A.X	Mouse monoclonal	1:200	Overnight	Millipore
α-BrdU	Mouse monoclonal	1:2000	1 hour	Sigma
α-mouse-Cy3	Goat polyclonal	1:2000	30 min	Sigma
α-rabbit-Cy3	Goat polyclonal	1:500	30 min	Sigma

Table II.3 Antibodies used for immunostaining in this study

CHAPTER III. THE CID1 HOLOENZYME

III.1. Activity of endogenous Cid1

As outlined in Chapter I, *S. pombe* Cid1 is a nucleotidyl transferase and was identified in a screen for components of the replication checkpoint pathway (Wang et al. 2000). When overexpressed, Cid1 confers resistance to a combination of hydroxyurea (HU) and caffeine. These drugs combined normally lead to lethality because of premature entry into mitosis with incomplete DNA replication. Biochemical analysis of Cid1 revealed its major activity to be uridylation of polyadenylated mRNA substrates (Rissland et al. 2007; Rissland and Norbury 2009). Although Cid1 was suggested to play a role in DNA checkpoint integrity, it was later found that its specificity for uridine was unaltered when Cid1 was isolated under conditions that perturb the cell cycle (Rissland et al. 2007). Curiously, TAP-tagged overexpressed Cid1 complexes isolated from *S. pombe* and recombinant Cid1 isolated from bacteria displayed specific differences in activity when assayed *in vitro.* Recombinant Cid1 showed strong PUP and PAP activity on either poly(A) or poly(U) substrates (Read et al. 2002; Rissland et al. 2007). In contrast, Cid1 complexes exhibited much stronger PUP than PAP activity on an $(A)_{15}$ RNA substrate and enhanced PAP activity only on an $(U)_{15}$ RNA. It was hypothesised that these discrepancies between recombinant Cid1 and native Cid1 complexes were caused by the absence of *S. pombe* specific regulatory factors when expressed in bacteria (Rissland et al. 2007).

The *in vitro* activities of recombinant Cid1 expressed in bacteria and overexpressed Cid1 (oCid1) in *S. pombe* have been analysed in detail previously. However, it remained unknown whether endogenous Cid1 (eCid1) would behave similarly, as previous attempts to isolate active eCid1 protein complexes form *S. pombe* had failed. To begin my studies, I sought to optimise purification and assay conditions in order to answer this question.

TAP-tagged Cid1, expressed from its own promoter, was affinity purified as previously described for overexpressed Cid1 (Rissland et al. 2007) but significant changes were made in order to recover sufficient amounts of active eCid1-TAP (see Chapter II). Successful recovery of the complexes was confirmed by western blot using an anti-mouse secondary antibody that is bound via its Fc region to the protein A moiety of the TAP. The band corresponding to eCid1-TAP was very faint when compared to oCid1, signifying the different expression levels (Figure III.1A).

Because of the originally discovered relationship of Cid1 with DNA checkpoint regulation, eCid1 was also purified from cells that had been treated with HU to test the effect of blocked DNA replication on its activity. The activity of eCid1 was examined in an *in vitro* assay, which measures the ability to add A, T, C or U residues to an $(A)_{15}$ RNA substrate (Figure III.1B). Similarly to overexpressed Cid1, eCid1 displayed strong incorporation of UTP on $(A)_{15}$ RNA and very weak activity towards ATP, CTP and GTP. In agreement with previous data, the addition of HU to the cells altered neither processivity nor nucleotide specificity of eCid1. In addition, the activity of Cid1 was compared on $(A)_{15}$ and $(U)_{15}$ RNA substrates to determine substrate-specific characteristics of eCid1 (Figure III.1C). Similar to oCid1, eCid1 showed enhanced PAP activity when presented with $(U)_{15}$ RNA. The PUP processivity of eCid1 was slightly reduced on $(U)_{15}$ RNA when compared to oCid1. This result could hint towards the presence of factors in the eCid1 complex inhibiting the extension of an oligouridine primer. It is possible that imbalance in complex stoichiometry on Cid1 overexpression would prevent

such factors from acting properly on oCid1. For these reasons, further investigations into the identification of the Cid1 complex used reduced levels of oCid1 (see Chapter III.5).

Taken together, these results show that endogenous Cid1 behaves very similarly to overexpressed Cid1 *in vitro* on $(A)_{15}$ RNA, the substrate most closely resembling known natural targets of Cid1 (Rissland and Norbury 2009). Consequently, the following experiments were all performed using ectopic Cid1 expressed from the *nmt1* promoter and $(A)_{15}$ RNA as a substrate.

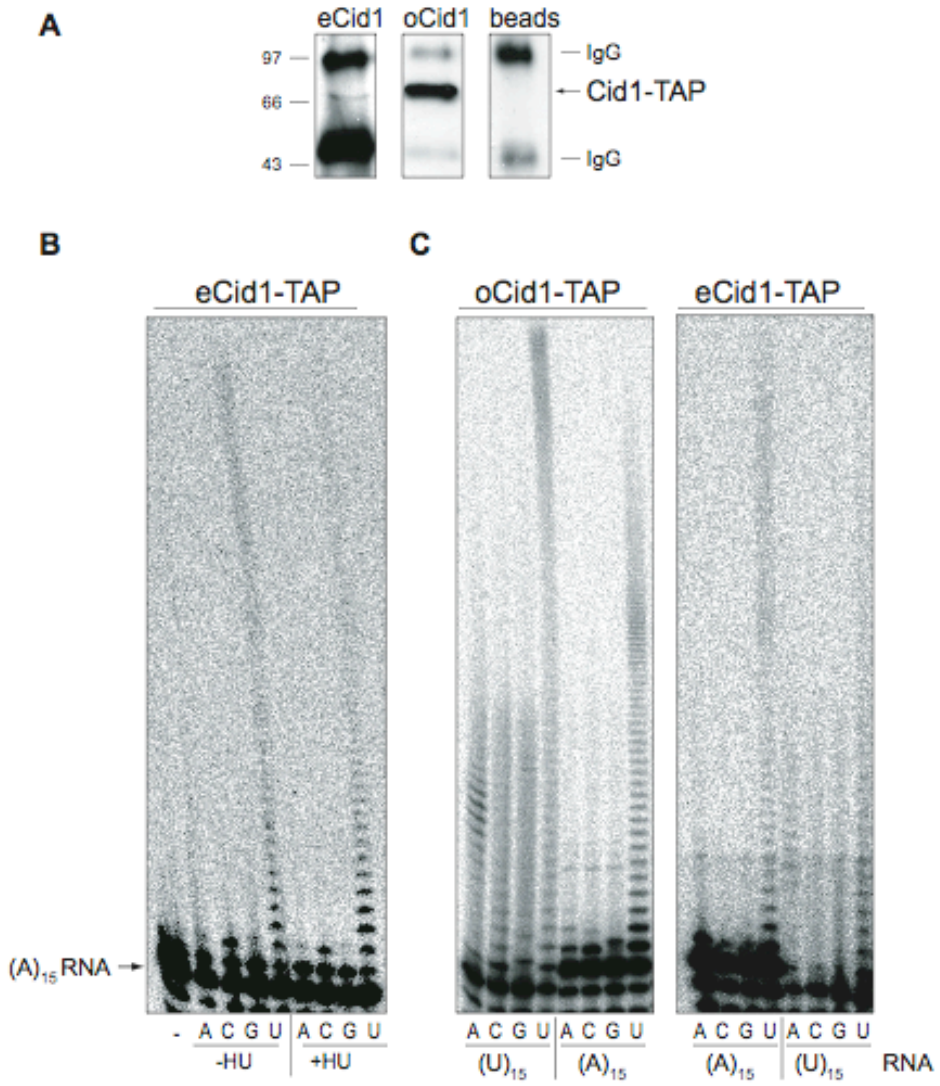

Figure III.1 Endogenous Cid1 activity

TAP-tagged endogenous Cid1 (eCid1) and overexpressed Cid1 (oCid1) were purified from cells on IgG beads. (A) A Western blot using an anti-rabbit antibody bound by the TAP moiety of the tag confirms elution of the protein. The bands corresponding to Cid1-TAP and immunoglobulin are indicated. (B) Endogenous Cid1 complex was purified from cells treated with and without 10mM HU for 60 min. Equal amounts of the protein complex were incubated with 5' end-labeled $(A)_{15}$ RNA and either ATP, CTP, GTP or UTP for 60 minutes at 30°C. (C) eCid1-TAP and oCid1-TAP were incubated with radiolabeled $(A)_{15}$ or $(U)_{15}$ RNA and each nucleotide for 45 minutes at 30°C. All assays were resolved on a 15% polyacrylamide gel and analysed by autoradiography. The position of the $(A)_{15}$ substrate RNAs is indicated by an arrow.

III.2. Testing Cid1 protein interactions with previously identified candidates

Given that Cid1 lacks a recognisable RNA-binding domain, it had been suggested that Cid1 forms a complex with potential RNA-binding proteins to regulate its activity. Aiming at unveiling such factors, a previous study has applied two approaches, yeast two-hybrid and affinity purification combined with mass spectrometry (MS), to identify Cid1-interacting proteins (Abigail Stevenson and Chris Norbury, unpublished). The yeast two-hybrid experiment using Cid1 as bait revealed an as yet uncharacterised protein called Hyd1 belonging to the metallo-β-lactamase family. The second method consisted of two consecutive affinity purification steps of TAP-tagged Cid1 on IgG and calmodulin beads followed by MS analysis of co-purifying proteins. Potential Cid1-interacting partners resulting from this analysis included the major poly(A) binding protein Pab1 and the multi-KH domain protein Vgl1, which has recently been identified as a component of heat stress-induced granules in fission yeast (Wen et al. 2010). A further candidate identified in this way was the RNA annealing factor Mlo3, previously implicated in nuclear export of poly(A)$^+$ RNA (Thakurta et al. 2005). Given that these proteins are associated with RNA metabolism, they represented interesting candidates as potential Cid1-regulators.

In order to verify a direct interaction between Cid1 and these putative candidates, co-immunoprecipitation experiments were performed under native conditions (Figure III.2). Each of the four candidate genes in addition to Cid1 was either myc-, HA- or GFP- tagged and the resulting strain was crossed to a strain harbouring a differently tagged version of Cid1. For every experiment either tagged version alone served as a negative control. Furthermore, every immunoprecipitation experiment was performed at least three times and in a reciprocal manner. RNase A was added in the Pab1

experiment (Figure III.2C), in order to test the possibility that any interaction was RNA-mediated. The results shown in Figure III.2 reveal that none of these proteins were pulled down by Cid1 or were themselves capable of co-purifying Cid1. It can be concluded either that Cid1 does not interact with these proposed candidates or that these interactions could not withstand the conditions used for co-immunoprecipitation in this study.

Interestingly, a very recent study has implicated Mlo3 in the production of centromeric siRNAs and the suppression of antisense RNA by linking heterochromatic factors with RNA turnover factors such as the TRAMP complex. Notably, FLAG-purification followed by MS identified Cid14 but not Cid1 as an interacting partner of Mlo3 (Zhang et al. 2011), in line with the results shown in Figure III.2A.

III.3. Cid1 activity in deletion mutants

In parallel to the verification of Cid1 protein interactions described above, the effect of the absence of some of these candidates on the activity of Cid1 *in vitro* was investigated. A TAP-tagged version of Cid1 was transformed into *hyd1*Δ and *vgl1*Δ deletion strains and affinity-purified on IgG-SEPHAROSE (Figure III.3A). The activity of Cid1 was tested using an $(A)_{15}$ RNA substrate and all four nucleotides. As shown in Figure III.3B, the activity of Cid1 complexes was not significantly altered when Vgl1 or Hyd1 were missing compared to WT Cid1 complex, as UTP but none of the other nucleotides were efficiently added to the primer. Furthermore, sequencing of *in vivo* targets of Cid1 showed that the absence of Pab1 did not affect nucleotide incorporation by Cid1 (Sophie Fleurdépine and Chris Norbury, unpublished). These results reaffirm the inability of Pab1, Hyd1 and Vgl1 to be involved in the regulation of Cid1.

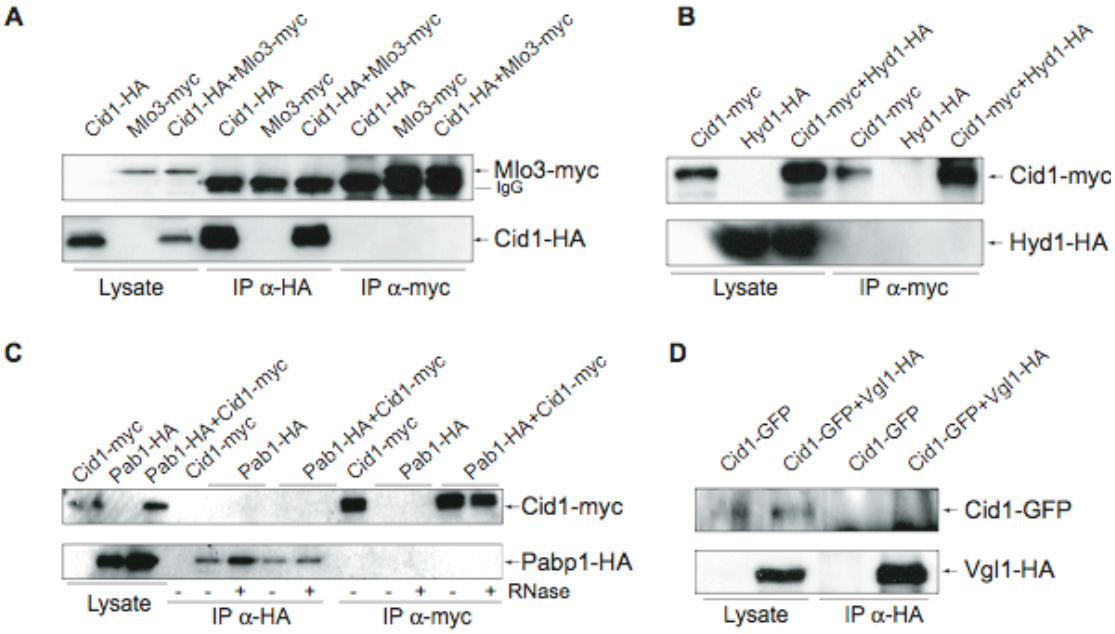

Figure III.2 Cid1 does not interact with previously found proteins

Native protein lysates were prepared from endogenously tagged strains. Anti-HA (α-HA) and anti-myc (α-myc) antibodies were used for immunoprecipitation as indicated. 5% of the lysate of each strain along with immunoprecipitates were analysed on a 10% SDS-PAGE. Detection of proteins by Western blot was enabled using antibodies against HA + myc (A-C) and HA + GFP (D). In (C), half of the immunoprecipitates were treated with 10μg/ml RNase A for 30 minutes. The migration of tagged proteins is indicated by an arrow in addition to bands corresponding to immunoglobulin.

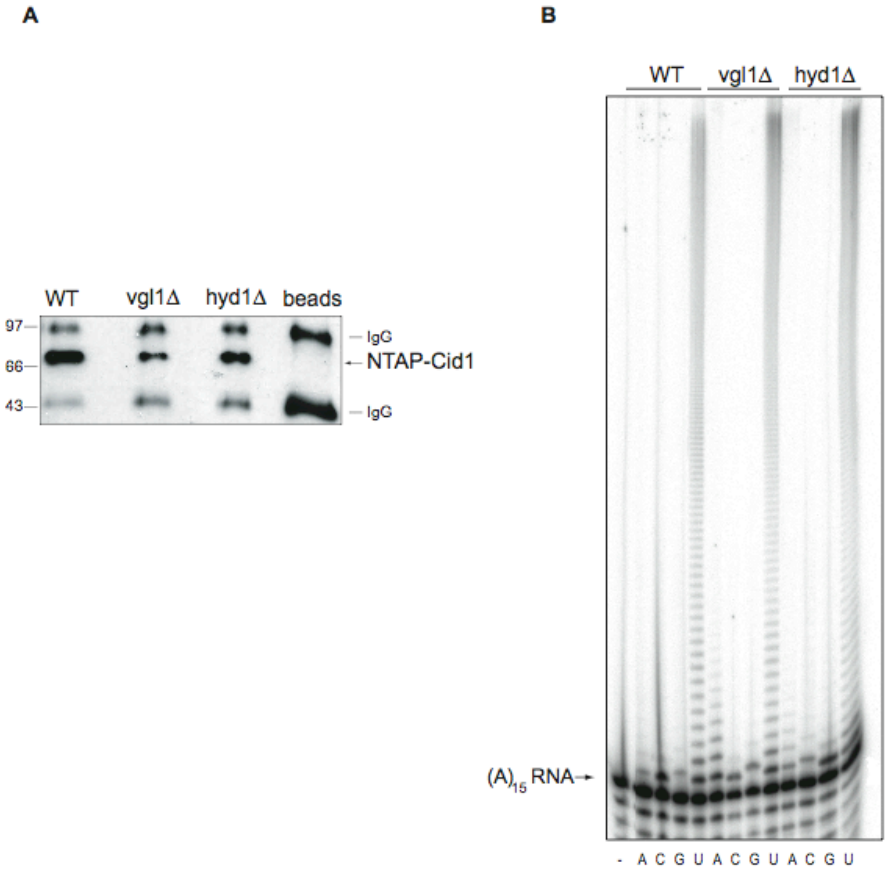

Figure III.3 Cid1 *in vitro* activity in deletion mutants

TAP-tagged overexpressed Cid1 was purified from *hyd1Δ* and *vgl1Δ* deletion strains and visualised by western blot. The migration of Cid1-TAP and immunoglobulin is indicated. (A). Equal amounts of the protein complex were incubated with 5' end-labeled $(A)_{15}$ RNA and either ATP, CTP, GTP or UTP for 30 minutes at 30°C. The reactions were resolved on a 15% polyacrylamide gel and analysed by autoradiography. The position of the substrate RNAs is indicated by an arrow.

III.4. Does Cid1 reside in a protein complex?

As numerous attempts to identify *bona fide* Cid1-interacting partners had been unsuccessful, the question remained whether Cid1 continuously resides in a stable protein complex in exponentially growing yeast cells, or whether accessory factors are dispensable for its activity *in vivo*. It needs to be taken into consideration that recombinant Cid1 in isolation is able to extend an RNA template without accessory factors although a clear RNA-binding domain in Cid1 has yet to be characterised. The processive and unspecific *in vitro* activity of recombinant Cid1 however differs significantly from its distributive uridylation activity *in vivo*, clearly implicating some regulatory elements in the cell.

To verify the presence of such factors in a different way, TAP-tagged Cid1 complexes were purified from *S. pombe* under both low and high salt conditions (0.2M and 1M NaCl, respectively). It was anticipated that the complex purified under high salt conditions might lack putative interacting proteins and so display a different activity *in vitro*. Under high salt conditions (Figure III.4A, see question marks), fewer proteins were associated with Cid1, indicating that the salt treatment destroyed at least some potential protein-protein interactions. Next, the activity of these Cid1 fractions was tested *in vitro* on an $(A)_{15}$ RNA oligonucleotide (Figure III.4B). Interestingly, the high salt wash decreased the specificity of the enzyme for UTP as both U and A residues were added with high efficiency, in contrast to the low PAP activity seen using Cid1 complexes isolated under low salt conditions. The enhanced PAP activity conferred by high salt purification is reminiscent of the activity of recombinant Cid1 in isolation (Rissland et al. 2007). Since Cid1 appears to act solely as a terminal U transferase *in vivo*, it seems plausible that an accessory factor that normally confers this specificity is lost after high salt treatment.

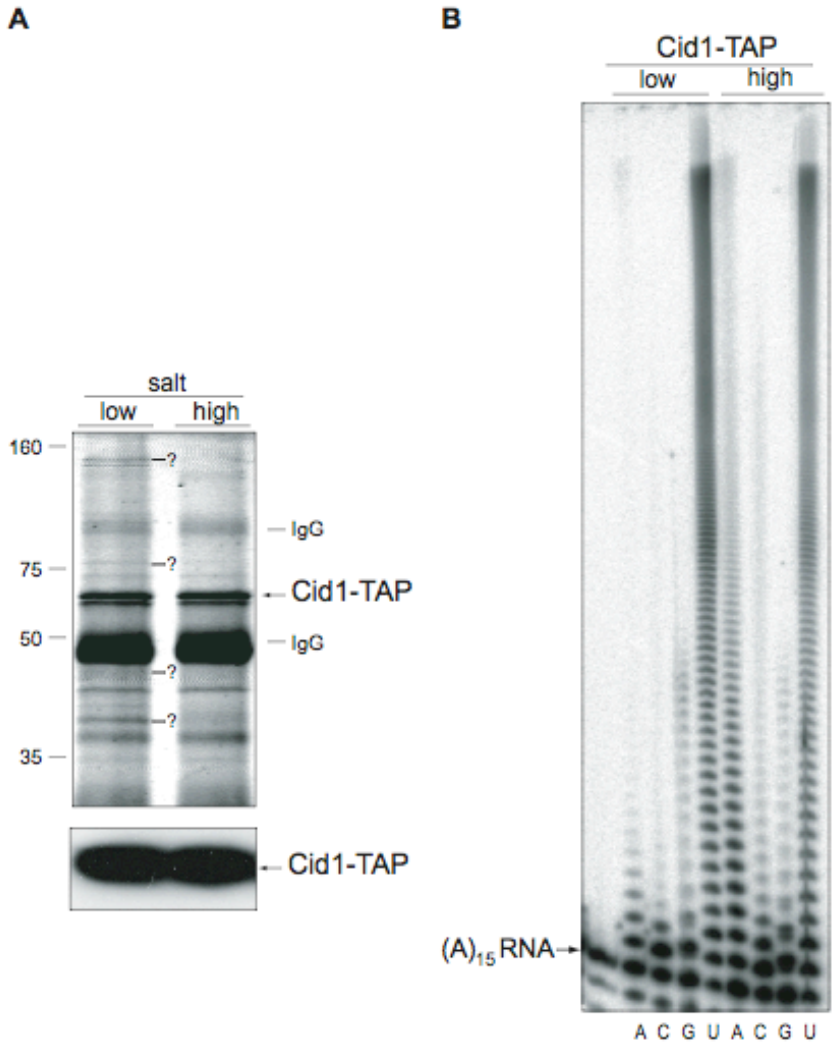

Figure III.4 High salt treatment affects the Cid1 complex *in vitro*

TAP-tagged overexpressed Cid1 was affinity purified under high (1M NaCl) and low (200 mM NaCl) salt conditions. (A) The complexes were resolved on a 10 % SDS-PAGE and stained with Sypro. The migration of Cid1-TAP and immunoglobulin is indicated. Bands missing in high salt washes are indicated with a question mark. The identity of Cid1 was confirmed by Western blot using an antibody recognizing the TAP (lower panel). (B) Equal amounts of the proteins were incubated with a 5' end-labeled $(A)_{15}$ RNA primer and either ATP, CTP, GTP or UTP for 40 minutes at 30°C. Reaction products were separated on a 15% polyacrylamide gel and visualised by autoradiography. The position of the substrate RNA is indicated by an arrow.

III.5. Cid1 TAP purification

To re-investigate the potential presence of Cid1-interacting proteins, the approach of affinity purification combined with MS analysis was repeated. This time however, the second affinity purification step on calmodulin beads was omitted in an attempt to preserve low-affinity interactions. Furthermore, the entire gel containing purified proteins was subjected to MS analysis rather than specific bands only (see Chapter II.2.7.2 for details). To control for background, a vector containing the TAP-tag alone was used. Both plasmids, pREPNTAP and pREPNTAP-Cid1, were transformed into *cid1*Δ cells. Their overexpression, driven from the *nmt1* promoter, was partially repressed by the addition of 0.1μM thiamine to the media in order to minimise saturation and sequestration of protein interactions.

TAP-tagged Cid1 and the TAP tag alone were simultaneously affinity purified under native conditions and subjected to MS. The elution profile of both samples is shown in Figure III.5. Unfortunately, for reasons that are presently unclear, a substantial number of Cid1 peptides were found in the negative control, complicating the identification of specific interacting candidates. Identified proteins by MS are listed in Appendix A. Cid1 co-purifying factors included proteins involved in ribosome biogenesis, stress response, metabolism and constituted mostly common background proteins found in TAP purifications. When high-scoring Cid1-TAP MS results were examined alone, the analysis unfortunately did not reveal the previously identified proteins Mlo3, Vgl1 or Hyd1, nor were proteins with obvious potential involvement in cytoplasmic RNA metabolism uncovered.

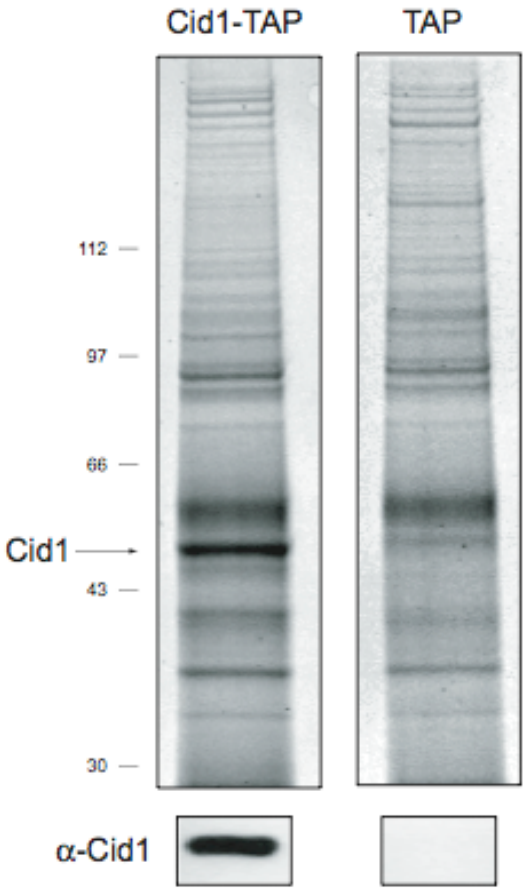

Figure III.5 Large-scale Cid1 TAP purification

TAP-tagged Cid1 and TAP alone expression was partially repressed by the addition of 10μM thiamine to the medium. Both were affinity purified from 10 liters yeast culture on IgG-SEPHARAROSE and eluted with TEV protease. The elution profiles were separated on a Bis-Tris gel and stained with Sypro. The band corresponding to Cid1 is indicated. A western blot using an antibody directed against Cid1 was used to confirm the identity of Cid1 (lower panel).

III.6. Cid1 is phosphorylated

The MS analysis fortuitously revealed a phosphorylation site on the C-terminus of the Cid1 polypeptide, which was present on serine 404 in eight out of ten peptides sequenced (indicated in Figure III.6A). To investigate the potential role of this modification, serine 404 was replaced by alanine on pREPNTAP-Cid1 (creating Cid1-S404A), which was subsequently transformed into *cid1*Δ cells. A potential role of the post-translational modification in the regulation of the yeast cell cycle was first examined in the assay that was initially used in the screen to identify Cid1. The ability of overexpressed Cid1-S404A to confer resistance to the combined drugs caffeine and HU was therefore investigated (Figure III.6B). No difference in drug sensitivity was observed when compared to WT, as both WT and mutant conferred resistance to the combination of caffeine and HU whilst the empty vector failed to do so. This result suggests that the phosphorylation may not interfere with the S-M checkpoint activation in response to replication stress when Cid1 is overexpressed.

Next the activity of Cid1-S404A was investigated *in vitro*. For this purpose, both TAP-tagged Cid1-WT and Cid1-S404A were purified on IgG-Sepharose. Equal recovery of both proteins was obtained (Figure III.6C). The activity was tested on an $(A)_{15}$ RNA oligo (Figure III.6D) and on $(U)_{15}$ RNA (data not shown). No significant and reproducible change in enzymatic activity could be observed in this assay. In agreement with these results, lambda protein phosphatase treatment of the purified complexes prior to activity tests did not alter the activity of Cid1 either.

It can be concluded from these data that removal of the phosphorylation on serine 404 of the Cid1 polypeptide does not impair its reported role in checkpoint activation nor does it affect nucleotide specificity *in vitro*.

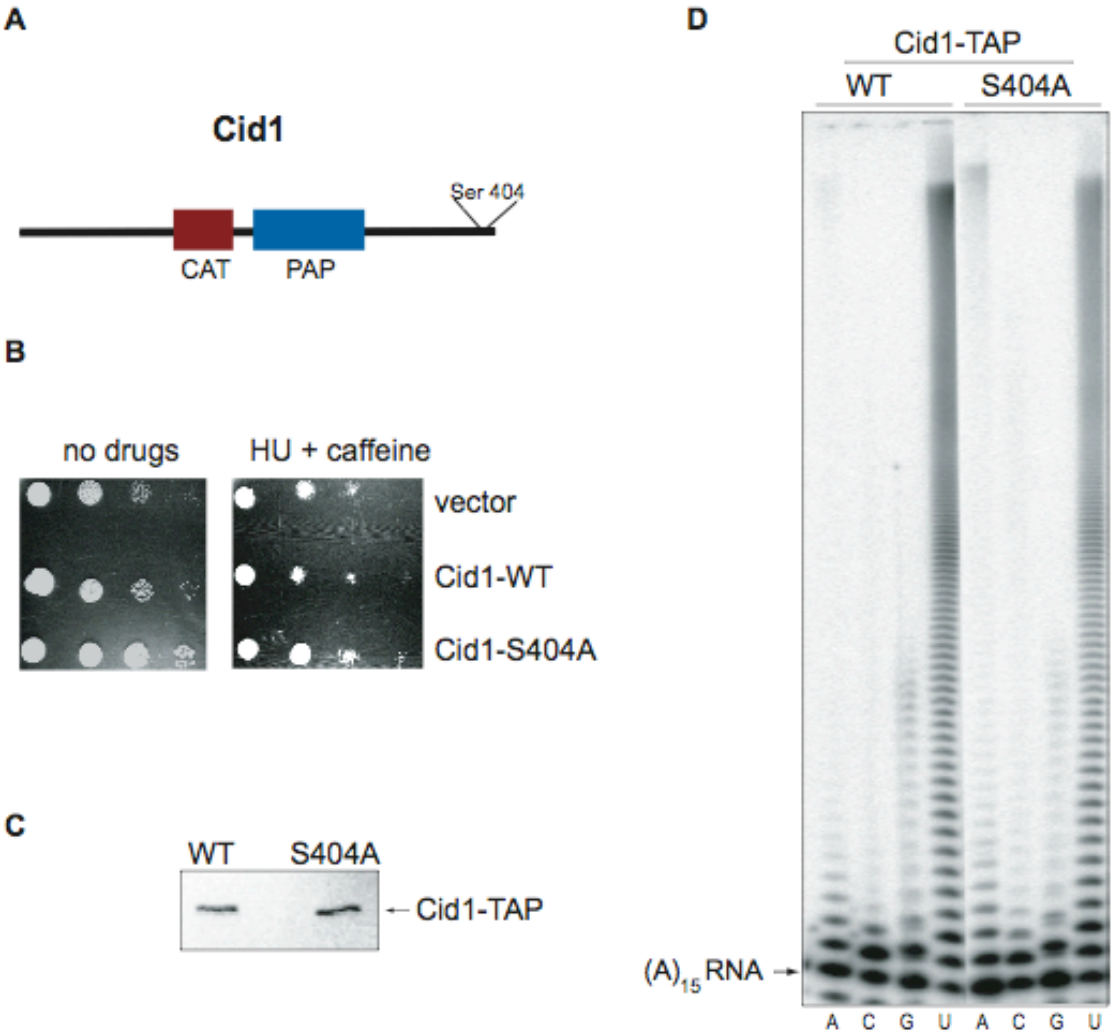

Figure III.6 Cid1 phosphorylation

(A) Diagram depicting Cid1 with its catalytic and PAP-associated domain in blue (CAT) and red (PAP), respectively. The position of the phosphorylation site serine 404 identified by MS is indicated. (B) *cid1Δ* cells were transformed with WT, Cid1 A404 (in which the identified phosphorylation site on serine 404 had been replaced by alanine) or the empty vector. Serial dilutions from 10^5 to 10^2 cells were spotted on YE5S agar plates containing either no drug or 2.5mM caffeine + 10mM HU as indicated. The plates were photographed 5 days after incubation at 30°C. (C) Overexpressed WT and Cid1A404 were affinity purified on IgG-Sepharose and verified by western blot using a secondary antibody recognising the Tag. (D) Equal amounts of the proteins were incubated with a 5' end-labeled $(A)_{15}$ RNA primer and either ATP, CTP, GTP or UTP for 40 minutes at 30°C. Reaction products were separated on a 15% polyacrylamide gel and visualised by autoradiography. The position of the substrate RNA is indicated by an arrow.

III.7. Discussion

Cid1 is a cytoplasmic nucleotidyl transferase that targets cytoplasmic mRNAs for degradation by adding one to a few uridyl residues to the 3' end of polyadenylated mRNAs (Rissland and Norbury 2009). *In vitro*, Cid1 is a highly processive poly(U) polymerase in its endogenous, overexpressed and recombinant form. Most members of the family of nucleotidyl transferases including Cid1 lack a canonical RNA binding domain and act in combination with RNA binding partners on their RNA targets. One example is the *S. cerevisiae* nuclear poly(A) polymerase Trf4, which stably interacts with zinc finger proteins Air1 and Air2 in order to bind its substrates (LaCava et al. 2005; Vanacova et al. 2005; Wyers et al. 2005). In an attempt to identify equivalent binding partners of Cid1, this and a previous study have applied TAP purification combined with MS analysis of TAP-tagged Cid1. Direct interactions between Cid1 and putative candidates involved in RNA metabolism were then tested by co-immunoprecipitation. Unfortunately, none of the proteins tentatively identified previously or in this study could be confirmed in co-immunoprecipitation experiments as direct interaction partners of Cid1 (Figure III.2). In addition, the absence of these putative candidates from living cells did not affect Cid1 activity (Figure III.3). From these results it can be hypothesised that Cid1 – in contrast to other nucleotidyl transferases - does not reside in a stable protein complex. Supporting this hypothesis is the observation that recombinant Cid1 is able to extend an RNA oligonucleotide by itself *in vitro* despite the lack of a recognisable RNA binding domain. Furthermore, recent data from electromobility shift assays indicate that recombinant Cid1 is also capable of binding its substrates very efficiently (Sophie Fleurdépine and Chris Norbury, unpublished). The domain(s) responsible for RNA binding are currently under investigation (see Chapter VI.1). However, these observations do not explain the high specificity of Cid1 towards UTP and distributive activity observed *in vivo* that is in such contrast to the processive activities of recombinant Cid1.

In order to re-investigate the involvement of regulatory factors, the Cid1 complex was compared under conditions that either preserve or destroy protein-binding capacities. When assayed *in vitro*, the two Cid1 complexes showed substantial differences in nucleotide choice (Figure III.4). This result hints towards the presence of some regulatory elements in *S. pombe* that yet need to be identified.

The MS analysis performed in this study did not identify Cid1-interacting proteins. However, it revealed a phosphorylation site on the C-terminus of Cid1 (Figure III.6) that was present on nearly all peptides sequenced. The C-terminus of Cid1 including the identified phosphorylation site is not conserved amongst other fungi, making a conserved regulatory function of the post-translational modification site unlikely. Nonetheless, its role was further investigated by mutational analysis, as this observation was the first to detail a post-translational modification of a non-canonical nucleotidyl transferase. Mutant Cid1, in which serine 404 was replaced by alanine, was tested for its capacity to reinforce the S-M checkpoint when DNA replication is inhibited (Wang et al. 2000), and for its activity *in vitro*. Unlike catalytically inactive Cid1, non-phosphorylated Cid1 fully resembled WT Cid1 both in activity *in vitro* and phenotypic characteristics *in vivo*. As such, the significance of the C-terminal post-translational modification of Cid1 remains to be unveiled. Other possible functional roles of the phosphorylation not investigated here could include alteration of protein half-life, protein interactions or subcellular localisation. On the other hand, it is also feasible that the identified phosphorylation site on Cid1 is unspecific. If the phosphorylation site was not associated with a selective disadvantage, there would have been no evolutionary pressure to change it (Lienhard 2008).

CHAPTER IV. ZCCHC11 and HISTONE mRNA METABOLISM

Histones have the capacity to interfere non-specifically with a variety of cellular processes, and hence to be toxic if they accumulate to levels that exceed the capacity of the cell to incorporate them into nucleosomes and chromatin (Osley 1991). Synthesis of most core histones is therefore tightly linked to ongoing DNA replication during S phase. This is achieved in large part by cell cycle-dependent changes in histone mRNA levels. Inhibition of DNA replication in mammalian cells, for example on exposure to the ribonucleotide reductase inhibitor HU, leads to the rapid and selective degradation of replication-dependent histone mRNAs.

A recent study suggested that 3' oligouridylation of replication-dependent histone mRNAs is a rate-limiting step in their cytoplasmic degradation, which occurs via both, 5' - 3' and 3' - 5' exonuclease activities. Two enzymes (PAPD1/hmtPAP/TUTase1 and PAPD5/TUTase3) were tentatively identified as candidates for performing the oligouridylation step (Mullen & Marzluff, 2008). However, these findings were unexpected for the following reasons. PAPD1 has been identified as the enzyme (hmtPAP) responsible for polyadenylation of mitochondrial mRNAs; and immunofluorescence microscopy data suggest that it is an exclusively mitochondrial protein (Tomecki et al. 2004; Nagaike et al. 2005). The amino acid sequence of PAPD5 indicates that it is one of two human orthologues of the well characterised yeast Trf4/Trf5 poly(A) polymerases. Furthermore, PAPD5 was recently shown to be responsible for the adenylation of incomplete ribosomal RNA transcripts in the nucleus (Shcherbik et al. 2010) and to catalise the

addition of AMP residues to RNA substrates *in vitro* (Rammelt et al. 2011).

Human cells possess two uridyl transferases, ZCCHC6 and ZCCHC11, which are orthologues of *S. pombe* Cid1 (see Chapter I.3.3.5). Their preference for uridines was initially identified by an RNA tethering approach in *Xenopus* oocytes (Kwak and Wickens 2007). In addition, the *in vitro* uridylation activity of ZCCHC6 and ZCCHC11 was also demonstrated using affinity-purified enzyme from human cells (Rissland et al. 2007; Heo et al. 2009; Jones et al. 2009). During this study, ZCCHC11 (with its orthologues in mouse and *C. elegans*) has been the subject of much recent attention due to its identification as the enzyme responsible for 3' uridylation of microRNAs (miRNAs) and their cytoplasmic precursors (Hagan et al. 2009; Heo et al. 2009; Jones et al. 2009; Lehrbach et al. 2009).

In this chapter, the possibility that either ZCCHC6 or ZCCHC11 could be responsible for uridylation of cytoplasmic replication-dependent histone mRNAs in human cells was investigated.

IV.1. ZCCHC6 and ZCCHC11 localisation

To begin this study, the intracellular localisations of ZCCHC6 and ZCCHC11 were examined. As these proteins are orthologues of the cytoplasmic protein Cid1 in *S. pombe*, it was hypothesised that ZCCHC6 and ZCCHC11 would also localise to the cytoplasm. With the aim of analysing endogenous protein levels, a protocol to affinity purify polyclonal antibodies, previously raised in the lab, was optimised successfully (see Chapter II.1.4.5). Nuclei from HEK293T cells were fractionated by centrifugation through a sucrose cushion and analysed by western blotting using these antibodies. In addition to endogenous protein, exogenous TAP-tagged versions of the same proteins were analysed in parallel in order to verify previous immunofluorescence

experiments performed in the lab. As a control for successful cytoplasmic and nuclear partition, antibodies against tubulin and topoisomerase IIα (Top2a) were used, respectively. ZCCHC6 (endogenous and overexpressed) was predominantly cytoplasmic although some protein was detected in the nuclear fraction (Figure IV.1A). In contrast, both forms of the ZCCHC11 protein localised exclusively to the cytoplasm (Figure IV.1B). These results suggested a closer similarity between Cid1 and ZCCHC11 than ZCCHC6 because Cid1 is also localised to the cytoplasm as judged by immunofluorescence. A direct comparison between both systems is however not possible as nuclear/cytoplasmic fractionation cannot be achieved in *S. pombe*. Note that the cytoplasmic fraction in Figure IV.1A is contaminated with the nuclear fraction. This, however, does not negate the conclusion that ZCCHC6 is present in both compartments, as cytoplasmic levels of ZCCHC6-TAP compared to nuclear levels were much higher than those of contaminating Top2a in the cytoplasmic fraction. Furthermore, the nuclear fraction was devoid of highly expressed tubulin, suggesting that the nuclear presence of ZCCHC6 was not a result of cytoplasmic contamination.

Taken together, these experiments indicate an exclusively cytoplasmic localisation for ZCCHC11, recently confirmed by immunofluorescence microscopy of endogenous ZCCHC11 performed by others (Heo et al. 2009); and the presence in both compartments of ZCCHC6, the significance of which remains to be investigated.

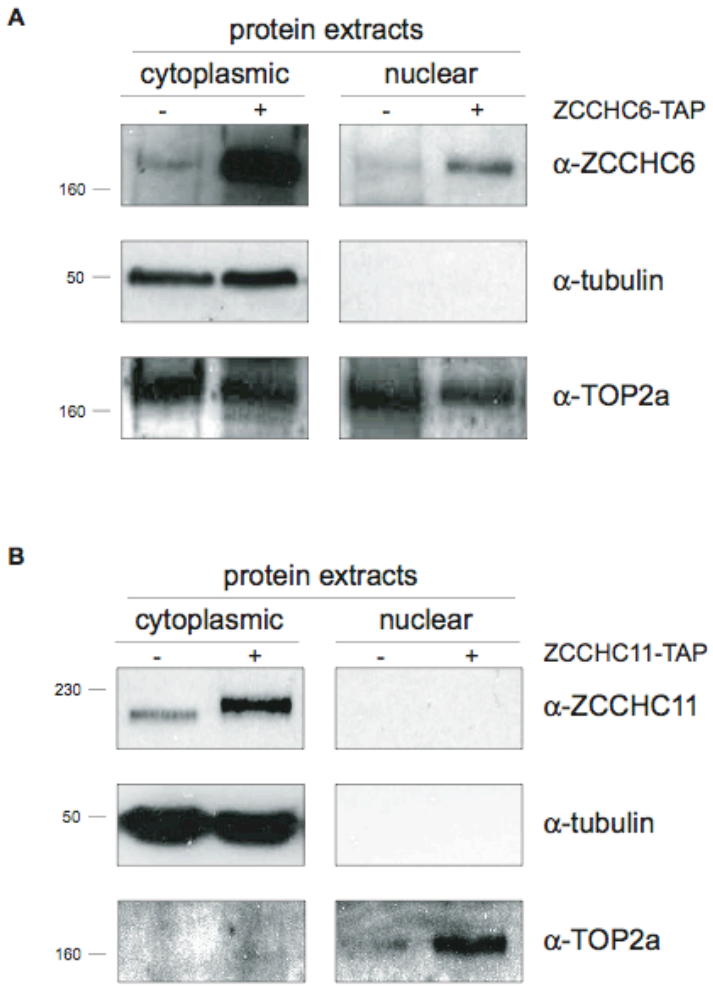

Figure IV.1 Intracellular localisation of ZCCHC6 and ZCCHC11

Cytoplasmic and nuclear HEK293T proteinl extracts were analysed by western blotting with a ZCCHC6 (A) and ZCCHC11 (B) specific antibody. Endogenous protein (-) and epitope-tagged ZCCHC6 and ZCCHC11 derived from pcDNA3 (+) were examined. Tubulin and topoisomerase IIα (α-Top2a) served as controls for cytoplasmic and nuclear localisation, respectively.

IV.2. ZCCHC11 associates with replication dependent histone mRNA

An involvement of the two uridyl transferases ZCCHC6 and ZCCHC11 in the metabolism of replication-dependent histone mRNAs was subsequently investigated by testing the possibility of an association between ZCCHC6 or ZCCHC11 and histone mRNAs *in vivo*. For this purpose, our specific antibodies were used to immunoprecipitate ZCCHC6 and ZCCHC11 along with associated RNAs from formaldehyde cross-linked cell extracts. The same experiment was performed without antibody as a negative control. Input and immunoprecipitates were analysed for the presence of histone HIST2H3 (H3) mRNA by RT-PCR. As shown in

Figure IV.2A, histone H3 mRNA was readily detectable specifically in association with ZCCHC11, but neither with ZCCHC6 nor in the negative control. In contrast, actin mRNA was not specifically immunoprecipitated by either antibody. Quantitative PCR using GAPDH mRNA as an additional negative control showed that H3 mRNA was present at four times higher levels in the α-ZCCHC11 immunoprecipitate compared to the precipitates of α-ZCCHC6 or without antibody (

Figure IV.2B). These data indicate that ZCCHC11 can bind to replication-dependent histone mRNAs *in vivo* and suggest a role for ZCCHC11 in histone mRNA metabolism in the cytoplasm.

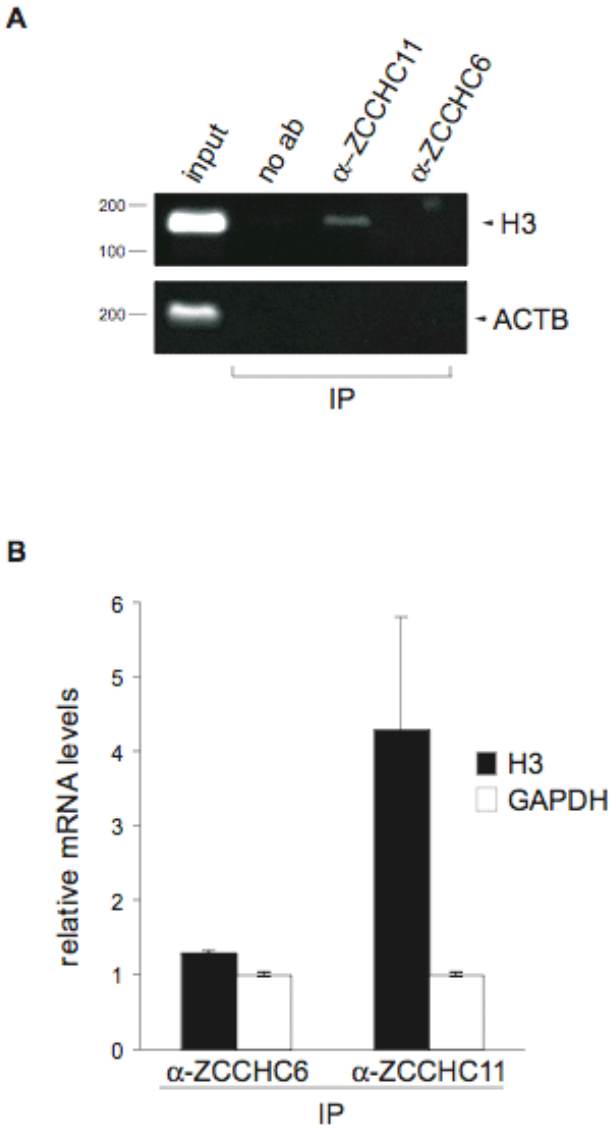

Figure IV.2 ZCCHC11 RNA immunoprecipitation

(A) Following formaldehyde cross-linking, RNPs were immunoprecipitated (IP) using specific antibody or no antibody (ab). Precipitates and 5% input were subjected to RT-PCR using primers specific for the ORF of replication-dependent histone HIST2H3 (H3) and Actin (ACTB) as a negative control. Products were separated by agarose gel electrophoresis. (B) As in (A), but H3 mRNA (and GAPDH mRNA as a control) were analysed using real time RT-PCR. Data (mean of three biological replicates, ±SD) are expressed relative to the signal obtained in the absence of antibodies, which was arbitrarily set to 1.

IV.3. Quantitative analysis of histone mRNA levels following inhibition of DNA replication

Its *in vitro* uridylation activity, localisation and association with HIST2H3 mRNA suggested a potential role for ZCCHC11 in histone mRNA degradation. Rapid decay of replication-dependent histone mRNAs can be induced by HU-mediated inhibition of DNA replication for a short time period, which reduces histone mRNA half-life to 10 minutes compared to one hour during unperturbed S phase (Heintz et al. 1983). Earlier studies have not observed variations between the histone mRNA degradation pathways when DNA replication is completed or inhibited (Kaygun and Marzluff 2005a; Mullen and Marzluff 2008). HU-mediated inhibition of DNA replication therefore represents a valuable means by which to study histone mRNA decay. To test a possible involvement of ZCCHC11 in histone mRNA decay, the rate of histone mRNA degradation was analysed upon short HU treatment (20-40 minutes) following specific gene knock-down of ZCCHC11. In addition, knock-down of Lsm1 was used as a positive control because the Lsm1 protein, and by extension the cytoplasmic Lsm1-7 heptameric complex, had previously been implicated in uridylation-dependent mRNA degradation in human cells and fission yeast (Mullen and Marzluff 2008; Rissland and Norbury 2009). siRNAs expressed from a plasmid as fold-back stem-loop structures and directed against the ORFs of ZCCHC11 and Lsm1 and a scrambled control were utilised to knock-down the expression of those genes in HEK293T cells. The level of down-regulation of all genes in this study is summarised in Table IV.1. Cells expressing the ZCCHC11- and Lsm1-specific or control non-specific siRNAs were then treated with HU for 30 minutes, and replication-dependent histone mRNA levels were determined by RT-PCR using primers specific for the ORF of Hist2H3 (H3, Figure IV.3A) and GAPDH along with a negative control lacking the reverse-trancriptase (Figure IV.3B). As expected, H3 mRNA but not control GAPDH mRNA was rapidly degraded in the control siRNA-expressing cells within 30

minutes of HU treatment. Expression of the ZCCHC11-specific siRNA largely prevented the HU-induced decrease in H3 mRNA levels, while Lsm1-specific siRNA expression abolished histone mRNA destabilisation as determined by real time PCR (Figure IV.3C).

Next, the kinetics of histone mRNA degradation were investigated in more detail. HU was added to the cells for 20 and 45 minutes following siRNA-mediated knock-down of ZCCHC11. In addition to H3 mRNA (Figure IV.4 upper panel), another replication-dependent histone mRNA, Hist2H2 (H2) was analysed by quantitative PCR (lower panel). Histone destabilisation upon HU treatment for 20 and 45 minutes was significantly impaired in the absence of ZCCHC11. The effect was most severe for H2 mRNA following 45 minutes of HU.

These results indicate a general requirement of ZCCHC11 in efficient degradation of replication-dependent histone mRNAs upon inhibition of DNA replication.

IV.4. ZCCHC11 catalytic activity is required for efficient histone mRNA degradation

The involvement of the catalytic nucleotidyl transferase activity of ZCCHC11 in efficient histone mRNA degradation was next investigated. This question was not trivial, as a previous study of the non-canonical poly(A) polymerase Trf4 had shown that in some cases, the presence of the protein, even when catalytically inactive, was sufficient to stimulate RNA degradation (Rougemaille et al. 2007). To this end, a siRNA was designed targeting the 3' UTR of ZCCHC11 mRNA such that ectopic expression of ZCCH11 from a plasmid that lacked its 3' UTR could be used to compensate for loss of endogenous protein. A catalytically inactive version of ZCCHC11 was

constructed (DADA) in which two aspartate residues essential for catalysis were replaced by alanine. These mutations were previously shown to abolish ZCCHC11 polymerase activity *in vitro* (Heo et al. 2009; Jones et al. 2009). Finally, a mutant lacking the phosphorylation site Ser773 was also constructed (SA) and tested. A large-scale proteomic analysis had previously revealed this consensus site on ZCCHC11, potentially recognised by the ATM checkpoint kinase upon DNA damage (Matsuoka et al. 2007). This site is conserved amongst mammals (see Chapter I.5.2.1 for more detail).

These plasmids, as well as an empty vector as a control, were transfected into HEK293T cells 48h post siRNA transfection and ZCCHC11 protein and mRNA levels were examined one day later. Crucially, endogenous ZCCHC11 levels were restored by introduction of the three ZCCHC11 expression plasmids (Figure IV.5A-B). Cells were then treated with HU as described above and histone mRNA levels were analysed. The negative effect of ZCCHC11 knock-down on histone mRNA degradation was completely reversed by co-expression of WT ZCCHC11 cDNA, reaffirming a direct role of ZCCHC11 in histone mRNA degradation and more specifically, ruling out off-target effects of the short hairpin RNA (Figure IV.5C). In contrast, the site-directed mutant version of ZCCHC11 lacking the two aspartate residues essential for catalysis was unable to support HU-induced histone mRNA turnover in this assay, indicating that ZCCHC11 catalytic activity is required for its mRNA destabilising function. Phosphorylation of Ser 773 did not appear to be important for ZCCHC11 function in this assay, as the SA mutant equaled the ability of WT ZCCHC11 to restore histone mRNAs degradation. In conclusion, these results show a direct requirement for catalytic activity of ZCCHC11 to stimulate H3 mRNA degradation upon inhibition of DNA replication.

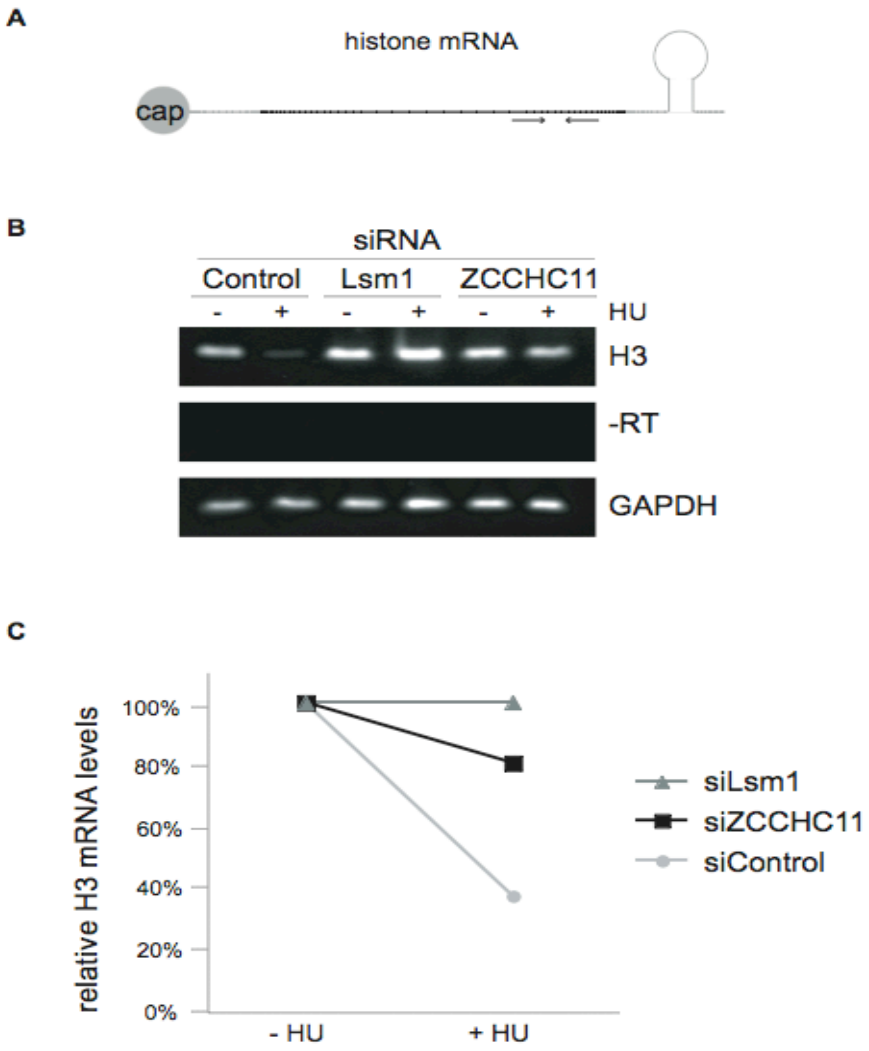

Figure IV.3 Degradation of Hist2H3 mRNA

(A) Diagram depicting position of PCR oligonucleotides used to amplify histone mRNA. (B) ZCCHC11 was knocked down using siRNAs directed against its ORF and expressed from a plasmid along with a scrambled negative siRNA control and Lsm1-specific siRNA. 72 hours following plasmid transfection, HEK293T cells were treated with (+) 5 mM hydroxyurea (HU) or not (-) for 30 minutes before being harvested. Total RNA was isolated and analysed by semi-quantitative (B) and quantitative (C) RT-PCR. (B) PCR products specific for H3 and GAPDH mRNA and lacking reverse transcriptase (-RT) as a negative control were separated by agarose gel electrophoresis. (C) H3 mRNA values were normalised to GAPDH mRNA and expressed relative to the RNA amount in untreated samples, which was arbitrarily set to 1.

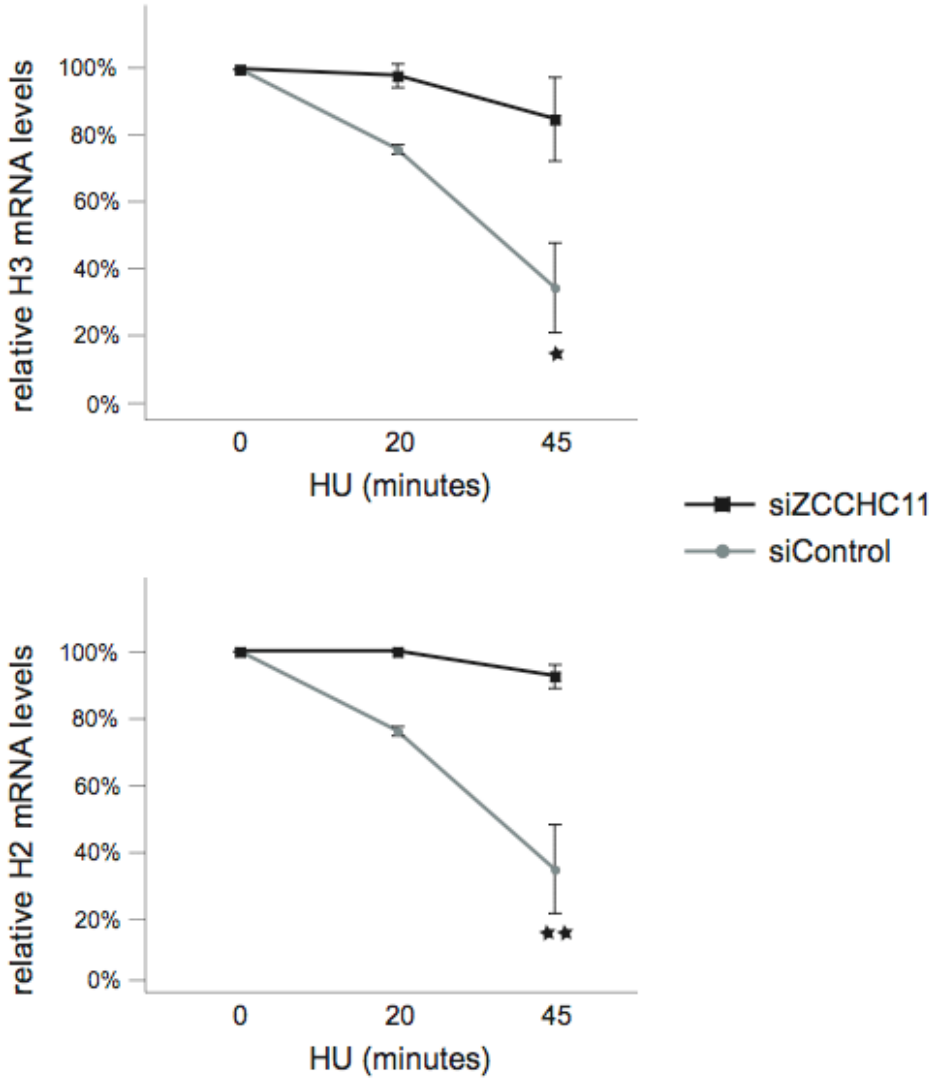

Figure IV.4 Requirement of ZCCHC11 in H2 and H3 mRNA degradation

As in Figure IV.3, but cells were treated with HU for 20 and 45 minutes following siRNA-mediated knock-down. Oligonucleotides for the ORF of Hist2H3 (A) and Hist2H2 (B) were used. Specific mRNA values (mean of three biological replicates ±SD) are indicated. One-tailed Student's t-test: * $P < 0.05$, ** $P < 0.01$

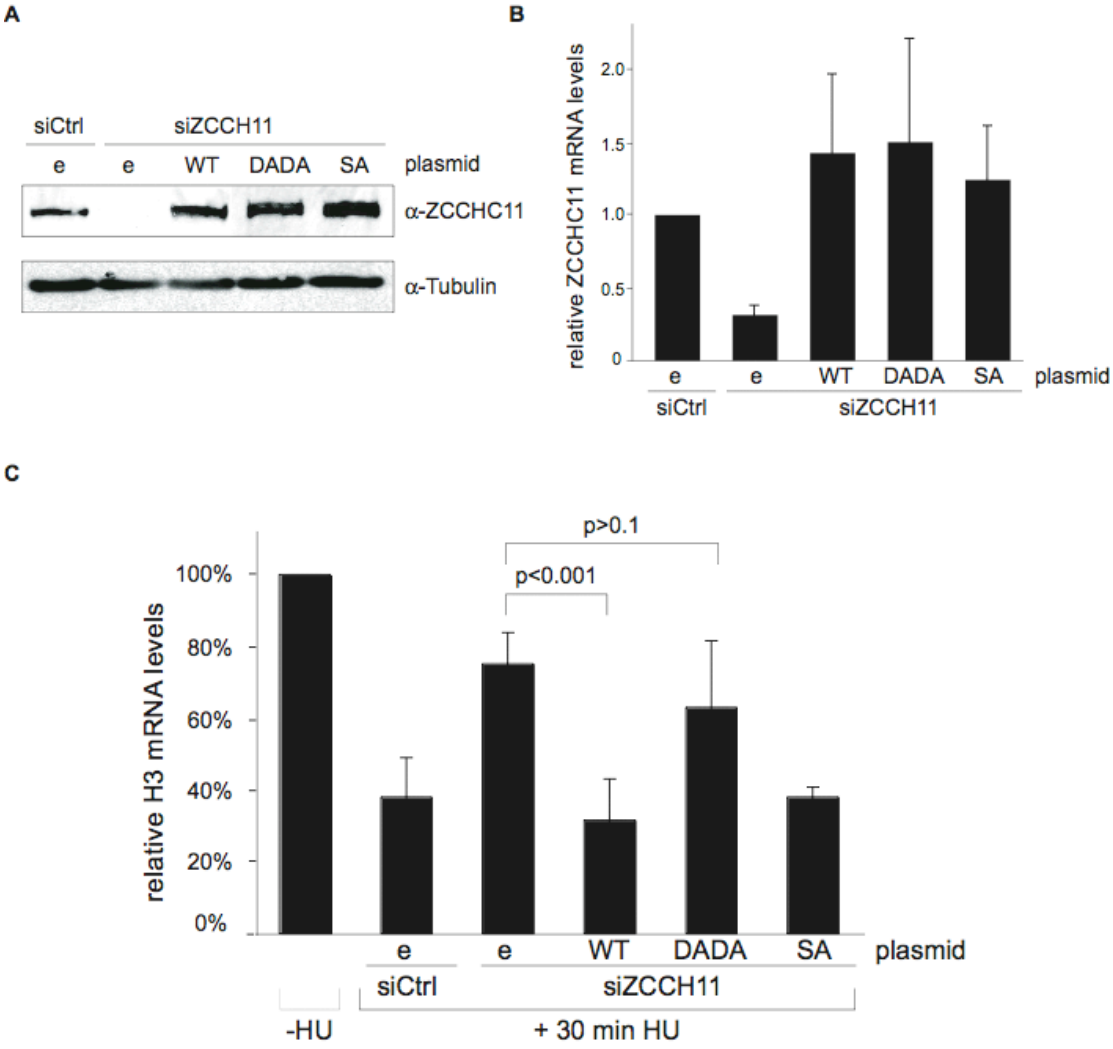

Figure IV.5 Requirement of ZCCHC11 activity in H3 mRNA degradation

(A, B) ZCCHC11 was knocked down using siRNAs directed against its 3' UTR along with a scrambled siRNA control (ctrl). 48 hours following siRNA transfection, HEK293T cells were transfected with either empty plasmid (e), or derivatives encoding WT, catalytically inactive mutant (DADA) or phosphorylation site Ser773 mutant (SA) ZCCHC11, as indicated. The expression of ZCCHC11 was analysed by western blot using anti-ZCCHC11 (A) and by quantitative RT-PCR (B) 72 hours after siRNA transfection. (C) As in (B) but cells were treated with (+) or without (-) 5 mM hydroxyurea (HU) for 30 minutes before being harvested. Total RNA was isolated and analysed by real time RT-PCR. H3 mRNA values (mean of five biological replicates ±SD) were normalised to GAPDH mRNA and expressed relative to the RNA amount in untreated samples, which was arbitrarily set to 1.

IV.5. Reduced histone mRNA uridylation on ZCCHC11 knock-down

The findings above suggested that the uridylation activity of ZCCHC11 might be directly responsible for the presence of U-tails previously observed on histone mRNAs (Mullen and Marzluff 2008). To address this possibility, a circularised rapid amplification of cDNA ends (cRACE) approach was used to detect terminal uridylation of histone mRNAs and to determine the effect of ZCCHC11 knock-down on these sequences (Figure IV.6A). This approach consisted of intra-molecular RNA ligation followed by RT-PCR using divergent primers across the ligation and sequencing of the PCR products. Using this technique, the precise determination of nucleotides from both 3' and 5' RNA ends was possible. In order to examine capped transcripts, which constituted the majority of transcripts in total RNA samples, the RNA was treated with tobacco acid pyrophosphatase (TAP) prior to intra-molecular ligation allowing removal of the 5' cap. Products representing decapped degradation intermediates resulted from untreated circularised RNA. Initial experiments recapitulated those described in an earlier study (Mullen and Marzluff 2008) and used RNA prepared from asynchronous HeLa cells. In the present study, the frequency of histone mRNA uridylation under these circumstances was too low to allow a statistically robust investigation of its dependence on ZCCHC11 activity. This low frequency suggests that uridylated mRNAs are turned over very rapidly *in vivo*, consistent with the documented roles of 3' UMP residues in RNA turnover pathways (Chapter I.2.2).

RNA isolated from cells synchronised in late S phase when uridylation of histone mRNAs is naturally occurring (Mullen and Marzluff 2008) was therefore utilised instead. Cells were synchronised by double thymidine blockade and release, a method that allows synchronous progression of HeLa cells through S phase (Whitfield et al. 2000). Under these

circumstances, the variant of the cRACE protocol using untreated RNA at the ligation step (to selectively monitor de-capped degradation intermediates; Figure IV.6A) yielded insufficient material for quantitative analysis. Nonetheless, capture of capped transcripts by pre-treatment of the RNA with TAP allowed the cloning and sequencing of substantial numbers of HIST2H2AC cDNAs. Approximately 30% of the sequences included terminal non-templated uridyl residues. When the cRACE protocol was carried out using TAP-treated RNA from cells in which ZCCHC11 had been knocked down, there was an almost two-fold reduction in the proportion of uridylated sequences (P= 0.15, chi-square test, Figure IV.6B). Sequence information of the cDNAs ends used in this statistical analysis showed that the start and the end of captured transcripts was distributed evenly between control and ZCCHC11 knock-down cells (Figure IV.7A). Interestingly, a few clones were isolated from decapped samples corresponding to RNAs that had undergone extensive 3' - 5' degradation and terminated in non-templated uridyl residues (Figure IV.7B). This observation suggests that 3' uridylation can continue during histone mRNA decay, and might serve, for example, to re-initiate stalled exonucleolysis.

It should be noted that the UMP tails detected in this study were of one or two residues in length and would be too short to allow their detection by oligo (dA)-primed reverse transcription as used by (Mullen and Marzluff 2008). The fact that longer oligo(U) tails were not observed suggests that such tails are comparatively rare and/or unstable. The data presented here are consistent with the notion that the mRNAs of HIST2H2AC, and potentially other replication-dependent histone genes, are direct targets of the ZCCHC11 uridyl transferase. The lack of a larger effect of proportional uridylation may be due to incomplete ZCCHC11 knock-down, or functional redundancy between ZCCHC11 and other uridyl transferases, even though ZCCHC11 knock-down alone was sufficient to stabilise histone mRNAs significantly (see section IV.6) whereas ZCCHC6 knock-down was not.

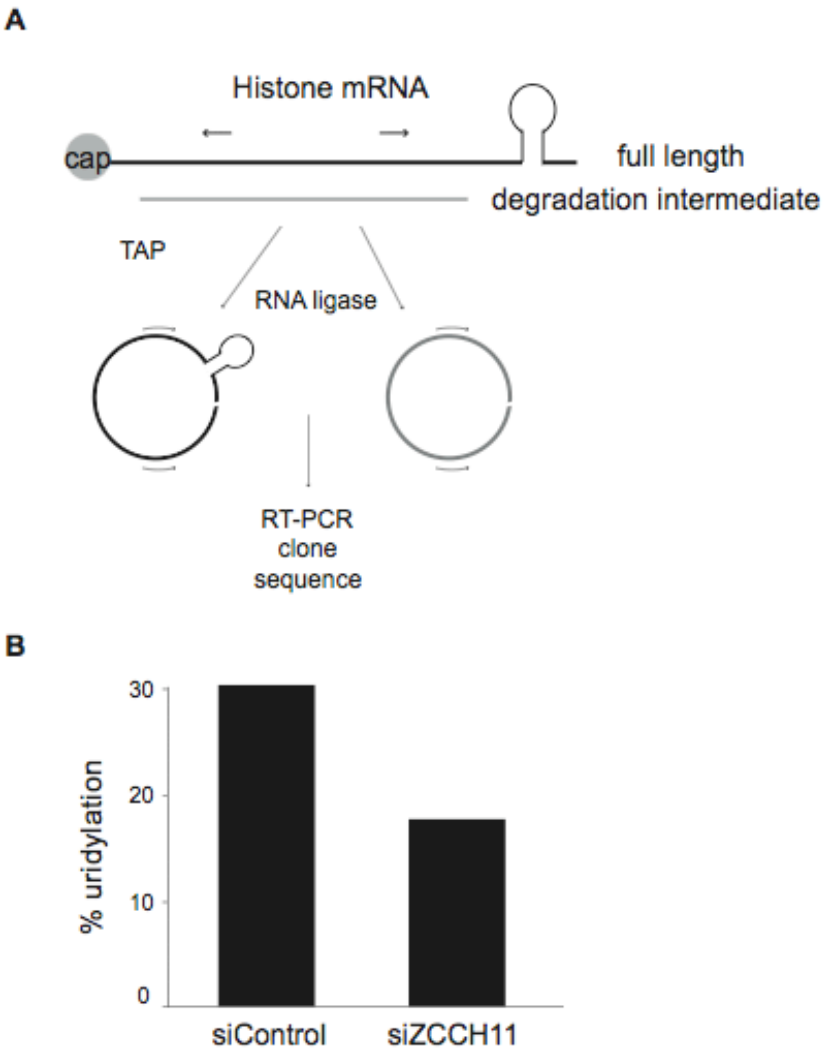

Figure IV.6 Histone mRNA uridylation

(A) Overview of the cRACE procedure used to capture capped HIST2H2AC transcripts (black) and degradation intermediates (grey). Arrows indicate the position of the PCR primers used. (B) cRACE was performed on TAP-treated RNA isolated from HeLa cells harvested at the end of S phase following siRNA-mediated knock-down. The percentage of cRACE products containing terminal uridyl residues is shown for control and ZCCHC11 knock-down cells (n=14/46, 8/48, respectively).

A

5' ends	siCtrl	siZCCHC11
TTCAATCTTATTTTGTTGCGAGGTTCTGAG	0	2
TCAATCTTATTTTGTTGCGAGGTTCTGAG	1	4
CAATCTTATTTTGTTGCGAGGTTCTGAG	1	3
AATCTTATTTTGTTGCGAGGTTCTGAG	30	21
ATCTTATTTTGTTGCGAGGTTCTGAG	4	9
TCTTATTTTGTTGCGAGGTTCTGAG	1	0
CTTATTTTGTTGCGAGGTTCTGAG	0	1
TTATTTTGTTGCGAGGTTCTGAG	1	1
TATTTTGTTGCGAGGTTCTGAG	2	4
ATTTTGTTGCGAGGTTCTGAG	3	3
TTTTGTTGCGAGGTTCTGAG	1	0
TGTTGCGAGGTTCTGAG	1	0
GTTGCGAGGTTCTGAG	1	0

3' ends	siCtrl	siZCCHC11
AAGGCTCTTTTTAGAGCCACCC	1	1
AAGGCTCTTTTTAGAGCCACC	7	4
AAGGCTCTTTTTAGAGCCACUU	1	1
AAGGCTCTTTTTAGAGCCACU	9	5
AAGGCTCTTTTTAGAGCCAC	7	12
AAGGCTCTTTTTAGAGCCAUU	4	2
AAGGCTCTTTTTAGAGCCA	5	5
AAGGCTCTTTTTAGAGCC	1	1
AAGGCTCTTTTTAGAGC	1	3
AAGGCTCTTTTTAGAG	8	13
AAGGCTCTTTTTAGA	2	1

stemloop
AAGGCTCTTTTTAGAGCCACCC

B

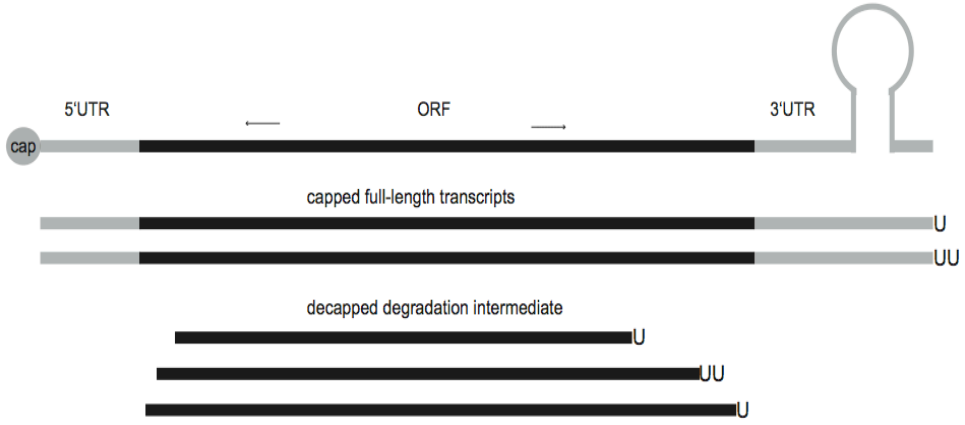

Figure IV.7 Sequence information of H2 mRNA

(A) Sequence information of HIST2H2AC cRACE product ends from TAP-treated (capped) RNA is shown along with the frequency of each sequence in Control and ZCCHC11 knock-down. Detected uridyl residues on 3' ends are highlighted. The 3' stem-loop sequence is indicated. (B) Diagram depicting a histone mRNA with its ORF, 5' and 3' UTRs. Arrows indicate the position of primers used for cRACE. The positions of uridyl residues detected by cRACE are shown on capped full length transcripts and decapped degradation intermediates.

IV.6. Involvement of other non-canonical PAPs in histone mRNA degradation

The reported functions of PAPD1 and PAPD5 in histone mRNA metabolism (Mullen and Marzluff 2008) were next investigated. RNAi was used to deplete PAPD1, PAPD5 or Lsm1 as a positive control. The effect on histone mRNA degradation following HU treatment was then tested. Although the extent of knock-down in each case was comparable to that achieved with ZCCHC11 (Table IV.1), neither siRNA against PAPD1 nor PAPD5 had any significant impact on HU-induced histone mRNA destabilisation (Figure IV.8A). These data are therefore at odds with those previously described, which implicated PAPD1 and PAPD5, but not ZCCHC11, in this process (Mullen and Marzluff 2008).

This RNA turnover pathway does not appear to operate only under the non-physiological condition of HU exposure, as steady-state histone H3 mRNA levels were significantly elevated in asynchronous cell populations expressing siRNAs targeting ZCCHC11 or Lsm1 (Figure IV.8B). Again, knock-down of PAPD1 or PAPD5 had no such effect.

ZCCHC11 was previously found to be responsible for the uridylation of cytoplasmic pre-miRNAs on recruitment by its RNA-binding partner Lin28, and for the uridylation of mature miRNAs in such a way as to influence their biological activity. To exclude the possibility that the ZCCHC11-dependent effect on histone mRNA turnover is mediated indirectly via miRNAs, the Drosha ribonuclease was knocked down in order to inhibit miRNA maturation. No changes in the rate of histone mRNA degradation were found upon S phase arrest under these conditions (Figure IV.8A) nor were any changes observed in steady-state histone mRNA levels (Figure IV.8B).

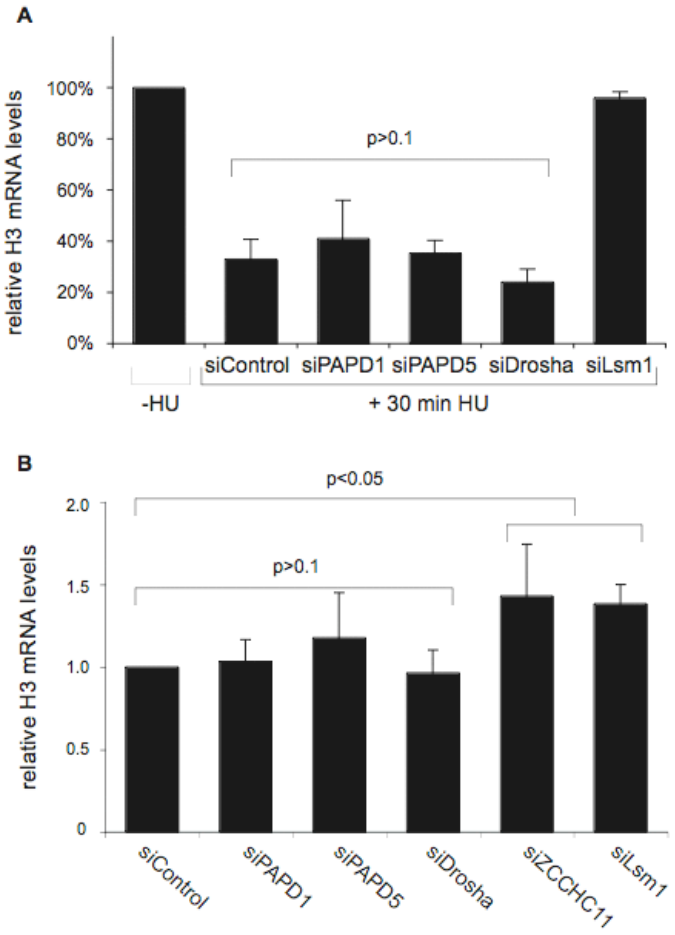

Figure IV.8 Involvement of other ncPAPs in histone mRNA degradation

(A) HEK293T cells were transfected with control or specific siRNAs directed against PAPD1, PAPD5, Drosha or Lsm1. 72h after transfection, cells were treated with (+) or without (-) 5mM hydroxyurea (HU) for 30 minutes. RNA was analysed as in Figure 2C. The mean of at least three biological replicates ±SD is indicated. (B) Steady state H3 mRNA levels in asynchronous cells transfected with the siRNA expression vectors indicated were compared to those in cells expressing the scrambled control siRNA.

shRNA	ZCCHC11	PAPD1	PAPD5	Lsm1	Drosha
Remaining RNA	40%	43%	35%	51%	36%

Table IV.1 shRNA knock-down efficiency

The efficiency of each knock-down was monitored by real-time qRT-PCR 72 hours after transfection.

IV.7. ZCCCH11 expression is regulated during S phase

As ZCCHC11 is required for histone mRNA regulation, a further interesting possibility would be that it might itself be regulated in some way during S phase progression. HeLa cells were synchronised by double thymidine block and release (Figure IV.9A), and mRNA levels were monitored during the subsequent progression through S phase. As expected, histone H3 mRNA levels rose to a peak by four hours after release, when cells were in mid-S phase, and were rapidly degraded by the end of S phase. By contrast, ZCCHC11 mRNA and protein levels declined slightly by the four hour time point, but subsequently recovered as cells completed S phase (Figure IV.9B). This pattern of expression would be consistent with suppression of ZCCHC11 activity during S phase progression and a physiological role for this activity in the degradation of histone mRNAs on completion of DNA replication, as suggested by the observation of histone mRNA accumulation on ZCCHC11 knock-down in asynchronous cells (Figure IV.9B). Comparable S phase-specific regulation was not seen in the case of PAPD1 or PAPD5 (data not shown).

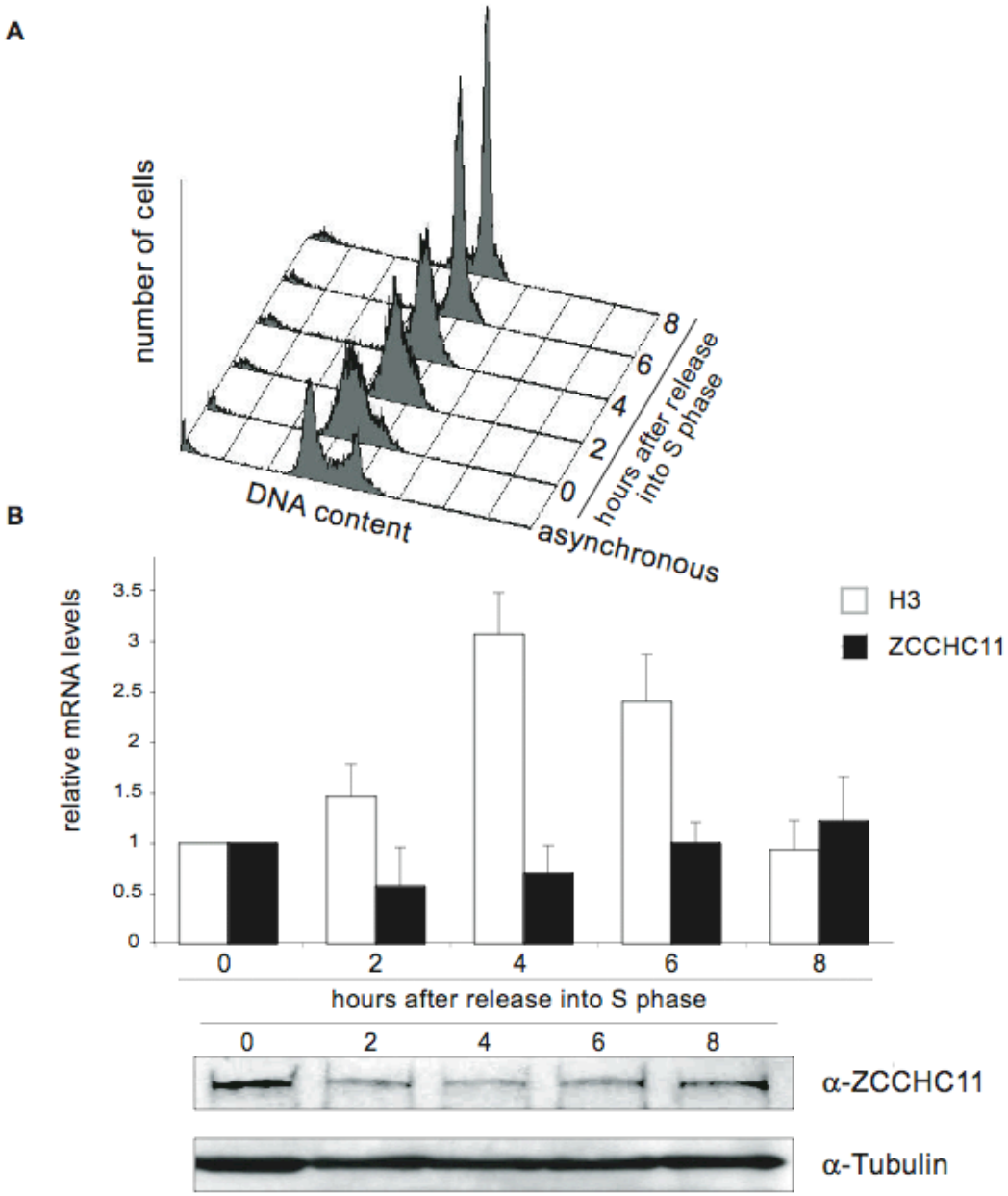

Figure IV.9 ZCCHC11 expression during S phase

HeLa cells were blocked in early S phase by a double thymidine block and then released. (A) The cell cycle distribution of propidium iodide stained cells was analysed by flow cytometry at the indicated times after release from the block, and in asynchronous cells. (B) Total RNA was isolated at time points indicated and analysed by real time RT-PCR using specific oligonucleotides (upper panel). H3 and ZCCHC11 mRNA levels (average of 3 replicates ±SD) were normalised to GAPDH mRNA and expressed in relation to RNA obtained from cells at the time when the block was removed (0 hours). ZCCHC11 and tubulin protein levels were measured by western blotting at the same time points (lower panel).

IV.8. Discussion

The data presented in this chapter implicate the human cytoplasmic uridyl transferase ZCCHC11 in the degradation of replication-dependent histone mRNAs following inhibition or completion of DNA replication. Histone mRNAs were selectively found in association with ZCCHC11 but not with ZCCHC6, an orthologue of ZCCHC11, which is also present in the cytoplasm. Knock-down of ZCCHC11 blocked mRNA degradation of two histone mRNAs following inhibition of DNA replication. This blockade could be relieved by co-expression of WT but not catalytically mutant ZCCHC11. Importantly, knock-down of PAPD1 or PAPD5, previously proposed as candidate histone mRNA uridyl transferases, had no such effect. The reason for this discrepancy with earlier published data is currently unclear, but given the involvement of 3' uridylation in the histone mRNA turnover pathway in the cytoplasm, it is easier to envisage a role in this pathway for the cytoplasmic terminal U-transferase ZCCHC11 than for the poly (A) polymerases PAPD1 or PAPD5, especially as the former is a mitochondrial and the latter a nuclear enzyme. Moreover, recent *in vitro* experiments performed by others using the 3' UTR of H2a as a substrate and recombinant PADP5 showed AMP but not UMP incorporation to the 3' end of the substrate (Rammelt et al. 2011).

Furthermore, a reduction in the proportion of histone transcripts that were uridylated at the end of S phase was observed following ZCCHC11 knock-down, indicating a direct role of the protein in modifying the 3' end of these RNAs. U-tails found on histone mRNAs by (Mullen and Marzluff 2008) were of up to eight residues in length, which is the only report to date of such long U-tails. In this study, as in numerous other reports of U-tails in fission yeast, worms and mammalian cells, the U-tails detected were short (1-3 residues). Again, the reason for this discrepancy is unclear. However, these modifications are rare and unstable as they serve to initiate very rapid 3' – 5' exonucleolytic RNA degradation and may therefore be difficult to capture. In

order to increase the frequency of uridyl residues found on histone mRNAs for statistical purposes here, RNA was specifically analysed from cells in late S phase when rapid histone mRNA decay takes place (Harris et al. 1991). The increased uridylation activity observed at the end of S phase suggests that ZCCHC11 is mostly active on histone mRNAs at this time point of the human cell cycle. In accordance with this, increased expression levels of ZCCHC11 were found at the end of S phase compared to mid S phase when histone mRNAs are produced. Furthermore, steady state histone mRNA levels were also increased upon ZCCHC11 knock-down in asynchronous cells. It can be hypothesised that these increased mRNA levels mainly arise from cells in S phase.

Efficient degradation of histone mRNAs also requires SLBP and Lsm1. It was suggested that SLBP remains bound to histone mRNAs while the oligouridine tract is added and the Lsm1-7 complex recruited, as SLBP was found in interaction with Lsm1 in an RNA-dependent manner (Mullen and Marzluff 2008). As such, SLBP was suggested to recruit the uridyl transferase to the 3' end of histone mRNAs. But since non-templated uridine residues were found in the body of histone mRNA upstream of the stem-loop sequence in this study, the necessity of SLBP in recruiting the uridyl transferase to the transcript is questionable. It will be interesting to investigate ZCCHC11 interactions with other factors involved in histone mRNA degradation (see Chapter I.4.4) in the future.

In addition to the role of ZCCHC11 in the uridylation-dependent pathway of histone mRNA turnover discussed here, the same enzyme has been implicated in miRNA regulation. The biological significance of the combination of these two important regulatory activities in a single RNA uridyl transferase awaits further clarification. Like *S. pombe* Cid1, ZCCHC11 does not display inherent substrate specificity *in vitro* (Jones et al. 2009) suggesting the involvement of other factors in targeting specific RNAs. One study has implicated Lin28 in the positive regulation of histone mRNAs in

embryonic cells by binding their open reading frame (Xu and Huang 2009). It will be interesting to determine whether Lin28 or a functional analog of Lin28 recruits ZCCHC11 to histone mRNAs in somatic cells and how the same enzyme exhibits these two different regulatory activities. Further studies may also help to explain the significance of the comparatively large size of ZCCHC11, its possession of zinc finger motifs and the duplication of the catalytic domain, while only one of the domains retains amino acid residues critical for activity.

Amino acid sequence comparisons and biochemical assays suggest that the ZCCHC6 protein might perform ZCCHC11-like roles, but these do not seem to relate to turnover of the histone mRNAs examined here or of miRNAs examined by others. The localisation of ZCCHC6 to the nucleus and the cytoplasm clearly distinguishes it from its orthologue ZCCHC11. It can be suggested that ZCCHC6 might perform two distinct functions related to its localisation. Another possibility could be that the protein shuttles between compartments, possibly in association with RNA. Surprisingly, immunofluorescence experiments of overexpressed ZCCHC6 showed an exclusively cytoplasmic localisation (Andrea Mikulasova and Chris Norbury, unpublished). Further investigations will be needed to explore the role of ZCCHC6. It will also be interesting to determine whether either ZCCHC6 or ZCCHC11 are also involved in the uridylation and turnover of polyadenylated mRNAs, as is the related uridyl transferase Cid1 in fission yeast (Rissland and Norbury 2009).

CHAPTER V. ZCCHC11 and the HUMAN CELL CYCLE

Data presented in Chapter IV implicate the uridyl transferase ZCCHC11 in the regulation of replication-dependent histone mRNAs. The tight coordination of replication-dependent histone levels with ongoing DNA replication is vital for the cell to ensure accurate assembly of newly synthesised DNA with nucleosomes. Disruption of chromatin assembly in S phase results in spontaneous DNA damage and cell cycle arrest in mammals (Ye et al. 2003). Furthermore, an excess of histones has detrimental cellular effects such as chromatin aggregation, saturation of chromatin-modifying enzymes and transcriptional interference as a result of suboptimal stoichiometry between DNA and histones (Gunjan et al. 2006). Hence, the regulation of histone levels is crucial to prevent DNA damage and genome instability.

To ensure genome integrity, specialised cell cycle checkpoints monitor successful DNA replication and segregation (see Chapter I.5). If DNA replication is not completed faithfully in S phase, the activated S phase-mitosis (S-M) checkpoint will lead to inhibition of cyclin-dependent kinase activity and hence prevent entry into mitosis. As a consequence of DNA damage, cell cycle progression is blocked to allow repair of the damaged DNA. Should the damage be irreparable, there is resultant permanent arrest of the cell cycle or cell death. Crucial events in the DNA damage response include phosphorylation of the effector kinases Chk1 and Chk2 and modification of chromatin. Both modifications are performed by the PIKKs ATM and ATR. Caffeine, an inhibitor of ATM/ATR, overrides the S-M checkpoint and triggers entry into mitosis despite incomplete or faulty DNA

replication. Notably, caffeine was one of the two drugs used in the screen that identified Cid1 (Wang et al. 1999), the orthologue of ZCCHC11 in *S. pombe.*

Recent studies have identified a role for ZCCHC11 in the regulation of microRNAs (miRNAs) (Hagan et al. 2009; Heo et al. 2009; Jones et al. 2009; Lehrbach et al. 2009). These miRNAs include the conserved regulator *let-7* and the cytokine-targeting miR26. ZCCHC11 function has consequently been associated with embryogenesis, development, tumorigenesis and immunity. However, a direct link between ZCCHC11 and the mammalian cell cycle has not yet been described. Indeed, no mammalian non-canonical poly (A/U) polymerase has so far been directly implicated in the regulation of the cell cycle or the activation of replication checkpoints.

This chapter explores the consequences of down-regulation of ZCCHC11 in human cells, with particular reference to cell cycle effects and the induction of DNA damage. The relationship between these phenotypes and the function of ZCCHC11 in histone mRNA turnover will also be discussed.

V.1. ZCCHC11 knock-down causes delays in S phase

ZCCHC11 expression is regulated during S phase (Chapter IV.7). This observation raised the question of whether ZCCHC11 has a role in regulation of the human cell cycle. To investigate the physiological function of ZCCHC11 in the completion of DNA replication and S phase, the effect of ZCCHC11 knock-down on cell cycle distribution was closely analysed in experiments described in the following sections.

Initially, the progression of cells through the cell cycle following release from S phase arrest was examined in more detail in control and ZCCHC11 knock-

down cells. Following optimisation of conditions, flow cytometric analysis of propidium iodide stained cells showed that almost all control and ZCCHC11 depleted cells were blocked in S phase after exposure to HU for 16 hours (Figure V.1, time 0). Interestingly, ZCCHC11 knock-down cells were as efficiently arrested as control cells following HU treatment, suggesting that there is no deficiency in the replication checkpoint under these conditions. Subsequent removal of HU allowed synchronous progression of the cells through S phase. No major difference between control and ZCCHC11 knock-down cells was observed at the time points 0, 1 and 3 hours, when cells resumed S phase efficiently. However, a change in cell cycle progression was detected after 5 hours, the time point corresponding to late S phase and completion of DNA replication. siZCCHC11-transfected cells showed a defect in the progression from S phase into G2 (Figure V.1B) as the peak seen in the control population was missing in the ZCCHC11 knock-down population. The delayed entrance of these cells into G2 suggested problematic but eventually successful completion of DNA replication. It can be hypothesised that this problem arose from inefficient histone mRNA degradation on ZCCHC11 depletion and defective chromatin assembly as a consequence. Moreover, this result provided a first link between ZCCHC11 and a defect in the human cell cycle and was therefore investigated further.

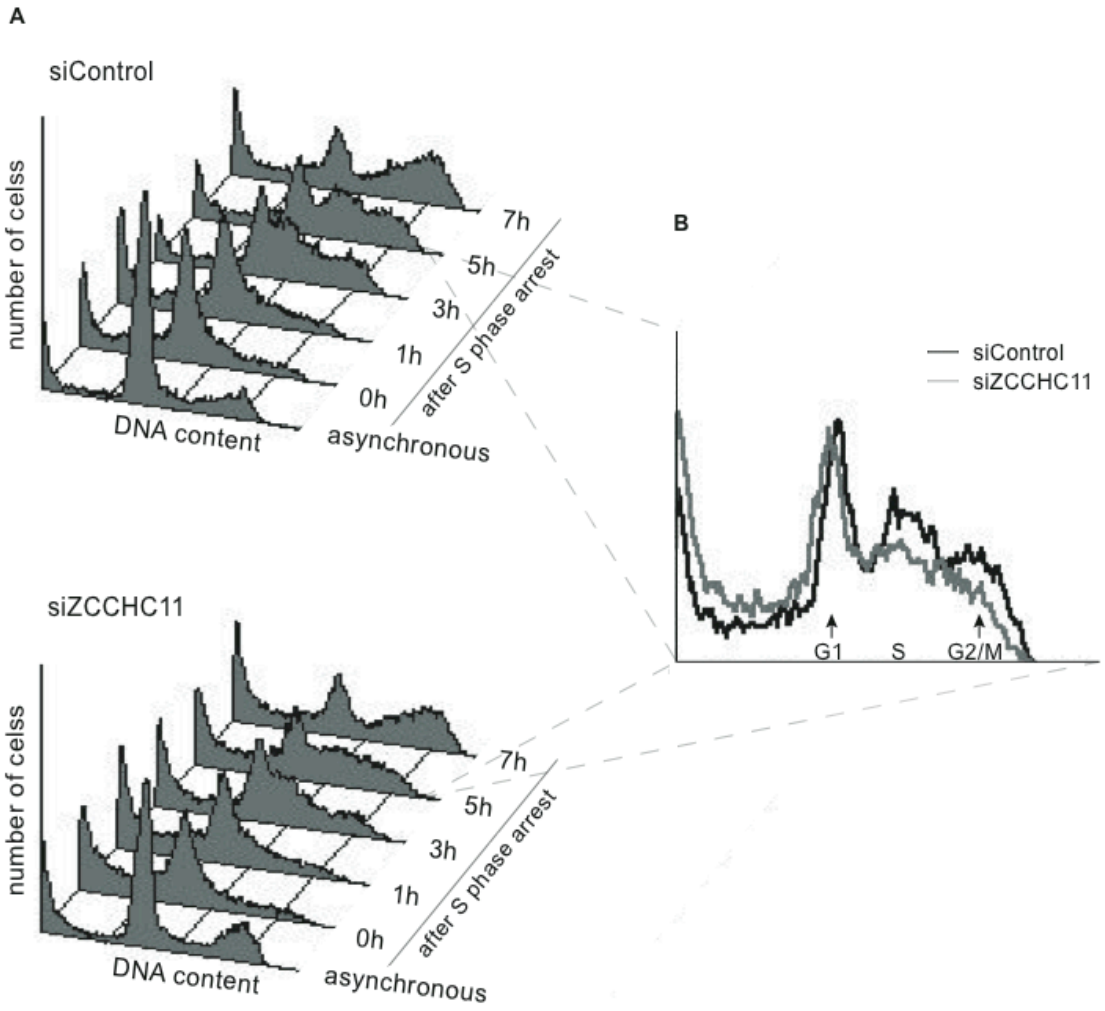

Figure V.1 Cell progression through S phase

Following siRNA knock-down, HeLa cells were arrested in S phase by the addition of 0.2 mM HU to the medium for 16 hours. HU was then removed and cells were harvested at indicated time points after HU removal. The cell cycle distribution of propidium iodide-stained cells was analysed by flow cytometry in asynchronous cells and at the indicated times after release from the arrest. (B) Histograms of siControl (black) and siZCCHC11 (grey) cells corresponding to the time point 5 hours were overlaid and enlarged. The positions of DNA contents corresponding to G1, S and G2/M are indicated.

V.2. Cell cycle distribution of cells in ZCCHC11 knock-down

With the aim of investigating this cell cycle phenotype in more depth, the establishment of stable ZCCHC11 knock-down in HEK293 and HeLa cells was attempted. It is worth noting that depletion of ZCCHC11 in embryonic stem cells as well as in a carcinoma cell line had previously caused significant technical difficulties, as ZCCHC11 levels recovered shortly after siRNA transfection in these cell types (Heo et al. 2009). However, such difficulties were not encountered in the system studied here and in several other studies using mammalian cell lines (Hagan et al. 2009; Jones et al. 2009). Nonetheless, it was not clear how the cell would cope with loss of ZCCHC11 over a long time period. For this purpose, plasmids expressing specific siRNAs and which contained a puromycin resistance gene were transfected and cells retaining the plasmids were selected by addition of low levels of puromycin. After three weeks, western blot experiments showed that the ZCCHC11 protein in HEK293 cells was still successfully depleted (Figure V.2A). It is possible that increased levels of ZCCHC6, the close homologue of ZCCHC11, could have compensated for loss of ZCCHC11 over this time period, but such increased ZCCHC6 levels were not observed as judged by quantitative RT-PCR. The effect of ZCCHC11 knock-down in comparison with control cells selected over three weeks was next examined by flow cytometry of propidium iodide (PI) stained cells (Figure V.2B). Strikingly, the cell cycle distribution showed substantial differences in the ZCCHC11 knock-down compared to the control. The proportions of cells in G1 with 2C DNA content and in S phase were reduced while that of cells containing 4C DNA content (in G2 or mitosis) was increased following depletion of ZCCHC11.

In order to quantify more accurately the S phase fraction, cells were pulse-labelled with the thymidine analogue bromo-deoxyuridine (BrdU) for 30

minutes before harvesting. BrdU incorporation was monitored using anti-BrdU and total DNA was stained with propidium iodide, allowing an estimate of the percentage of cells that were undergoing S phase during the time of labelling. The contour plot in Figure V.2C indicates a reduced proportion of cells incorporating BrdU in the siZCCHC11 sample compared to the siControl. In particular, cells in early S phase were affected (R1: 16.6% versus 4.9%). These results showed that absence of ZCCHC11 over a prolonged time period caused serious cell cycle perturbations. These data also opened up several questions as to the nature and consequences of the ZCCHC11 phenotype.

Attempts to maintain ZCCHC11-specific shRNAs in HEK293 cells for longer than three weeks following puromycin selection were not successful. This suggests that there was substantial selective pressure on cells to recover ZCCH11 levels or in some way compensate for its depletion. This finding indirectly highlights the importance of ZCCHC11 to the cells and also explains the difficulties encountered by others to deplete ZCCHC11 in embryonic stem cells, where ZCCHC11 could be of even greater importance as a miRNA regulator (Heo et al. 2009). As a consequence, further investigations into the ZCCHC11 knock-down phenotype used transient siRNA transfections as described earlier. As shown in Figure V.3, the impact of ZCCHC11 knock-down on the cell cycle following a three-day siRNA treatment period in HEK293 cells was still substantial. A representative histogram of PI stained cells showed again a reduced proportion of cells in G1 and an accumulation of cells in G2 or mitosis. When cells undergoing DNA replication were specifically analysed by BrdU incorporation, the proportion of those entering S phase was reduced while the amount of cells containing 4C DNA content was again increased. Taken together, these results suggested that depletion of ZCCHC11 caused an accumulation of cells in G2 or M, with a corresponding decrease in the proportions of cells in other stages of the cell cycle, accompanied by an increase in the proportion of dead cells. It is worthwhile mentioning that a direct positive correlation

between the extent of knock-down obtained and the extent of the cell cycle changes was observed for each experiment. This confirmed a direct relationship between loss of ZCCHC11 and the cell cycle defect observed.

V.3. G2 arrest upon ZCCCH11 knock-down

The increased abundance of cells with 4C DNA content upon loss of ZCCHC11 suggested that they were delayed either in G2 or in mitosis, since flow cytometry of PI stained cells cannot differentiate between cells in these two phases, as their DNA content is identical. In order to differentiate delay in mitosis from G2, the mitotic indices of control and ZCCHC11 knock-down cells were determined by immunofluorescence microscopy using the mitotic marker ph-H3. Phosphorylation of H3 is coupled with mitotic chromosome condensation and as such allows very specific visualisation of mitotic cells. Figure V.4A shows representative fields of control and ZCCHC11 knock-down cells labelled with ph-H3 and stained with DAPI. Statistical analysis (Figure V.4B) indicated an average reduction of 45% in the proportion of mitotic cells in the ZCCHC11 knock-down compared to the control. As a consequence, it can be suggested that the cells accumulating with 4C DNA content observed in Figures V.2. and V.3. resided in G2 rather than in mitosis.

Next, the question was asked whether the cells accumulating in G2 upon ZCCHC11 knock-down were temporarily or permanently arrested. To this end, cells were labelled with the thymidine analogue BrdU for 24 hours, on the basis that most cells in an unperturbed population would incorporate BrdU during this labelling period. If a fraction of the ZCCHC11 knock-down cells were permanently blocked in G2, the proportion of BrdU-negative cells would be increased under these conditions. Following BrdU labelling, HEK293 cells were analysed by flow cytometry as in section V.2. A contour

blot depicting total DNA content versus BrdU incorporation showed that the proportion of BrdU-negative cells was only slightly decreased upon depletion of ZCCHC11 (Figure V.5A). Equivalent results were obtained when BrdU-labelled HeLa cells were analysed by immunofluorescence microscopy and counted manually (Figure V.5B).

From these results it can be concluded that cells in which ZCCHC11 had been knocked down were only temporarily blocked in G2, and were able to enter mitosis and pass through S phase within 24 hours. Nonetheless, the increased amount of BrdU incorporation in cells containing 4C DNA may reflect repair DNA synthesis and further suggest complications in completing faultless DNA replication. This is in agreement with the delayed entry into G2/mitosis observed in Figure V.1. Taken together, the findings above hint towards the activation of a G2 specific checkpoint, possibly as a result of some abnormal DNA structure when ZCCHC11 is depleted. These possibilities were further investigated in the next sections.

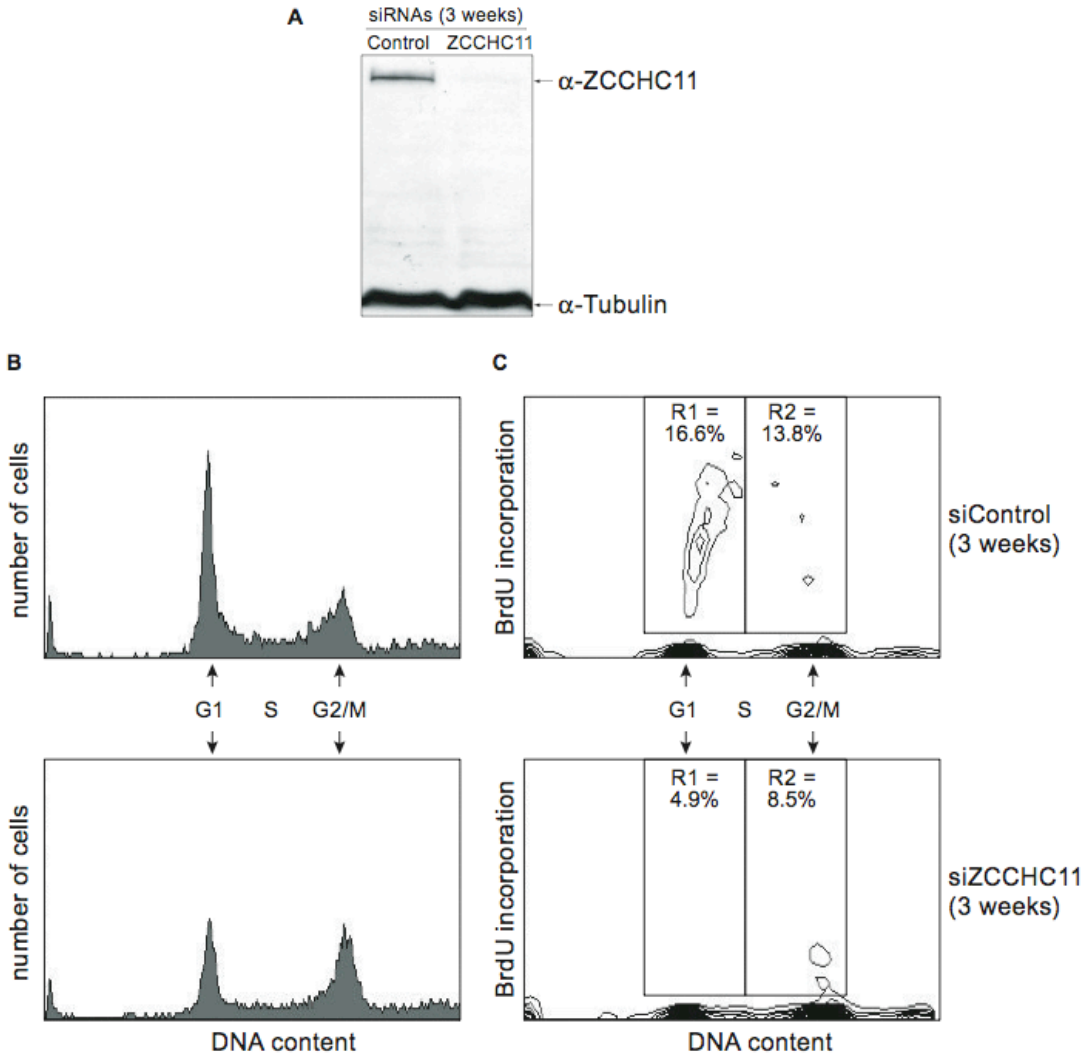

Figure V.2 Cell cycle kinetics upon prolonged ZCCHC11 knock-down

ZCCHC11 was knocked down in HEK293 cells using specific siRNA (or a scrambled control) expressed from a plasmid as a fold-back stem-loop structure. Specific siRNA expression was maintained in cells for 3 weeks by addition of 3μg/ml puromycin. (A) A western blot using specific antibodies shows ZCCHC11 and tubulin as a loading control. (B) Histogram showing the cell cycle distribution of propidium iodide stained cells analysed by flow cytometry. (B) HEK293 cells were pulse-labeled with 10 μM BrdU for 30 minutes prior to harvest. BrdU incorporation (abscissa) and DNA content (ordinate) were analysed by flow cytometry using anti-BrdU and FITC-conjugated secondary antibody. R1 and R2 define the percentage of BrdU-positive cells present in indicated regions. The positions of DNA contents corresponding to G1, S and G2/M are indicated by arrows.

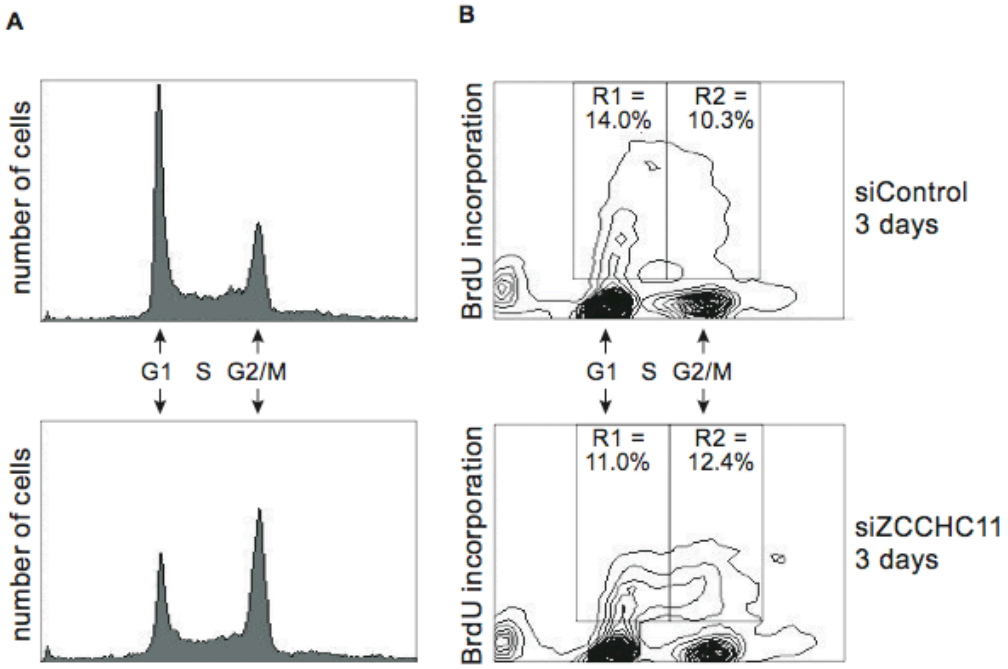

Figure V.3 Cell cycle kinetics following transient ZCCHC11 knock-down

HEK293 cells were harvested 72 hours following siRNA-plasmid transfection. Cells were processed as in Figure V.2.

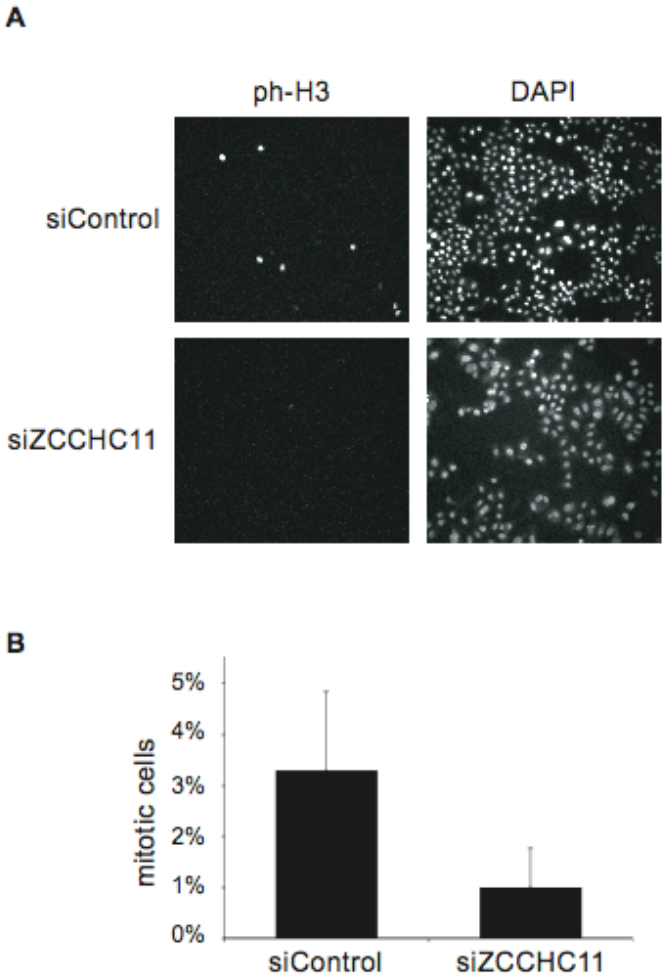

Figure V.4 Determination of mitotic index

(A) ZCCHC11 was knocked down in HeLa cells prior to immunofluorescence analysis using the mitotic marker phH3 (left panel). Nuclei were also stained with DAPI (right panel). (B) Total and ph-H3 stained cells were counted using CellProfiler software and results were verified by manual counting. Quantitation of the mitotic index is expressed as the percentage of phH3 positive (mitotic) cells in relation to total cells (N≈1500). The average of 4 experiments (± SD) is shown for ZCCHC11 knock-down and control cells.

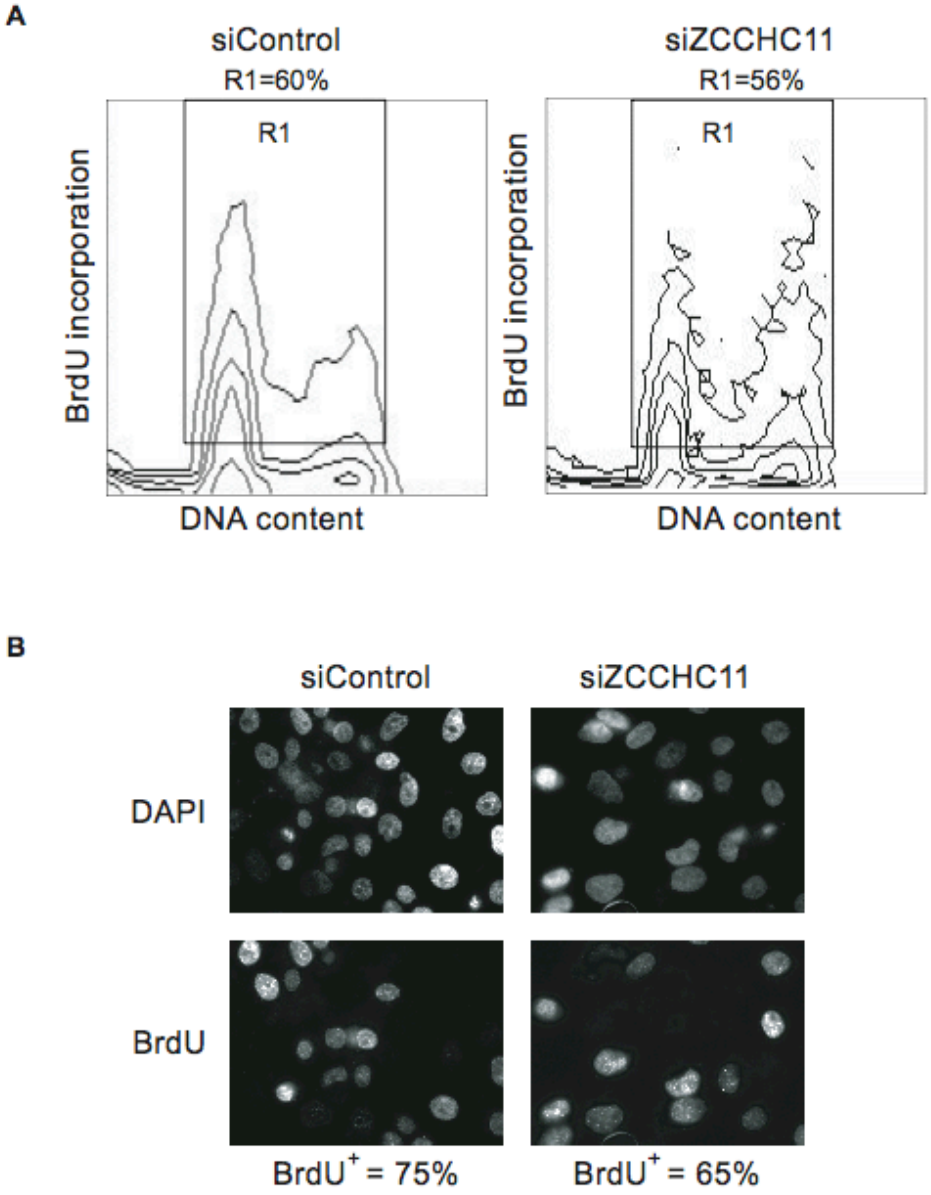

Figure V.5 BrdU incorporation over 24 hours

Cells were labeled with 10 μM BrdU for 24 hours. (A) HEK293 cells were analysed as in Figure V.3. The region R1 defines BrdU positive cells and is expressed as a percentage of all cells analysed. (C) HeLa cells were analysed by immunofluorescence microscopy using anti-BrdU and anti-mouse-FITC. $BrdU^+$ denotes the proportion of cells that have incorporated BrdU during the labelling period.

V.4. DNA damage occurs when ZCCHC11 is depleted

One possible cause of cell cycle delays in S phase or G2 is the activation of replication and/or DNA damage checkpoints. These responses, mediated by the PIKKs ATM and ATR, block cell cycle progression to allow for repair of the DNA (Bartek and Lukas 2007) before it is segregated in mitosis. To investigate whether DNA damage was occurring as a consequence of loss of ZCCHC11, HeLa cells were analysed for the presence of γ-H2A.X by immunofluorescence microscopy. Phosphorylation of the histone variant H2A.X constitutes an early event in the cell response to DNA damage (Rogakou et al. 1998) and can be visualised using a specific antibody. As a positive control for the formation of γ-H2A.X foci, cells were treated with methyl methanesulfonate (MMS), an alkylating agent. Under these conditions, γ-H2AX foci were induced in nearly all cells (Figure V.6A). Notably, γ-H2A.X foci were also largely detected in cells in which ZCCHC11 had been knocked down. Statistical analyses of three independent experiments revealed a significant increase of γ-H2AX foci in ZCCHC11 knock-down cells compared to control cells; 15% of all cells analysed were γ-H2A.X positive in contrast to 4% in control cells. Interestingly, individual cells in the ZCCHC11 knock-down cell population contained either several or no γ-H2A.X foci. This suggested that some but not all ZCCHC11 knock-down cells were activating the DNA damage response and in those that did, the activation was similar to the extent of the MMS-induced response.

Another hallmark of the DNA damage response is the phosphorylation and activation of Chk1 by ATR and or ATM. In addition to its well-documented role in the DNA damage response, Chk1 is also important for the negative regulation of cell cycle progression in response to inhibition of DNA replication in vertebrates (Zachos et al. 2003). The possibility of Chk1 activation as a consequence of ZCCHC11 depletion was therefore

investigated. Following ZCCHC11 knock-down, HEK293 protein extracts treated with phosphatase inhibitors were prepared and analysed by western blot. They were specifically examined for the presence of a shift in electrophoretic mobility using anti-Chk1 and a band corresponding to phosphorylated Chk1 using anti-ph-Chk1. Blots were also probed using α-ZCCHC11 to monitor successful knock-down of the ZCCHC11 protein and anti-tubulin to control for equal loading. Strikingly, a Chk1 band of reduced mobility was observed when ZCCHC11 was knocked down but not in control cells (Figure V.6B). These results were confirmed by western blot experiments probing directly for phosphorylated Chk1. The efficacy of the ph-Chk1 antibody was additionally tested by treatment of cells with MMS, which led to extensive Chk1 phosphorylation (Figure V.6B, lanes 2 and 4). Importantly, a band corresponding to ph-Chk1 was also present in the untreated siZCCHC11 sample but not in the control. This signal was not a consequence of increased total protein levels as judged by equal tubulin levels.

Taken together, the presence of phosphorylated H2A.X and Chk1 upon depletion of ZCCHC11 indicated an activation of the DNA damage response in these cells. Whether the response was due to stalled replication forks, structural DNA damage such as double strand breaks or to other forms of DNA damage remains to be investigated. However, the findings above suggested that a DNA integrity checkpoint was activated under these conditions, which presumably caused delayed entry into mitosis.

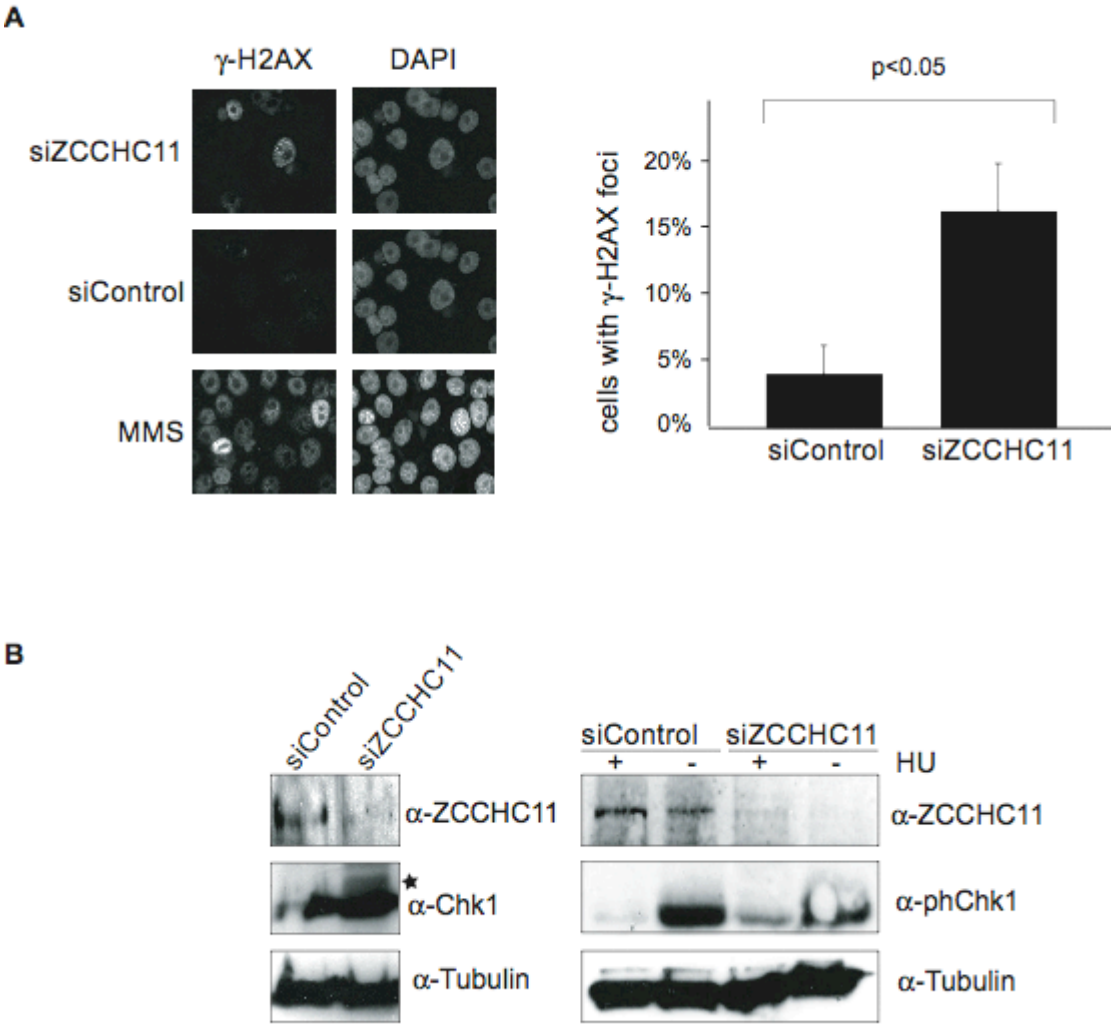

Figure V.6 DNA damage response in ZCCHC11 knock-down

(A) ZCCHC11 knock-down and control HeLa cells were analysed by immunofluorescence microscopy using an antibody recognising γ-H2AX (left panel). As a positive control, cells were treated with MMS for 3 hours. The average of 3 experiments (±SD) is depicted as a percentage of cells showing γ-H2AX foci in control and ZCCHC11 knock-down cells. (B) Phosphatase inhibitor-treated total protein extracts from HEK293 cells were analysed by western blot using specific antibodies as indicated. The star (left panel) indicates phosphorylated Chk1. The treatment of cells with 5mM HU for 16 hours was used as a positive control for the presence of phosphorylated Chk1 in the right panel. A western blot for ZCCHC11 (α-ZCCHC11) confirms successful knock-down and tubulin serves as a loading control.

V.5. Activation of the DNA replication checkpoint

The orthologue of ZCCHC11 in fission yeast, Cid1, has been suggested to be important for S-M checkpoint integrity as its deletion in combination with mutations in the repair polymerases DNA pol δ or ε caused specific checkpoint defects (Wang et al. 2000). The previous sections established a link between ZCCHC11 and S phase delay, G2 arrest and DNA damage, strongly suggesting an activation of the replication checkpoint when ZCCHC11 is depleted. In order to investigate further whether such a checkpoint had been activated, use was made of caffeine, a drug that can override the S-M checkpoint in fission yeast and mammalian cells (Schlegel and Pardee 1986; Wang et al. 1999). It was reasoned that, if ZCCHC11-depleted cells were delayed in G2 because of the activation of the S-M checkpoint, the addition of caffeine to the cells would force them through the checkpoint and result in a proportional increase of mitotic cells. In order to accumulate mitotic cells following caffeine treatment, cells were also treated with nocodazole, which specifically blocks them in mitosis. A schematic representation of the experimental design with the effects on cell cycle progression of DNA damage and the drugs used is depicted in Figure V.7A.

Following specific RNAi-mediated knock-down of ZCCHC11 and subsequent drug treatment, HeLa cells were fixed and analysed by immunofluorescence microscopy using α-ph-H3 as described in section V.3. The proportion of mitotic cells in untreated samples in control and ZCCHC11 knock-down cells was arbitrarily set to 1. This allowed a direct comparison between the abundance of cells entering mitosis following treatment with or without caffeine in siControl and siZCCHC11 cells (Figure V.7B). The proportion of mitotic cells increased gradually upon addition of nocodazole alone with no major significant difference between control and ZCCHC11 depleted cells indicating a normal progression of cells from G2 into mitosis. Furthermore,

the combination of caffeine and nocodazole had no strong additive effects on the mitotic index in control cells, presumably because ATM/ATR-dependent checkpoints were not activated in these cells. Strikingly, the proportion of mitotic cells in the ZCCHC11-depleted population increased significantly after 2 and 5 hours of treatment with caffeine. This result suggested that a proportion of the cells in which ZCCHC11 was depleted were held in G2 prior to caffeine treatment because of activation of an ATM/ATR-dependent checkpoint. Overall, these findings are consistent with the occurrence of DNA damage and a transient arrest of cells in G2 as a result of ZCCHC11 depletion.

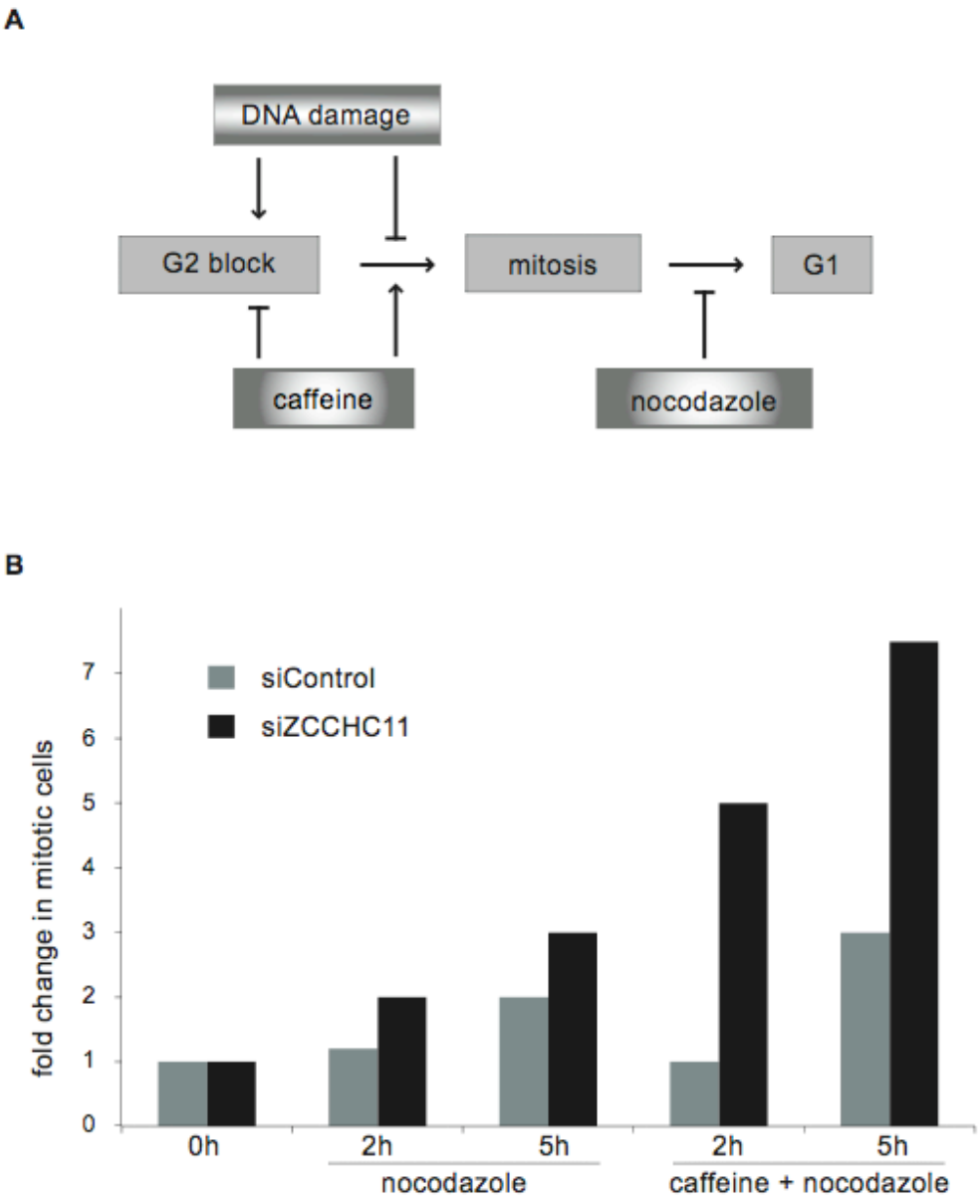

Figure V.7 DNA replication checkpoint activation

(A) A diagram depicting checkpoint activation in response to DNA damage and the effects of the drugs caffeine and nocodazole on cell cycle progression. (B) HeLa cells grown on cover slips were transfected with siRNA-expressing plasmids prior to treatment with 10mM caffeine and 1μg/ml nocodazole for the time in hours (h) indicated. Cells were fixed and analysed for mitotic index as in Figure 4. The program CellProfiler was used to count cells. The average of two independent experiments is shown and expressed in relation to the timepoint 0, which was arbitrarily set to 1.

V.6. Discussion

The findings presented in this chapter showed a distinct cellular phenotype resulting from knocking down the poly(U) polymerase ZCCHC11 by means of RNAi. This phenotype consisted of a transient G2 arrest and a consequently proportionate reduction of cells in mitosis, early S phase and G1. Furthermore, progression of cells through S phase in cells released from a HU block was delayed when ZCCHC11 was depleted. The arrest of cells in G2 was most likely due to checkpoint activation and a response to DNA damage, as early events in the DNA damage signalling cascade such as phosphorylation of Chk1 and H2A.X could be detected. In addition, drug treatments inhibiting checkpoint activation reversed the effect of cell accumulation in G2 and promoted progression into mitosis.

Taken together, these observations strongly suggest that cells deficient in ZCCHC11 experience some form of DNA damage that activates checkpoint mechanisms and hence delays completion of S phase and entry into mitosis. Given its role in histone mRNA degradation at the end of S phase discovered in this study, it could be envisaged that it is loss of this function of ZCCHC11 that gives rise to the cell cycle phenotype observed. Failure to degrade histone mRNAs efficiently could result in an unbalanced overproduction of histone mRNAs and hence histone proteins, which in turn could interfere with accurate chromatin assembly. Disruption of chromatin assembly has previously been associated with DNA damage and cell cycle arrest (Ye et al. 2003). It can therefore be hypothesised that the response to DNA checkpoint activation observed in this study occurs as a consequence of inefficient histone mRNA degradation (Figure V.8).

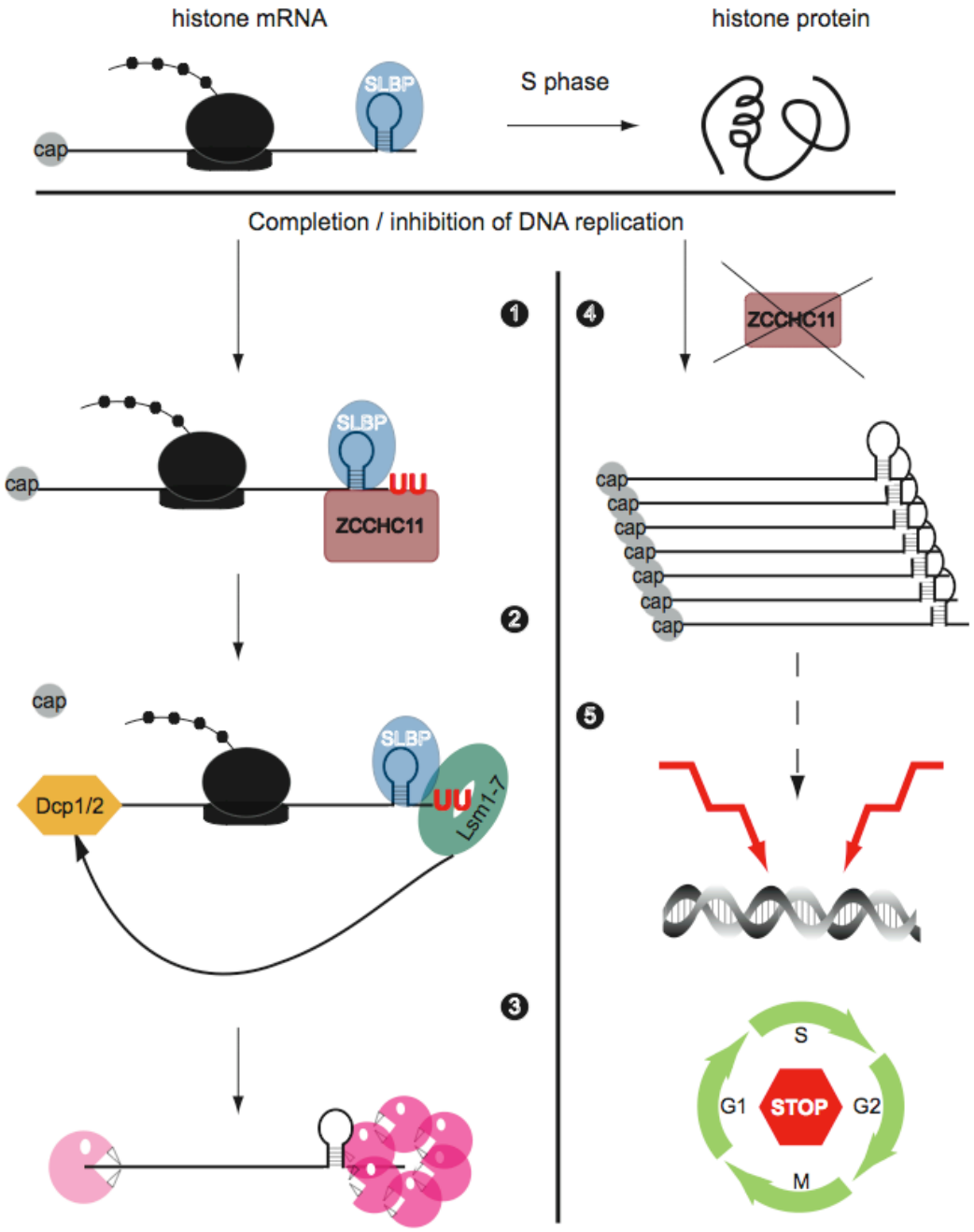

Figure V.8 Speculative model of the role of ZCCHC11

This model proposes the involvement of ZCCHC11 in uridylation of histone mRNAs following completion of histone synthesis and DNA replication or upon inhibition of DNA replication (1). The Lsm1-7 complex is subsequently recruited to the 3' end, where it also interacts with the stem-loop binding protein (SLBP). Lsm1-7 then stimulates decapping (2) and exonucleolytic decay (3). If ZCCHC11 protein is missing, cytoplasmic histone mRNAs accumulate to high extent (4). This may lead to defective chromatin assembly and abnormal DNA structures, with consequent activation of the DNA damage checkpoint and cell cycle delay (5). See text for further details.

It is important to mention that although the ZCCHC11 protein is clearly important for the initiation of rapid histone mRNA degradation, the cell can eventually find alternative pathways to eliminate these transcripts when ZCCHC11 is absent, in line with the general redundancy of RNA degradation pathways. In support of this view, highly increased histone protein levels were not detected upon ZCCHC11 knock-down in asynchronous cells. This suggests that ZCCHC11-depleted cells are able to circumvent the defects in efficient uridylation-dependent histone mRNA degradation. Reliance on an alternative pathway is illustrated by inefficient histone mRNA degradation as well as delay but not permanent arrest in late S phase and G2 when the uridylation-mediated degradation pathway is impaired.

So far, no mammalian non-canonical poly(A/U) polymerase has been directly implicated in the regulation of the cell cycle or the activation of replication checkpoints, in contrast to studies performed in yeast. One report proposed a link between the non-canonical polymerases Trf4 and Trf5 in *S. cerevisiae* and genome instability through regulation of histone mRNA levels, though the direct modification of histone mRNAs by Trf4/Trf5 could not be demonstrated (Reis and Campbell 2007). Additionally, Cid1, originally implicated in the activation of the replication checkpoint (Wang et al. 2000), has been linked to histone mRNA levels. Microarray experiments in *S. pombe* from our lab identified increased histone mRNA levels in the absence of Cid1 upon activation of the replication checkpoint (Abigail Stevenson and Chris Norbury; unpublished). These results were directly confirmed by Northern blots, though their interpretation is complicated because of unequal proficiency in checkpoint activation between *cid1Δ* and WT cells. Moreover, a direct involvement of Cid1 in histone mRNA uridylation remains to be demonstrated. Nonetheless, these studies in yeast proposed a relationship between at least one nucleotidyl transferase and efficient degradation of histone mRNAs. Failure to do so was associated with DNA damage and checkpoint activation.

This study implicates the uridyl transferase ZCCHC11 in histone mRNA degradation in mammalian cells and proposes that inefficient destabilisation of histone mRNAs results in DNA damage, checkpoint activation and cell cycle delay in G2 (Model, Figure V.8). Further investigations into the direct relationship between increased histone levels and cell cycle defects will be needed to investigate this hypothesis further.

CHAPTER VI. CONCLUSIONS

This final chapter aims to bring together the results from Chapter III, IV and V in one final comprehensive conclusion. Experimental data were obtained from both yeast and mammalian systems regarding the uridyl transferase Cid1 in *S. pombe* and ZCCHC11 in human cells. This thesis strongly suggests that not only the biochemical properties and intracellular localisation of these two proteins are conserved but also their role in the DNA integrity checkpoint.

VI.1. The dual life of Cid1

Cid1 was originally identified a decade ago as a component involved in the DNA replication checkpoint (Wang et al. 2000; Read et al. 2002). Later, it was found that Cid1 exhibits RNA poly(A) and poly(U) activity *in vitro*, but adds uridyl residues to cytoplasmic bulk polyadenylated RNA 3' ends *in vivo*. This modification then acts as a signal for exonucleolytic degradation of RNAs (Rissland et al. 2007; Rissland and Norbury 2009). Despite major advances made into the characterisation of the Cid1 protein in our lab, several questions remained, namely how is Cid1 recruited to its targets and how is the difference in processivity between highly processive *in vitro* and very distributive *in vivo* explained?

Chapter III aims at answering some of these questions, in particular with regards to potential accessory factors that drive Cid1 specificity. To this end,

the role of putative interacting partners and a phosphorylation site on the Cid1 polypeptide were analysed and validated. In summary, no factors could be identified as bona fide regulators of Cid1 activity by the methods used in this study; Cid1-TAP purification combined with MS. It should be noted though that previous attempts in discovering such factors using various techniques had also largely failed (Abigail Stevenson and Chris Norbury, unpublished). These results led to the conclusion that a stable Cid1 complex similar to the TRAMP complex (see Chapter I.1) either does not exist in exponentially growing fission yeast cells or could not be captured to date using standard techniques. The autonomy of Cid1 from accessory factors can now be partially explained by very recent data arising from the crystal structure of Cid1 (Luke Yates, Robert Gilbert and Chris Norbury, unpublished). On its surface, Cid1 possesses regions of basic amino acids, which in combination confer RNA-binding capacity to Cid1 (Sophie Fleurdépine and Chris Norbury, unpublished). Furthermore, preliminary experiments reveal that the biochemical properties of Cid1 with regards to its processivity can be greatly influenced by the salt concentration in the assay buffer. These biochemical investigations in addition to the crystal structure of Cid1 will hopefully soon resolve the current uncertainties concerning Cid1 activity.

One unanswered question, however, is the connection between the dual roles of Cid1 as a nucleotidyl transferase involved in bulk RNA decay on the one hand and the replication checkpoint on the other hand. Early studies from our laboratory suggest an involvement of Cid1 in heterochromatin formation during S phase arrest, which could explain the originally identified function of Cid1 in the replication checkpoint (Daniel Scott, Abigail Stevenson and Chris Norbury, unpublished). Finally, data from the human cell system presented in this study may possibly provide a step closer in unravelling the link between RNA regulation and cell cycle checkpoint activation.

VI.2. The dual functions of ZCCHC11

ZCCHC11 and its homologue PUP-2 in *C. elegans* have repeatedly been reported to play a major role in miRNA regulation in the cytoplasm. By adding 1-3 uridyl residues to the 3' ends of pre-miRNAs (Hagan et al. 2009; Heo et al. 2009; Lehrbach et al. 2009) and miRNAs (Jones et al. 2009), ZCCHC11 was shown to target these RNAs for degradation and crucially, to regulate miRNA levels in this way. Identified substrates of ZCCHC11 include precursors of the universally important *let-7* miRNA family and the cytokine targeting miRNA *miR26*. As such, ZCCHC11 was suggested to be indirectly involved in developmental biology, embryogenesis, oncogenesis and immunology.

This thesis unravels a new role for ZCCHC11; it shows that efficient histone mRNA degradation at the end of S phase or when S phase is arrested requires catalytically active ZCCHC11. Uridyl residues added by ZCCHC11 were found on mature histone mRNA 3' ends as well as on degradation intermediates. This modification presumably serves to recruit the Lsm1-7 complex to the transcript, which in turn stimulates decapping and exonucleolytic degradation of the RNA (see Model in Figure V.8). As for Cid1 in *S. pombe*, the question remains how ZCCHC11 is recruited to histone mRNAs. In the case of miRNAs, it has been shown that the pluripotency factor Lin28 is essential to target pre-*let-7* for uridylation by ZCCHC11 (Hagan et al. 2009; Heo et al. 2009; Lehrbach et al. 2009). There is one report suggesting that Lin28 also binds replication-dependent histone mRNAs (Xu and Huang 2009), though in this case Lin28 was found to stabilise histone messages rather than destabilise them as is the case for miRNAs. Further experiments are needed to fully understand how ZCCHC11 is targeted to histone mRNAs.

Moreover, data in Chapter IV.7 and V show that ZCCHC11 expression itself is regulated to some extent during S phase, with its expression peaking towards the end, when histone transcripts are degraded. Notably, the transition of cells from S phase into G2/M was delayed upon knock-down of ZCCHC11, suggesting the involvement of ZCCHC11 in the G2/M checkpoint. In agreement with this suggestion, depletion of ZCCHC11 resulted in striking accumulation of cells in late S phase and/or G2, occurrence of DNA damage as indicated by the presence of phosphorylated H2A.X and Chk1, and DNA checkpoint activation (Figure V.8).

These results tentatively support the idea that inefficient histone mRNA degradation following ZCCHC11 knock-down is the prevalent cause of the ZCCHC11 phenotype observed here. It is conceivable that accumulation of histone mRNAs and possibly also histone proteins at the end of S phase would lead to defective chromatin assembly and as a result, activation of the DNA integrity checkpoint. A similar phenotype has been observed by others following Lsm1 deletion in budding yeast (Herrero and Moreno 2011). Using yeast genetics, these authors could link the phenotype directly to accumulation of histone mRNAs; experimental evidence that would be very challenging to obtain in human cells. Nevertheless, Lin28 has also been suggested to be important for the transition from S phase into G2/M as changes in the cell cycle distribution had been observed upon depletion of Lin28 from mouse embryonic stem cells (Xu and Huang 2009; Xu et al. 2009). This phenotype was proposed to arise as a result of defective regulation of histone mRNAs in the absence of Lin28, which is reminiscent of the proposed ZCCHC11 phenotype here. Based on current data, it is however unlikely that ZCCHC11 and Lin28 act together to target histone mRNAs for degradation since both proteins have been suggested to have opposing effects on histone mRNA stability (positive regulation by Lin28 in mouse embryonic cells (Xu and Huang 2009) and negative regulation by ZCCHC11 in somatic cells).

Finally, the documented role of ZCCHC11 in miRNA regulation cannot be excluded as a potential cause for the cell cycle phenotype since it is becoming evident that the cell cycle is regulated by multiple miRNAs (Carleton et al. 2007). For example, overexpression of pre-*let-7* in human primary fibroblasts led to accumulation of cells in G2/M following cell synchronisation by serum starvation (Legesse-Miller et al. 2009), which partially reflects the phenotype observed here. The authors proposed that stabilisation of the mitosis-inhibiting kinase Wee1 prevented entry into mitosis due to *let-7*-mediated down-regulation of the Wee1-targeting protein Cdc34. However, this reported accumulation of cells in G2/M did not occur in asynchronous cells, nor did it appear to be as dramatic as that observed upon ZCCHC11 knock-down in this study. As such, explanation of the ZCCHC11 phenotype simply by up-regulation of the miRNA *let-7* family alone does not appear straightforward. Overall, the nature of the DNA checkpoint activation caused by ZCCHC11 depletion awaits further clarification, as do several additional questions, which are discussed below.

VI.3. Future directions

In the last three years, we have learned a great deal about ZCCHC11. ZCCHC11 is a cytoplasmic uridyl transferase that targets precursor and mature miRNAs, histone mRNAs and probably also siRNAs for degradation. Through its RNA-regulatory functions, ZCCHC11 has been implicated in scores of biological processes such as development, tumorigenesis and cell cycle regulation. However, there are still many open questions regarding this protein that will require much research in the future.

Very recent advances using sophisticated single-molecule studies for example, have dissected the binding and uridylation mechanism of ZCCHC11 and pre-*let-7* in mammalian cells (Yeom et al. 2011). Nonetheless,

high-resolution structural information from crystallography or nuclear magnetic resonance analysis of ZCCHC11 in complex with RNA and UTP will be needed to identify precisely the catalytic mechanism and RNA binding properties of the protein. In addition, structural data might also give indications about the duplication of the catalytic and PAP-associated domains and the various zinc finger motifs within the ZCCHC11 polypeptide. Furthermore, a knock-out mouse model of ZCCHC11 would be highly valuable for phenotypic studies of, for instance, the ZCCHC11-related cell cycle phenotype observed in this study. The model could overcome several disadvantages associated with RNAi-mediated knock-down of ZCCHC11 in mammalian cells including inefficiency and off-target effects. Finally, it is highly plausible that ZCCHC11 also acts on substrates other than miRNAs or histone mRNAs. Research using genome-wide techniques such as high-throughput sequencing combined with either ZCCHC11 pull-down or ZCCHC11 knock-down would be of great use to uncover further substrates of ZCCHC11. It will be particularly interesting to investigate whether mammalian polyadenylated mRNAs are also uridylated prior to mRNA decay similar to the situation in *S. pombe*. Likewise, are *S. pombe* non-polyadenylated histone mRNAs uridylated upon completion or inhibition of S phase, and does this activity explain the role of Cid1 in the DNA replication checkpoint?

References

Aravind, L. and Koonin, E.V. 1999. DNA polymerase beta-like nucleotidyltransferase superfamily: identification of three new families, classification and evolutionary history. *Nucleic Acids Res* **27**(7): 1609-1618.

Bai, Y., Srivastava, S.K., Chang, J.H., Manley, J.L., and Tong, L. 2011. Structural Basis for Dimerization and Activity of Human PAPD1, a Noncanonical Poly(A) Polymerase. *Molecular Cell* **41**(3): 311.

Balbo, P.B. and Bohm, A. 2007. Mechanism of poly(A) polymerase: structure of the enzyme-MgATP-RNA ternary complex and kinetic analysis. *Structure* **15**(9): 1117-1131.

Bartek, J. and Lukas, J. 2003. Chk1 and Chk2 kinases in checkpoint control and cancer. *Cancer Cell* **3**: 421.

Bartek, J. and Lukas, J. 2007. DNA damage checkpoints: from initiation to recovery or adaptation. *Current Opinion in Cell Biology* **19**(2): 238.

Bayne, E.H., Portoso, M., Kagansky, A., Kos-Braun, I.C., Urano, T., Ekwall, K., Alves, F., Rappsilber, J., and Allshire, R.C. 2008. Splicing factors facilitate RNAi-directed silencing in fission yeast. *Science* **322**(5901): 602-606.

Benoit, P., Papin, C., Kwak, J.E., Wickens, M., and Simonelig, M. 2008. PAP- and GLD-2-type poly(A) polymerases are required sequentially in cytoplasmic polyadenylation and oogenesis in Drosophila. *Development* **135**(11): 1969-1979.

Branzei, D. and Foiani, M. 2005. The DNA damage response during DNA replication. *Curr Opin Cell Biol* **17**(6): 568-575.

Burns, D.M., D'Ambrogio, A., Nottrott, S., and Richter, J.D. 2011. CPEB and two poly(A) polymerases control miR-122 stability and p53 mRNA translation. *Nature* **473**(7345): 105-108.

Bähler, J., Wu, J.Q., Longtine, M.S., Shah, N.G., McKenzie, A., Steever, A.B., Wach, A., Philippsen, P., and Pringle, J.R. 1998. Heterologous modules for efficient and versatile PCR-based gene targeting in Schizosaccharomyces pombe. *Yeast* **14**(10): 943-951.

Bühler, M., Haas, W., Gygi, S.P., and Moazed, D. 2007. RNAi-dependent and -independent RNA turnover mechanisms contribute to heterochromatic gene silencing. *Cell* **129**(4): 707-721.

Calonge, T.M. and O'Connell, M.J. 2008. Turning off the G2 DNA damage checkpoint. *DNA Repair* **7**(2): 136.

Caponigro, G. and Parker, R. 1995. Multiple functions for the poly(A)-binding protein in mRNA decapping and deadenylation in yeast. *Genes & Development* **9**(19): 2421-2432.

Carleton, M., Cleary, M.A., and Linsley, P.S. 2007. MicroRNAs and cell cycle regulation. *Cell Cycle* **6**(17): 2127-2132.

Carpousis, A.J., Vanzo, N.F., and Raynal, L.C. 1999. mRNA degradation. A tale of poly(A) and multiprotein machines. *Trends Genet* **15**(1): 24-28.

Celeste, A., Fernandez-Capetillo, O., Kruhlak, M.J., Pilch, D.R., Staudt, D.W., Lee, A., Bonner, R.F., Bonner, W.M., and Nussenzweig, A. 2003. Histone H2AX phosphorylation is dispensable for the initial recognition of DNA breaks. *Nat Cell Biol* **5**(7): 675-679.

Chang, Y.-F., Imam, J.S., and Wilkinson, M.F. 2007. The Nonsense-Mediated Decay RNA Surveillance Pathway. *Annual Review of Biochemistry* **76**(1): 51-74.

Chowdhury, A., Mukhopadhyay, J., and Tharun, S. 2007. The decapping activator Lsm1p-7p-Pat1p complex has the intrinsic ability to distinguish between oligoadenylated and polyadenylated RNAs. *RNA* **13**(7): 998-1016.

Coller, J. and Parker, R. 2004. Eukaryotic mRNA Decapping. *Annual Review of Biochemistry* **73**: 861-890.

Decker, C.J. and Parker, R. 1993. A turnover pathway for both stable and unstable mRNAs in yeast: evidence for a requirement for deadenylation. *Genes Dev* **7**(8): 1632-1643.

Deng, J., Ernst, N.L., Turley, S., Stuart, K.D., and Hol, W.G. 2005. Structural basis for UTP specificity of RNA editing TUTases from Trypanosoma brucei. *Embo J* **24**(23): 4007-4017.

Dominski, Z. and Marzluff, W.F. 2007. Formation of the 3' end of histone mRNA: getting closer to the end. *Gene* **396**(2): 373-390.

Dominski, Z., Yang, X.-c., and Marzluff, W.F. 2005. The Polyadenylation Factor CPSF-73 Is Involved in Histone-Pre-mRNA Processing. *Cell* **123**(1): 37.

Erkmann, J.A., Sànchez, R., Treichel, N., Marzluff, W.F., and Kutay, U. 2005. Nuclear export of metazoan replication-dependent histone mRNAs is dependent on RNA length and is mediated by TAP. *RNA* **11**(1): 45-58.

Feng, Y., Huang, H., Liao, J., and Cohen, S.N. 2001. Escherichia coli poly(A)-binding proteins that interact with components of degradosomes or impede RNA decay mediated by polynucleotide phosphorylase and RNase E. *J Biol Chem* **276**(34): 31651-31656.

Gallie, D.R., Lewis, N.J., and Marzluff, W.F. 1996. The Histone 3'-Terminal Stem-Loop is Necessary for Translation in Chinese Hamster Ovary Cells. *Nucleic Acids Research* **24**(10): 1954-1962.

Gao, M., Wilusz, C.J., Peltz, S.W., and Wilusz, J. 2001. A novel mRNA-decapping activity in HeLa cytoplasmic extracts is regulated by AU-rich elements. *EMBO J* **20**(5): 1134-1143.

Gatei, M., Sloper, K., Sørensen, C., Syljuåsen, R., Falck, J., Hobson, K., Savage, K., Lukas, J., Zhou, B.B., Bartek, J., and Khanna, K.K. 2003. Ataxia-telangiectasia-mutated (ATM) and NBS1-dependent phosphorylation of Chk1 on Ser-317 in response to ionizing radiation. *Journal of Biological Chemistry* **278**(17): 14806.

Gorgoni, B., Andrews, S., Schaller, A., Schümperli, D., Gray, N.K., and Müller, B. 2005. The stem-loop binding protein stimulates histone translation at an early step in the initiation pathway. *RNA* **11**(7): 1030-1042.

Graves, R.A., Pandey, N.B., Chodchoy, N., and Marzluff, W.F. 1987. Translation is required for regulation of histone mRNA degradation. *Cell* **48**(4): 615-626.

Gunjan, A., Paik, J., and Verreault, A. 2006. The emergence of regulated histone proteolysis. *Current Opinion in Genetics & Development* **16**(2): 112.

Hagan, J.P., Piskounova, E., and Gregory, R.I. 2009. Lin28 recruits the TUTase Zcchc11 to inhibit let-7 maturation in mouse embryonic stem cells. *Nat Struct Mol Biol* **16**(10): 1021-1025.

Hamill, S., Wolin, S.L., and Reinisch, K.M. 2010. Structure and function of the polymerase core of TRAMP, a RNA surveillance complex. *Proceedings of the National Academy of Sciences* **107**(34): 15045-15050.

Harris, M.E., Bohni, R., Schneiderman, M.H., Ramamurthy, L., Schumperli, D., and Marzluff, W.F. 1991. Regulation of histone mRNA in the unperturbed cell cycle: evidence suggesting control at two posttranscriptional steps. *Mol Cell Biol* **11**(5): 2416-2424.

Hartwell, L.H. and Kastan, M.B. 1994. Cell cycle control and cancer. *Science* **266**(5192): 1821-1828.

Hastings, M.L. and Krainer, A.R. 2001. Pre-mRNA splicing in the new millennium. *Curr Opin Cell Biol* **13**(3): 302-309.

Heintz, N., Sive, H.L., and Roeder, R.G. 1983. Regulation of human histone gene expression: kinetics of accumulation and changes in the rate of synthesis and in the half-lives of individual histone mRNAs during the HeLa cell cycle. *Mol Cell Biol* **3**(4): 539-550.

Heo, I., Joo, C., Cho, J., Ha, M., Han, J., and Kim, V.N. 2008. Lin28 mediates the terminal uridylation of let-7 precursor MicroRNA. *Mol Cell* **32**(2): 276-284.

Heo, I., Joo, C., Kim, Y.-K., Ha, M., Yoon, M.-J., Cho, J., Yeom, K.-H., Han, J., and Kim, V.N. 2009. TUT4 in Concert with Lin28 Suppresses MicroRNA Biogenesis through Pre-MicroRNA Uridylation. *Cell* **138**(4): 696.

Herrero, A.B. and Moreno, S. 2011. Lsm1 promotes genomic stability by controlling histone mRNA decay. *EMBO J* **30**(10): 2008.

Hoeijmakers, J.H. 2001. Genome maintenance mechanisms for preventing cancer. *Nature* **411**(6835): 366-374.

Holm, L. and Sander, C. 1995. DNA polymerase β belongs to an ancient nucleotidyltransferase superfamily. *Trends Biochem Sci* **20**(9): 345-347.

Houseley, J., LaCava, J., and Tollervey, D. 2006. RNA-quality control by the exosome. *Nat Rev Mol Cell Biol* **7**(7): 529-539.

Houseley, J. and Tollervey, D. 2008. The nuclear RNA surveillance machinery: the link between ncRNAs and genome structure in budding yeast? *Biochim Biophys Acta* **1779**(4): 239-246.

Huang, Y. and Carmichael, G.C. 1996. Role of polyadenylation in nucleocytoplasmic transport of mRNA. *Mol Cell Biol* **16**(4): 1534-1542.

Jones, M.R., Quinton, L.J., Blahna, M.T., Neilson, J.R., Fu, S., Ivanov, A.R., Wolf, D.A., and Mizgerd, J.P. 2009. Zcchc11-dependent uridylation of microRNA directs cytokine expression. *Nat Cell Biol* **11**: 1137-1163.

Jones-Rhoades, M.W., Bartel, D.P., and Bartel, B. 2006. MicroRNAs and their regulatory roles in plants. *Annual Review of Plant Biology* **57**: 19-53.

Kadaba, S., Krueger, A., Trice, T., Krecic, A.M., Hinnebusch, A.G., and Anderson, J. 2004. Nuclear surveillance and degradation of hypomodified initiator tRNAMet in S. cerevisiae. *Genes Dev* **18**(11): 1227-1240.

Katoh, T., Sakaguchi, Y., Miyauchi, K., Suzuki, T., Kashiwabara, S., Baba, T., and Suzuki, T. 2009. Selective stabilization of mammalian microRNAs by 3' adenylation mediated by the cytoplasmic poly(A) polymerase GLD-2. *Genes Dev* **23**(4): 433-438.

Kaufmann, I., Martin, G., Friedlein, A., Langen, H., and Keller, W. 2004. Human Fip1 is a subunit of CPSF that binds to U-rich RNA elements and stimulates poly(A) polymerase. *EMBO J* **23**(3): 616-626.

Kaygun, H. and Marzluff, W.F. 2005a. Regulated degradation of replication-dependent histone mRNAs requires both ATR and Upf1. *Nat Struct Mol Biol* **12**(9): 794-800.

Kaygun, H. and Marzluff, W.F. 2005b. Translation termination is involved in histone mRNA degradation when DNA replication is inhibited. *Mol Cell Biol* **25**(16): 6879-6888.

Keller, C., Woolcock, K., Hess, D., and Bühler, M. 2010. Proteomic and functional analysis of the noncanonical poly(A) polymerase Cid14. *RNA* **16**(6): 1124-1129.

Kim, M., Krogan, N.J., Vasiljeva, L., Rando, O.J., Nedea, E., Greenblatt, J.F., and Buratowski, S. 2004. The yeast Rat1p exonuclease promotes transcription termination by RNA polymerase II. *Nature* **432**(7016): 517-522.

Kim, S.T., Xu, B., and Kastan, M.B. 2002. Involvement of the cohesin protein, Smc1, in Atm-dependent and independent responses to DNA damage. *Genes Dev* **16**(5): 560-570.

Kolev, N.G. and Steitz, J.A. 2005. Symplekin and multiple other polyadenylation factors participate in 3' end maturation of histone mRNAs. *Genes & Development* **19**(21): 2583-2592.

Kornberg, R.D. 1977. Structure of Chromatin. *Annual Review of Biochemistry* **46**: 931-954.

Koseoglu, M.M., Graves, L.M., and Marzluff, W.F. 2008. Phosphorylation of threonine 61 by cyclin a/Cdk1 triggers degradation of stem-loop binding protein at the end of S phase. *Mol Cell Biol* **28**(14): 4469-4479.

Kushner, S.R. 2002. mRNA decay in Escherichia coli comes of age. *J Bacteriol* **184**(17): 4658-4665.

Kwak, J.E., Drier, E., Barbee, S.A., Ramaswami, M., Yin, J.C., and Wickens, M. 2008. GLD2 poly(A) polymerase is required for long-term memory. *Proc Natl Acad Sci U S A* **105**(38): 14644-14649.

Kwak, J.E., Wang, L., Ballantyne, S., Kimble, J., and Wickens, M. 2004. Mammalian GLD-2 homologs are poly(A) polymerases. *Proc Natl Acad Sci U S A* **101**(13): 4407-4412.

Kwak, J.E. and Wickens, M. 2007. A family of poly(U) polymerases. *RNA* **13**(6): 860-867.

LaCava, J., Houseley, J., Saveanu, C., Petfalski, E., Thompson, E., Jacquier, A., and Tollervey, D. 2005. RNA degradation by the exosome is promoted by a nuclear polyadenylation complex. *Cell* **121**(5): 713-724.

Laishram, R.S. and Anderson, R.A. 2010. The poly A polymerase Star-PAP controls 3[prime]-end cleavage by promoting CPSF interaction and specificity toward the pre-mRNA. *EMBO J* **29**(24): 4132.

Legesse-Miller, A., Elemento, O., Pfau, S.J., Forman, J.J., Tavazoie, S., and Coller, H.A. 2009. let-7 Overexpression Leads to an Increased Fraction of Cells in G2/M, Direct Down-regulation of Cdc34, and Stabilization of Wee1 Kinase in Primary Fibroblasts. *Journal of Biological Chemistry* **284**(11): 6605-6609.

Lehrbach, N.J., Armisen, J., Lightfoot, H.L., Murfitt, K.J., Bugaut, A., Balasubramanian, S., and Miska, E.A. 2009. LIN-28 and the poly(U) polymerase PUP-2 regulate let-7 microRNA processing in Caenorhabditis elegans. *Nat Struct Mol Biol* **16**(10): 1016-1020.

Li, J., Yang, Z., Yu, B., Liu, J., and Chen, X. 2005. Methylation protects miRNAs and siRNAs from a 3'-end uridylation activity in Arabidopsis. *Curr Biol* **15**(16): 1501-1507.

Lienhard, G.E. 2008. Non-functional phosphorylations? *Trends in Biochemical Sciences* **33**(8): 351.

Lukas, C., Bartkova, J., Latella, L., Falck, J., Mailand, N., Schroeder, T., Sehested, M., Lukas, J., and Bartek, J. 2001. DNA damage-activated kinase Chk2 is independent of proliferation or differentiation yet correlates with tissue biology. *Cancer Research* **61**(13): 4990.

Lykke-Andersen, S., Brodersen, D.E., and Jensen, T.H. 2009. Origins and activities of the eukaryotic exosome. *J Cell Sci* **122**(Pt 10): 1487-1494.

Lüscher, B., Stauber, C., Schindler, R., and Schümperli, D. 1985. Faithful cell-cycle regulation of a recombinant mouse histone H4 gene is controlled by sequences in the 3'-terminal part of the gene. *Proc Natl Acad Sci U S A* **82**(13): 4389-4393.

Ma, T., Van Tine, B.A., Wei, Y., Garrett, M.D., Nelson, D., Adams, P.D., Wang, J., Qin, J., Chow, L.T., and Harper, J.W. 2000. Cell cycle-regulated phosphorylation of p220(NPAT) by cyclin E/Cdk2 in Cajal bodies promotes histone gene transcription. *Genes Dev* **14**(18): 2298-2313.

Martin, F., Schaller, A., Eglite, S., Schumperli, D., and Muller, B. 1997. The gene for histone RNA hairpin binding protein is located on human chromosome 4 and encodes a novel type of RNA binding protein. *EMBO J* **16**(4): 769.

Martin, G., Doublie, S., and Keller, W. 2008. Determinants of substrate specificity in RNA-dependent nucleotidyl transferases. *Biochim Biophys Acta* **1779**(4): 206-216.

Marzluff, W.F. 2005. Metazoan replication-dependent histone mRNAs: a distinct set of RNA polymerase II transcripts. *Current Opinion in Cell Biology* **17**(3): 274.

Marzluff, W.F. and Duronio, R.J. 2002. Histone mRNA expression: multiple levels of cell cycle regulation and important developmental consequences. *Current Opinion in Cell Biology* **14**(6): 692.

Marzluff, W.F., Wagner, E.J., and Duronio, R.J. 2008. Metabolism and regulation of canonical histone mRNAs: life without a poly(A) tail. *Nat Rev Genet* **9**(11): 843-854.

Mata, J., Lyne, R., Burns, G., and Bahler, J. 2002. The transcriptional program of meiosis and sporulation in fission yeast. *Nat Genet* **32**(1): 143-147.

Matsuoka, S., Ballif, B.A., Smogorzewska, A., McDonald, E.R., 3rd, Hurov, K.E., Luo, J., Bakalarski, C.E., Zhao, Z., Solimini, N., Lerenthal, Y., Shiloh, Y., Gygi, S.P., and Elledge, S.J. 2007. ATM and ATR substrate analysis reveals extensive protein networks responsive to DNA damage. *Science* **316**(5828): 1160-1166.

Matsuyama, A., Arai, R., Yashiroda, Y., Shirai, A., Kamata, A., Sekido, S., Kobayashi, Y., Hashimoto, A., Hamamoto, M., Hiraoka, Y., Horinouchi, S., and Yoshida, M. 2006. ORFeome cloning and global analysis of protein localization in the fission yeast Schizosaccharomyces pombe. *Nat Biotechnol* **24**(7): 841-847.

Mellman, D.L. and Anderson, R.A. 2009. A novel gene expression pathway regulated by nuclear phosphoinositides. *Adv Enzyme Regul* **49**(1): 11-28.

Mellman, D.L., Gonzales, M.L., Song, C., Barlow, C.A., Wang, P., Kendziorski, C., and Anderson, R.A. 2008. A PtdIns4,5P2-regulated nuclear poly(A) polymerase controls expression of select mRNAs. *Nature* **451**(7181): 1013-1017.

Minoda, Y., Saeki, K., Aki, D., Takaki, H., Sanada, T., Koga, K., Kobayashi, T., Takaesu, G., and Yoshimura, A. 2006. A novel Zinc finger protein, ZCCHC11, interacts with TIFA and modulates TLR signaling. *Biochem Biophys Res Commun* **344**(3): 1023-1030.

Motamedi, M.R., Verdel, A., Colmenares, S.U., Gerber, S.A., Gygi, S.P., and Moazed, D. 2004. Two RNAi complexes, RITS and RDRC, physically interact and localize to noncoding centromeric RNAs. *Cell* **119**(6): 789-802.

Mowry, K.L. and Steitz, J.A. 1987. Identification of the human U7 snRNP as one of several factors involved in the 3' end maturation of histone premessenger RNA's. *Science* **238**(4834): 1682-1687.

Mullen, T.E. and Marzluff, W.F. 2008. Degradation of histone mRNA requires oligouridylation followed by decapping and simultaneous degradation of the mRNA both 5' to 3' and 3' to 5'. *Genes Dev* **22**(1): 50-65.

Murakami, H. and Nurse, P. 2000. DNA replication and damage checkpoints and meiotic cell cycle controls in the fission and budding yeasts. *Biochem J* **349**(Pt 1): 1-12.

Nagaike, T., Suzuki, T., Katoh, T., and Ueda, T. 2005. Human mitochondrial mRNAs are stabilized with polyadenylation regulated by mitochondria-specific poly(A) polymerase and polynucleotide phosphorylase. *J Biol Chem* **280**(20): 19721-19727.

Nakanishi, T., Kubota, H., Ishibashi, N., Kumagai, S., Watanabe, H., Yamashita, M., Kashiwabara, S., Miyado, K., and Baba, T. 2006. Possible role of mouse poly(A) polymerase mGLD-2 during oocyte maturation. *Dev Biol* **289**(1): 115-126.

Newman, M.A., Thomson, J.M., and Hammond, S.M. 2008. Lin-28 interaction with the Let-7 precursor loop mediates regulated microRNA processing. *RNA* **14**(8): 1539-1549.

Norbury, C.J. 2010. 3' Uridylation and the regulation of RNA function in the cytoplasm. *Biochem Soc Trans* **38**(4): 1150-1153.

Nyberg, K.A., Michelson, R.J., Putnam, C.W., and Weinert, T.A. 2002. Toward Maintaining The Genome: DNA Damage and Replication Checkpoints. *Annual Review of Genetics* **36**: 617-656.

Ojala, D., Montoya, J., and Attardi, G. 1981. tRNA punctuation model of RNA processing in human mitochondria. *Nature* **290**(5806): 470-474.

Osley, M.A. 1991. The regulation of histone synthesis in the cell cycle. *Annu Rev Biochem* **60**: 827-861.

Pandey, N.B. and Marzluff, W.F. 1987. The stem-loop structure at the 3' end of histone mRNA is necessary and sufficient for regulation of histone mRNA stability. *Mol Cell Biol* **7**(12): 4557-4559.

Proudfoot, N.J., Furger, A., and Dye, M.J. 2002. Integrating mRNA processing with transcription. *Cell* **108**(4): 501-512.

Rammelt, C., Bilen, B., Zavolan, M., and Keller, W. 2011. PAPD5, a noncanonical poly(A) polymerase with an unusual RNA-binding motif. *RNA*.

Read, R.L., Martinho, R.G., Wang, S.W., Carr, A.M., and Norbury, C.J. 2002. Cytoplasmic poly(A) polymerases mediate cellular responses to S phase arrest. *Proc Natl Acad Sci U S A* **99**(19): 12079-12084.

Reis, C.C. and Campbell, J.L. 2007. Contribution of Trf4/5 and the Nuclear Exosome to Genome Stability Through Regulation of Histone mRNA Levels in Saccharomyces cerevisiae. *Genetics* **175**(3): 993-1010.

Richter, J.D. 2007. CPEB: a life in translation. *Trends Biochem Sci* **32**(6): 279-285.

Rissland, O.S., Mikulasova, A., and Norbury, C.J. 2007. Efficient RNA polyuridylation by noncanonical poly(A) polymerases. *Mol Cell Biol* **27**(10): 3612-3624.

Rissland, O.S. and Norbury, C.J. 2009. Decapping is preceded by 3' uridylation in a novel pathway of bulk mRNA turnover. *Nat Struct Mol Biol* **16**(6): 616-623.

Rogakou, E.P., Boon, C., Redon, C., and Bonner, W.M. 1999. Megabase chromatin domains involved in DNA double-strand breaks in vivo. *J Cell Biol* **146**(5): 905-916.

Rogakou, E.P., Pilch, D.R., Orr, A.H., Ivanova, V.S., and Bonner, W.M. 1998. DNA Double-stranded Breaks Induce Histone H2AX Phosphorylation on Serine 139. *Journal of Biological Chemistry* **273**(10): 5858-5868.

Rougemaille, M., Gudipati, R.K., Olesen, J.R., Thomsen, R., Seraphin, B., Libri, D., and Jensen, T.H. 2007. Dissecting mechanisms of nuclear mRNA surveillance in THO/sub2 complex mutants. *EMBO J* **26**(9): 2317.

Rouhana, L., Wang, L., Buter, N., Kwak, J.E., Schiltz, C.A., Gonzalez, T., Kelley, A.E., Landry, C.F., and Wickens, M. 2005. Vertebrate GLD2 poly(A) polymerases in the germline and the brain. *RNA* **11**(7): 1117-1130.

Rouhana, L. and Wickens, M. 2007. Autoregulation of GLD-2 cytoplasmic poly(A) polymerase. *RNA* **13**(2): 188-199.

Rybak, A., Fuchs, H., Smirnova, L., Brandt, C., Pohl, E.E., Nitsch, R., and Wulczyn, F.G. 2008. A feedback loop comprising lin-28 and let-7 controls pre-let-7 maturation during neural stem-cell commitment. *Nat Cell Biol* **10**(8): 987-993.

Sachs, A.B., Sarnow, P., and Hentze, M.W. 1997. Starting at the beginning, middle, and end: translation initiation in eukaryotes. *Cell* **89**(6): 831-838.

Saitoh, S., Chabes, A., McDonald, W.H., Thelander, L., Yates, J.R., and Russell, P. 2002. Cid13 is a cytoplasmic poly(A) polymerase that regulates ribonucleotide reductase mRNA. *Cell* **109**(5): 563-573.

San Paolo, S., Vanacova, S., Schenk, L., Scherrer, T., Blank, D., Keller, W., and Gerber, A.P. 2009. Distinct roles of non-canonical poly(A) polymerases in RNA metabolism. *PLoS Genet* **5**(7): e1000555.

Sancar, A., Lindsey-Boltz, L.A., Ünsal-Kaçmaz, K., and Linn, S. 2004. Molecular Mechanisms of Mammalian DNA Repair and the DNA Damage Checkpoint. *Annual Review of Biochemistry* **73**(1): 39-85.

Sanchez, R. and Marzluff, W.F. 2002. The Stem-Loop Binding Protein Is Required for Efficient Translation of Histone mRNA In Vivo and In Vitro. *Mol Cell Biol* **22**(20): 7093-7104.

Scharl, E.C. and Steitz, J.A. 1994. The site of 3' end formation of histone messenger RNA is a fixed distance from the downstream element recognized by the U7 snRNP. *EMBO J* **13**(10): 2432-2440.

Schlegel, R. and Pardee, A.B. 1986. Caffeine-induced uncoupling of mitosis from the completion of DNA replication in mammalian cells. *Science* **232**(4755): 1264-1266.

Schmid, M., Kuchler, B., and Eckmann, C.R. 2009. Two conserved regulatory cytoplasmic poly(A) polymerases, GLD-4 and GLD-2, regulate meiotic progression in C. elegans. *Genes Dev* **23**(7): 824-836.

Schmidt, M.-J. and Norbury, C.J. 2010. Polyadenylation and beyond: emerging roles for noncanonical poly(A) polymerases. *Wiley Interdisciplinary Reviews - RNA* **1**(1): 142.

Schuster, G. and Stern, D. 2009. RNA polyadenylation and decay in mitochondria and chloroplasts. *Prog Mol Biol Transl Sci* **85**: 393-422.

Shatkin, A.J. and Manley, J.L. 2000. The ends of the affair: Capping and polyadenylation. *Nat Struct Mol Biol* **7**(10): 838-842.

Shcherbik, N., Wang, M., Lapik, Y.R., Srivastava, L., and Pestov, D.G. 2010. Polyadenylation and degradation of incomplete RNA polymerase I transcripts in mammalian cells. *EMBO Rep* **11**(2): 106-111.

Shen, B. and Goodman, H.M. 2004. Uridine addition after microRNA-directed cleavage. *Science* **306**(5698): 997.

Slomovic, S., Laufer, D., Geiger, D., and Schuster, G. 2005. Polyadenylation and degradation of human mitochondrial RNA: the prokaryotic past leaves its mark. *Mol Cell Biol* **25**(15): 6427-6435.

Smolka, M.B., Albuquerque, C.P., Chen, S.-H., and Zhou, H. 2007. Proteome-wide identification of in vivo targets of DNA damage checkpoint kinases. *Proceedings of the National Academy of Sciences* **104**(25): 10364-10369.

Song, M.G. and Kiledjian, M. 2007. 3' Terminal oligo U-tract-mediated stimulation of decapping. *RNA* **13**(12): 2356-2365.

Sorensen, C.S., Syljuasen, R.G., Lukas, J., and Bartek, J. 2004. ATR, Claspin and the Rad9-Rad1-Hus1 complex regulate Chk1 and Cdc25A in the absence of DNA damage. *Cell Cycle* **3**(7): 941-945.

Stevenson, A.L. and Norbury, C.J. 2006. The Cid1 family of non-canonical poly(A) polymerases. *Yeast* **23**(13): 991-1000.

Stimac, E., Groppi, V.E., Jr., and Coffino, P. 1984. Inhibition of protein synthesis stabilizes histone mRNA. *Mol Cell Biol* **4**(10): 2082-2090.

Strub, K. and Birnstiel, M.L. 1986. Genetic complementation in the Xenopus oocyte: co-expression of sea urchin histone and U7 RNAs restores 3' processing of H3 pre-mRNA in the oocyte. *EMBO J* **5**(7): 1675-1682.

Stucki, M., Clapperton, J.A., Mohammad, D., Yaffe, M.B., Smerdon, S.J., and Jackson, S.P. 2005. MDC1 Directly Binds Phosphorylated Histone H2AX to Regulate Cellular Responses to DNA Double-Strand Breaks. *Cell* **123**(7): 1213.

Thakurta, A.G., Gopal, G., Yoon, J.H., Kozak, L., and Dhar, R. 2005. Homolog of BRCA2-interacting Dss1p and Uap56p link Mlo3p and Rae1p for mRNA export in fission yeast. *EMBO J* **24**(14): 2512.

Tharun, S., He, W., Mayes, A.E., Lennertz, P., Beggs, J.D., and Parker, R. 2000. Yeast Sm-like proteins function in mRNA decapping and decay. *Nature* **404**(6777): 515.

Tharun, S. and Parker, R. 2001. Targeting an mRNA for Decapping: Displacement of Translation Factors and Association of the Lsm1p-7p Complex on Deadenylated Yeast mRNAs. *Molecular Cell* **8**(5): 1075.

Thiriet, C. and Hayes, J.J. 2005. Chromatin in Need of a Fix: Phosphorylation of H2AX Connects Chromatin to DNA Repair. *Molecular Cell* **18**(6): 617.

Tomecki, R., Dmochowska, A., Gewartowski, K., Dziembowski, A., and Stepien, P.P. 2004. Identification of a novel human nuclear-encoded mitochondrial poly(A) polymerase. *Nucleic Acids Res* **32**(20): 6001-6014.

Tomecki, R., Kristiansen, M.S., Lykke-Andersen, S., Chlebowski, A., Larsen, K.M., Szczesny, R.J., Drazkowska, K., Pastula, A., Andersen, J.S., Stepien, P.P., Dziembowski, A., and Jensen, T.H. 2010. The human core exosome interacts with differentially localized processive RNases: hDIS3 and hDIS3L. *EMBO J* **29**(14): 2342-2357.

Trippe, R., Guschina, E., Hossbach, M., Urlaub, H., Luhrmann, R., and Benecke, B.J. 2006. Identification, cloning, and functional analysis of the human U6 snRNA-specific terminal uridylyl transferase. *RNA* **12**(8): 1494-1504.

Trippe, R., Sandrock, B., and Benecke, B.J. 1998. A highly specific terminal uridylyl transferase modifies the 3'-end of U6 small nuclear RNA. *Nucleic Acids Res* **26**(13): 3119-3126.

van Wolfswinkel, J.C., Claycomb, J.M., Batista, P.J., Mello, C.C., Berezikov, E., and Ketting, R.F. 2009. CDE-1 affects chromosome segregation through uridylation of CSR-1-bound siRNAs. *Cell* **139**(1): 135-148.

Vanacova, S., Wolf, J., Martin, G., Blank, D., Dettwiler, S., Friedlein, A., Langen, H., Keith, G., and Keller, W. 2005. A new yeast poly(A) polymerase complex involved in RNA quality control. *PLoS Biol* **3**(6): e189.

Vasudevan, S. and Peltz, S.W. 2001. Regulated ARE-mediated mRNA decay in Saccharomyces cerevisiae. *Mol Cell* **7**(6): 1191-1200.

Viswanathan, S.R., Powers, J.T., Einhorn, W., Hoshida, Y., Ng, T.L., Toffanin, S., O'Sullivan, M., Lu, J., Phillips, L.A., Lockhart, V.L., Shah, S.P., Tanwar, P.S., Mermel, C.H., Beroukhim, R., Azam, M., Teixeira, J., Meyerson, M., Hughes, T.P., Llovet, J.M., Radich, J., Mullighan, C.G., Golub, T.R., Sorensen, P.H., and Daley, G.Q. 2009. Lin28 promotes transformation and is associated with advanced human malignancies. *Nat Genet* **41**(7): 843-848.

Wagner, E.J. and Marzluff, W.F. 2006. ZFP100, a component of the active U7 snRNP limiting for histone pre-mRNA processing, is required for entry into S phase. *Mol Cell Biol* **26**(17): 6702-6712.

Wahle, E. and Ruegsegger, U. 1999. 3' end processing of pre-mRNA in eukaryotes. *FEMS Microbiology Rev* **23**(3): 277-295.

Wang, L., Eckmann, C.R., Kadyk, L.C., Wickens, M., and Kimble, J. 2002. A regulatory cytoplasmic poly(A) polymerase in Caenorhabditis elegans. *Nature* **419**(6904): 312-316.

Wang, S.W., Norbury, C., Harris, A.L., and Toda, T. 1999. Caffeine can override the S-M checkpoint in fission yeast. *J Cell Sci* **112** (6): 927-937.

Wang, S.W., Toda, T., MacCallum, R., Harris, A.L., and Norbury, C. 2000. Cid1, a fission yeast protein required for S-M checkpoint control when DNA polymerase delta or epsilon is inactivated. *Mol Cell Biol* **20**(9): 3234-3244.

Wang, Z.F., Whitfield, M.L., Ingledue, T.C., Dominski, Z., and Marzluff, W.F. 1996. The protein that binds the 3' end of histone mRNA: a novel RNA-binding protein required for histone pre-mRNA processing. *Genes & Development* **10**(23): 3028-3040.

Ward, I.M. and Chen, J. 2001. Histone H2AX Is Phosphorylated in an ATR-dependent Manner in Response to Replicational Stress. *Journal of Biological Chemistry* **276**(51): 47759-47762.

Weinert, T.A. and Hartwell, L.H. 1988. The RAD9 gene controls the cell cycle response to DNA damage in Saccharomyces cerevisiae. *Science* **241**(4863): 317-322.

Wen, W.L., Stevenson, A.L., Wang, C.Y., Chen, H.J., Kearsey, S.E., Norbury, C.J., Watt, S., Bahler, J., and Wang, S.W. 2010. Vgl1, a multi-KH domain protein, is a novel component of the fission yeast stress granules required for cell survival under thermal stress. *Nucleic Acids Res* **38**(19): 6555-6566.

West, S., Gromak, N., Norbury, C.J., and Proudfoot, N.J. 2006. Adenylation and exosome-mediated degradation of cotranscriptionally cleaved pre-messenger RNA in human cells. *Mol Cell* **21**(3): 437-443.

West, S., Gromak, N., and Proudfoot, N.J. 2004. Human 5'-3' exonuclease Xrn2p promotes transcription termination at co-transcriptional cleavage sites. *Nature* **432**(7016): 522-525.

Whitfield, M.L., Kaygun, H., Erkmann, J.A., Townley-Tilson, W.H.D., Dominski, Z., and Marzluff, W.F. 2004. SLBP is associated with histone mRNA on polyribosomes as a component of the histone mRNP. *Nucleic Acids Research* **32**(16): 4833-4842.

Whitfield, M.L., Zheng, L.X., Baldwin, A., Ohta, T., Hurt, M.M., and Marzluff, W.F. 2000. Stem-loop binding protein, the protein that binds the 3' end of histone mRNA, is cell cycle regulated by both translational and posttranslational mechanisms. *Mol Cell Biol* **20**(12): 4188-4198.

Win, T.Z., Draper, S., Read, R.L., Pearce, J., Norbury, C.J., and Wang, S.W. 2006a. Requirement of fission yeast Cid14 in polyadenylation of rRNAs. *Mol Cell Biol* **26**(5): 1710-1721.

Win, T.Z., Stevenson, A.L., and Wang, S.W. 2006b. Fission yeast Cid12 has dual functions in chromosome segregation and checkpoint control. *Mol Cell Biol* **26**(12): 4435-4447.

Wyers, F., Rougemaille, M., Badis, G., Rousselle, J.C., Dufour, M.E., Boulay, J., Regnault, B., Devaux, F., Namane, A., Seraphin, B., Libri, D., and Jacquier, A. 2005. Cryptic pol II transcripts are degraded by a nuclear quality control pathway involving a new poly(A) polymerase. *Cell* **121**(5): 725-737.

Wyman, S.K., Knouf, E.C., Parkin, R.K., Fritz, B.R., Lin, D.W., Dennis, L.M., Krouse, M.A., Webster, P.J., and Tewari, M. 2011. Post-transcriptional generation of miRNA variants by multiple nucleotidyl transferases contributes to miRNA transcriptome complexity. *Genome Research %R 101101/gr118059110*.

Xu, B. and Huang, Y. 2009. Histone H2a mRNA interacts with Lin28 and contains a Lin28-dependent posttranscriptional regulatory element. *Nucleic Acids Res* **37**(13): 4256-4263.

Xu, B., Zhang, K., and Huang, Y. 2009. Lin28 modulates cell growth and associates with a subset of cell cycle regulator mRNAs in mouse embryonic stem cells. *RNA* **15**(3): 357-361.

Yazdi, P.T., Wang, Y., Zhao, S., Patel, N., Lee, E.Y., and Qin, J. 2002. SMC1 is a downstream effector in the ATM/NBS1 branch of the human S-phase checkpoint. *Genes Dev* **16**(5): 571-582.

Ye, X., Franco, A.A., Santos, H., Nelson, D.M., Kaufman, P.D., and Adams, P.D. 2003. Defective S Phase Chromatin Assembly Causes DNA Damage, Activation of the S Phase Checkpoint, and S Phase Arrest. *Molecular Cell* **11**(2): 341.

Yee, K.S. and Vousden, K.H. 2005. Complicating the complexity of p53. *Carcinogenesis* **26**(8): 1317-1322.

Yeom, K.-H., Heo, I., Lee, J., Hohng, S., Kim, V.N., and Joo, C. 2011. Single-molecule approach to immunoprecipitated protein complexes: insights into miRNA uridylation. *EMBO Rep*.

Yu, J., Vodyanik, M.A., Smuga-Otto, K., Antosiewicz-Bourget, J., Frane, J.L., Tian, S., Nie, J., Jonsdottir, G.A., Ruotti, V., Stewart, R., Slukvin, II, and Thomson, J.A. 2007. Induced pluripotent stem cell lines derived from human somatic cells. *Science* **318**(5858): 1917-1920.

Zachos, G., Rainey, M., and Gillespie, D.A. 2003. Lethal errors in checkpoint control--life without Chk1. *Cell Cycle* **2**(1): 14-16.

Zhang, K., Fischer, T., Porter, R.L., Dhakshnamoorthy, J., Zofall, M., Zhou, M., Veenstra, T., and Grewal, S.I.S. 2011. Clr4/Suv39 and RNA Quality Control Factors Cooperate to Trigger RNAi and Suppress Antisense RNA. *Science* **331**(6024): 1624-1627.

Zhao, J., Kennedy, B.K., Lawrence, B.D., Barbie, D.A., Matera, A.G., Fletcher, J.A., and Harlow, E. 2000. NPAT links cyclin E-Cdk2 to the regulation of replication-dependent histone gene transcription. *Genes Dev* **14**(18): 2283-2297.

Zheng, L., Dominski, Z., Yang, X.C., Elms, P., Raska, C.S., Borchers, C.H., and Marzluff, W.F. 2003. Phosphorylation of stem-loop binding protein (SLBP) on two threonines triggers degradation of SLBP, the sole cell cycle-regulated factor required for regulation of histone mRNA processing, at the end of S phase. *Mol Cell Biol* **23**(5): 1590-1601.

Zhou, B.B. and Elledge, S.J. 2000. The DNA damage response: putting checkpoints in perspective. *Nature* **408**(6811): 433-439.

Appendices

Appendix A Proteins identified by MS

Cid1-TAP co-purifying proteins and their associated function, sorted according to the protein score obtained by MASCOT. The score reflects the probability that identified peptide masses match non-random events.

Identified Protein	Associated Function	Score
Probable heat shock protein Ssa2	Stress response	606
Caffeine-induced death protein 1 (Cid1)	RNA turnover, replication checkpoint	571
Glyceraldehyde-3-phosphate dehydrogenase 1	Glycolysis	524
Elongation factor 1-alpha-B/C	Translation	479
Actin	Cytoskeleton	457
Elongation factor 1-alpha-A	Translation	456
Heat shock 70 kDa protein	Stress response	435
Heat shock protein Sks2	Stress response	405
Heat shock protein 60 (HSP60)	Stress response	226
PABP (Polyadenylate tail-binding protein)	RNA processing	214
Acetolactate synthase	Amino-acid biosynthesis	171
Fatty acid synthase subunit alpha	Lipid synthesis	155
Alcohol dehydrogenase	Metabolic oxidation	145
Heat shock protein homolog pss1	Stress response	132
RNA polymerase I subunit RPA2	Transcription	116
60S ribosomal protein L35	Translation	115
rRNA 2'-O-methyltransferase fibrillarin	Ribosome biogenesis	113
6-phosphofructokinase	Glycolysis	105
Plasma membrane ATPase 1	Ion transport	100
RNA helicase Ded1	Translation	98
Putative coatomer subunit alpha	ER-Golgi	98
60S ribosomal protein L3-B	Translation	96
60S ribosomal protein L12	Translation	96
Carbamoyl-phosphate synthase	Nucleotide synthesis	92
DNA-binding protein TG1-3	Telomere binding	92
Sulfite reductase [NADPH] subunit beta	Metabolic oxidation	91
60S ribosomal protein L30-1	Translation	85
Heat shock protein 90 homolog	Stress response	83
78 kDa glucose-regulated protein	Glycolysis	80
60S acidic ribosomal protein P1-alpha 1	Translation	78
Homocitrate synthase, mitochondrial precursor	Amino-acid biosynthesis	73
Probable 60S ribosomal protein L28e	Translation	73
Probable aspartate-semialdehyde dehydrogenase	Amino-acid biosynthesis	73
U3 small nucleolar RNA-associated protein 10	Ribosome biogenesis	72
60S acidic ribosomal protein P2-alpha	Translation	72
60S ribosomal protein L22	Translation	72
Elongation factor 2 (EF-2)	Translation	70
3-isopropylmalate dehydrogenase	Amino-acid biosynthesis	70
60S ribosomal protein L8	Translation	69
60S ribosomal protein L18-A	Translation	67
DNA-directed RNA polymerase I subunit RPA1	Transcription	65

Triosephosphate isomerase	Metabolism	63
COPII coat assembly protein sec16	ER-Golgi	59
40S ribosomal protein S4-C	Translation	59
Serine/threonine-protein kinase cdk9	Transcription	57
60S ribosomal protein L13	Translation	55
60S ribosomal protein L4-A	Translation	55
Arg11, mitochondrial	Amino-acid biosynthesis	55
60S acidic ribosomal protein P1-alpha 5	Translation	54
Endo-1,3(4)-beta-glucanase 1	Cell division	54
60S ribosomal protein L6.	Translation	51
60S ribosomal protein L30-2.	Translation	51
60S ribosomal protein L25-A.	Translation	50
Sik1	Ribosome biogenesis	49
60S acidic ribosomal protein P0.	Translation	49
40S ribosomal protein S3aE-A	Translation	47
Cell division control protein 2	Cell division	46
S-adenosylmethionine synthetase	Carbon metabolism	46
RNA polymerases I and III subunit RPAC2	Transcription	45
Saccharopine dehydrogenase	Amino-acid biosynthesis	44
40S ribosomal protein S3	Translation	42
RNA helicase Has1	Ribosome biogenesis	41
DNA damage checkpoint protein Rad24	DNA damage response	41
Uncharacterised glutamine amidotransferase	?	41
60S ribosomal protein L4-B	Translation	41
Probable ketol-acid reductoisomerase	Amino-acid biosynthesis	40
Eukaryotic translation initiation factor 4 gamma	Translation	40
Bromodomain-containing protein	Chromatin remodeling	39
60S ribosomal protein L2	Translation	35
RNA helicase Drs1	Ribosome biogenesis	35
F-box/TPR repeat protein Pof3	Transcription	35
Probable methionyl-tRNA synthetase	Protein biosynthesis	35
60S ribosomal protein L24-B	Translation	35
60S ribosomal protein L7-C	Translation	34
Ribose-phosphate pyrophosphokinase 3	Glycolysis	34
Serine/threonine-protein kinase Gcn2	Protein phosphorylation	34
Fatty acid synthase subunit beta	Lipid synthesis	33
Putative alpha-trehalose-phosphate synthase	Glycolysis	33
Anaphase-promoting complex subunit 3	Cell division	31
Pyruvate carboxylase	Gluconeogenesis	31
UPF0202 protein	Ribosome biogenesis	30
Uncharacterised protein C146.01	?	30
DNA ligase 4	DNA repair	30
40S ribosomal protein S14	Translation	30
Probable pyruvate decarboxylase C1F8.07c	Metabolism	30
Translation initiation factor 6 (eIF-6)	Translation	29
60S ribosomal protein L26	Translation	29
ATP-dependent RNA helicase Dbp6	Ribosome biogenesis	29
Probable translation initiation factor 3	Translation	28
40S ribosomal protein S5-A	Translation	28
Putative peptide chain release factor 1	Translation	28
RuvB-like helicase 2	DNA damage response	27
Uncharacterised oxidoreductase C2F3.05c	?	27
Phosphoglycerate mutase	Glycolysis	27

60S ribosomal protein L14	Translation	27
Dihydrolipoyllysine-residue acetyltransferase	Amino-acid biosynthesis	26
Rho1 guanine nucleotide exchange factor 3	Cell division	26
Probable homocysteine methyltransferase	Amino-acid biosynthesis	26
Centromere protein 3	Cell division	26
Casein kinase II subunit alpha	Protein phosphorylation	26
Dual specificity protein kinase Pom1	Protein phosphorylation	26
40S ribosomal protein S18	Translation	26
Pyruvate dehydrogenase E1 component subunit beta	Glycolysis	25
Translation initiation factor 2-alpha kinase 2	Translation	25
Dihydrolipoyl dehydrogenase	Metabolic oxidation	25
Vacuolar segregation protein Pep7	Protein sorting	25
Uncharacterised ATPase protein C16E9.10c	?	25
40S ribosomal protein S9-B	Translation	24
Uncharacterised protein C2F7.08c	?	24
Switch-activating protein 1	Mating type	24
Casein kinase I homolog 3	Protein phosphorylation	24
60S ribosomal protein L7-B	Translation	24
Glucose-insensitive transcription protein 7	Glycolysis	24
Chitin synthase regulatory factor 4	Polysaccharide synthesis	23
ATP-dependent RNA helicase Suv3	Mitochondrial RNA processing	23
Uncharacterised protein C777.11	?	23
KH domain-containing protein Vgl1	RNA binding	23
E3 ubiquitin-protein ligase Ptr1	mRNA transport	23
Protein Hob3	Cell division	23
Autophagy-related protein 2	Autophagy	22
Pyruvate kinase (PK)	Glycolysis	22
Rho1 guanine nucleotide exchange factor 1	Cell division	22
Serine/threonine-protein kinase Ppk25	Phosphorylation	21
DNA polymerase delta catalytic subunit	DNA replication	21
60S ribosomal protein L17-A	Translation	21
Uncharacterised protein C19G7.18c	?	21
Uncharacterised NOC2 family protein C1142.04	?	21
Probable mitochondrial intermediate peptidase	Proteolysis	21
Histone H2B-alpha (H2B.1).	Nucleosome	21
Transcriptional repressor tup12	Transcription	21
Uncharacterised protein C20G4.08	?	20
Kinetochore protein Fta6	Cell division	20
Division mal foutue 1 protein	Cell division	20
RNA helicase Prp16	mRNA-splicing	20
Putative protein disulfide-isomerase	Protein folding	20
ERO1-like protein 1 precursor	Electron transport ER	20
Meiotically up-regulated gene 131 protein	?	20
Probable translation initiation factor eIF-2B	Translation	20

Appendix B Plasmids used in this study

Name	Source	Use
	S. pombe	
pREPNTAP	K. Gould	Empty vector used as negative control for MS
pREPNTAP-Cid1	A. Stevenson	TAP purification + MS
pREPNTAP-Cid1 S404A	This study	Investigation of phosphorylation site
pFA6a series	J. Bähler	Myc-/HA-tagging for Co-IP
	Human cells	
pGEX-Hs3	A. Mikulasova	Antibody production
pGEX-Hs2	A. Mikulasova	Antibody production
pcDNA3-TAP	A. Mikulasova	Complementation assays
pcDNA3-Hs3TAP	A. Mikulasova	Complementation assays
pcDNA3-Hs3TAP-DADA	A. Mikulasova	Complementation assays
pcDNA3-Hs3TAP-S773A	This study	Complementation assays
pcDNA3-Hs2TAP	A. Mikulasova	Complementation assays

Appendix C Oligonucleotides used in this study

Name	Sequence	Use
	S. pombe	
Mlo3_myc_F	GAACTCCTAATCGTCCTAAAAAATCCGCCGAAGAGCTC GACAAGGAGATGGATGATTATTTTGGATCAAATGAGAA GGAGCGGATCCCCGGGTTAATTAA	Gene-tagging
Mlo3_myc_R	AATCCATTACGAAAGACCCAAAACACAAAAACAACTTC AAGAACTGCCATTCGAAACAGCATTATATTGCCAATATT ATTGAATTCGAGCTCGTTTAAAC	Gene-tagging
Cid1_myc_F	TTCCGCCTCGTCGCCAGAAAAAAACGGATGAACAATCT AACAAAAAATTGTTGAATGAAACCGATGGTGACAATTCT GAGCGGATCCCCGGGTTAATTAA	Gene-tagging
Cid1_myc_R	GAGGTTGTACATAAAACAAAGGGGGAAAGGTATTAGAA ACAAGAGGTCAAAATTTTTAAAGAAAAATAAAAACATTC CATGAATTCGAGCTCGTTTAAAC	Gene-tagging
C1_S404A__F	GATGGTGACAATgCTGAGTGAGCGGCCGC	Cid1-Mutagenesi
C1_S404A__R	GCGGCCGCTCACTCAGcATTGTCACCATC	Cid1-Mutagenesi

Human cells		
HC11DADA__F	CGTGATAGTGCTCTGGCTATTTGTATGACC	ZCCHC11-Mutagenesi
HC11DADA__F	GGTCATACAAATAGCCAGAGCACTATCACG	ZCCHC11-Mutagenesi
HC11SA__F	GAAATGGACTGTACAGCACAGAGATGTATTATTG	ZCCHC11-Mutagenesi
HC11SA__F	CAATAATACATCTCTGTGCTGTACAGTCCATTTC	ZCCHC11-Mutagenesi
ZCCHC11__F	TCAACAGGTGGCTGGTTCAGCTCAG	qRT-PCR
ZCCHC11__R	TAGCAGCTGACTGGGAAGAGTTCTG	qRT-PCR
PAPD5_F	AATCTCAGCATGGATCAGCA	qRT-PCR
PAPD5_R	TGGATTTGCCTTGATGTTGT	qRT-PCR
PAPD1_F	GCTTTGAAGACAAGATTCCC	qRT-PCR
PAPD1_R	GGAGCAGATGGTAGCAATAG	qRT-PCR
Lsm1_F	TACGGTGATATTCCTCGAGG	qRT-PCR
Lsm1_R	CTTCCAGCTTGGTCTGCTG	qRT-PCR
H2A_F	AACGACGAGGAACTGAACAA	qRT-PCR
H2A_R	TTTGCCTTGTGGTGACTCTC	qRT-PCR
H3_F	CGCAGGACTTTAAGACGGA	qRT-PCR
H3_R	ATGTCCTTGGGCATAATGGT	qRT-PCR
GAPDH_F	ATGGGTGTGAACCATGAGAA	qRT-PCR
GAPDH_R	GTGCTAAGCAGTTGGTGGTG	qRT-PCR
H2A_5'_R	GTTGCCTTTGCGCAGCAAG	cRACE
H2A_3'_F	AACGACGAGGAACTGAACAA	cRACE
shZCCHC11_F	TCTCGGTTGCTTCAGACTTTATATTCAAGAGATATAAAGTCTGAAGCAACCCT	shRNA
shZCCHC11_R	CTGCAGGGTTGCTTCAGACTTTATATCTCTTGAATATAAAGTCTGAAGCAACC	shRNA
shPAPD5_F	TCTCGGATCGAGAGTGTAATTAATTCAAGAGATTAATTACACTCTCGATCCCT	shRNA
shPAPD5_R	CTGCAGGGATCGAGAGTGTAATTAATCTCTTGAATTAATTACACTCTCGATCC	shRNA
shPAPD1_F	TCTCGTCCTTTACCAAGAAGAAATTCAAGAGATTTCTTCTTGGTAAAGGACCT	shRNA
shPAPD1_R	CTGCAGGTCCTTTACCAAGAAGAAATCTCTTGAATTTCTTCTTGGTAAAGGAC	shRNA
shLsm1_F	TCTCGAGCAGATACTCTTGATGATTCAAGAGATCATCAAGAGTATCTGCTCCT	shRNA
shLsm1_R	CTGCAGGAGCAGATACTCTTGATGATCTCTTGAATCATCAAGAGTATCTGCTC	shRNA

Appendix D Media

Luria-Bertani (LB) medium

1% w/v bacto-tryptone
0.5% w/v bacto-yeast extract
1% w/v NaCl
For agar: add 1.5% w/v bacto-agar
Ampicillin was added before use to a final concentration of 100μg/ml

The following media was supplied by Cancer Research UK.

YE5S medium

0.5% w/v bacto-yeast extract
3% w/v glucose
225μg/ml leucine, uracil, adenine, histidine, lysine
For agar: add 2% w/v bacto-agar

ME4S agar

2% w/v bacto-malt extract
225μg/ml leucine, uracil, adenine, histidine
2% w/v bacto agar

Edinburgh Minimal Medium (EEM2)

14.7mM potassium hydrogen phthallate
15.5mM Na2HPO4
93.5mM NH4Cl
2% w/v Glucose
Salts: 5.2mM $MgCl_2$, 0.1mM $CaCl_2$, 13.4mM GCl, 0.28mM Na_2SO_4
Vitamins: 4.2μM pantothenic acid, 81.2μM nicotinic acid, 55.5μM inositol, 40.8μM biotin)
Minerals: 8.1μM boric acid, 2.37μM $MnSO_4$, 1.39μM $ZnSO_4$, 0.74μM $FeCl_3$, 0.25μM molybdic aicd, 0.6μM KI, 4.76μM citric acid, 0.16μM $CuSO_4$)
For agar: add 2% w/v bacto-agar